Institute of Earth Sciences
NAWI Graz Geocenter
University & TU of Graz

Department of Geography and Geology
University Salzburg

The Sattnitz-Conglomerate of the Klagenfurt-Basin - Carinthia

Orogenesis - Sedimentology – Diagenesis - Morphology – Use as Building Material

Master Thesis
submitted by Ewald Mothwurf
on Nov. 15, 2018

Supervisor
Univ. Prof. Dr. Franz Neubauer

ABSTRACT

In the South of the present-day Klagenfurt Basin, the Upper Miocene-Pliocene Sattnitz Conglomerate dominates the landscape. It stretches East – West over 50 km and North – South over 2 - 5 km. The ca. 200 to 400 m thick succession is a poorly sorted conglomerate with sub-rounded cobbles and rounded pebbles. The clasts comprise carbonate/dolomite, arenite and crystalline phyllosilicates, the sandy matrix is composed of monocrystalline siliciclastic grains, which include quartz, white mica, K-feldspar, biotite, chlorite and carbonate cement, the latter formed by diagenesis.

Within the possible conglomerate deposition time frame between Pannonian and the cool ages in Late Pliocene, an extraordinary climatic event, the Messinian Salinity Crisis of the Mediterranean area potentially generated an extreme climate in this area. At the partly desiccated Mediterranean Sea the air was hot with temperatures above 50°C and also high water temperatures leading to a high evaporation rate. The desiccation led to a semiarid climate with extreme rainfalls in the surrounding land including the catchments of the Sattnitz Conglomerate where torrential downpours provoked floods out of three valleys joining at Villach from where the debris, encapsulated in sheet floods, flushed down the depositional area. There is no other climatic event known within the possible depositional time that could have provoked this conglomerate deposition.

The provenance of the conglomerate is allocated by the exhumation ages from detrital white mica dated by the Ar-Ar method and the known exhumation dates within the catchments. The clasts can be assigned to three major groups, (1) unmetamorphic limestone, dolomites and marls, (2) sandstones and (3) metamorphic clasts. Some clast's origin can be assigned to limited areas giving a clue to the provenance.

Diagenesis was likely in two stages: a poorly preserved stage of thin dolomite coatings, and then the main stage by precipitation of calcite.

The post-diagenetic overprint of the Sattnitz Conglomerate was due to the glaciations. The younger conglomerates (Hollenburg Nagelfluh) was formed in the interglacial stages. These rocks were the preferred construction material for houses,

castles and churches versus the Sattnitz Conglomerate. The main buildings constructed using these conglomerates are presented in this thesis.

KURZFASSUNG

Der Süden des gegenwärtigen Klagenfurter Beckens wird vom großräumigen Plateau des Sattnitz-Konglomerats eingenommen. Es erstreckt sich über 50 km Ost–West und 2–5 km Nord-Süd. Es ist ein schlecht sortiertes Konglomerat mit mäßig gerundeten Komponenten. Die Klasten sind Karbonat/Dolomit, Sandstein und kristalline Schiefer, Die Matrix enthält monokristalline siliziklastische Körner aus Quarz, Hellglimmer, K-Feldspat, Biotit, Chlorit führenden Gangquarz, Schichtsilikate und Karbonatzement, letzteren als diagenetische Bindung.

Innerhalb des möglichen Zeitraumes der Konglomeratablagerung zwischen dem späteren Pannonium und den frühen Kaltzeiten im späten Pliozän, ein außergewöhnliches klimatisches Ereignis, die Messinianische Salzkrise des Mittelmeeres, bewirkte ein extremes Klima in dieser Region. Am teilweise ausgetrockneten Mittelmeer war die Luft heiß mit Temperaturen über 50°C und hohen Wassertemperaturen, was zu einer enormen Verdunstung führte. Die Austrocknung führte zu einem semiariden Klima mit sintflutartigen Regengüssen im umgebenden Gebiet inklusive der Einzugsgebiete des Sattnitz-Konglomerats, in denen Sturzfluten entstanden, die aus den drei Tälern, die sich in Villach vereinen und Geröll enthalten, in Schwallen mit Schichtfluten in das Ablagerungsgebiet transportierten. Kein anderes Klimaereignis in diesem Zeitraum kann zur Bildung dieses Konglomerats geführt haben.

Die Herkunft des Konglomerates wurde über die Exhumationsalter von detritischen Hellglimmern mittels Ar-Ar-Datierung und den bekannten Exhumationsaltern im Einzugsgebiet bestimmt. Die Klasten können drei Hauptgruppen zugeordnet werden, nicht metamorphosierter Kalkstein, Dolomite und Mergel, Sandstein und metamorphe Klasten. Der Ursprung einiger Klasten ist auf ein sehr begrenztes Gebiet beschränkt.

Die postdiagenetische Formung des Sattnitz Konglomerates erfolgte durch die Vergletscherung. In Interglazialen wurden jüngere Konglomerate gebildet (Hollenburger Nagelfluh), welche bevorzugt als Bausteine für Gebäude, Schlösser und

Kirchen eingesetzt wurden. Es werden die wesentlichsten Gebäude in Unterkärnten beschrieben, bei denen Konglomerate eingesetzt wurden.

Acknowledgements

I want to express my gratitude to all who facilitated and supported this thesis.

First of all, to my supervisor Prof. Franz Neubauer, University Salzburg, for the conception of the theme, the scientific topics of this master's thesis, for the time spent on our joint field work and all I could learn as the thesis progressed.

My thank goes: To the professors of the University of Graz, Ulrich Foelsche – Meteorology Department - for our discussions on the climatic influence, and from our Geology Department Harry Fritz for general advice and feedback and Gerfried Winkler for our discussions around the hydrology of the floods, to Karl Ettinger for his support at the SEM-EDX and to Werner Piller for the pollen literature references.

To Prof. Franz Neubauer for the joint elaboration of the chapters Provenance analysis and Diagenesis which will be the kernel of a planned publication.

To Karl Krainer for the images provided.

To Dagmar Gallé who sparked my geology study with a present of the book "High Above the Alps" by Kurt Stuewe and was, as may partner, patiently accompanying this study.

Table of Content

Scientific questions of this thesis on the Sattnitz Conglomerate

- Sedimentological model, provenance of the clastic detritus
- Climatic conditions during the time of deposition and diagenesis
- Postdiagenetic tectonics and morphogenesis
- Use of Sattnitz- and interglacial conglomerates as construction material

Introduction

Geography and Geology of the Study Area

The Sattnitz Conglomerate (SC) is situated within the Neogene Klagenfurt Basin (KB), the only flexural basin inside the Alps (Heberer et al., 2017), in Carinthia, in the southern part of Austria. The Rosental Valley in the S of the SC separates it from the Karawanken Mountain (KW) chain the northern flanks of which are exposing the Bärental Cnglomerate (BC). The SC stretches 56 km from West to East from Faaker See in the W to Eberndorf in the E where the conglomerate dives under the Holocene and the recent alluvial plane. The SC thickness is in the range of 200 to 400m, it is deposited above a pre-Alpine polymetamorphic crystalline basement (Altkristallin in the further text) which has partially a rare Permian and a Triassic cover. The SC main ridge stretches from St. Egyden / Penken in the W to Annabrücke (east of Mieger) in the E over 32 km, it is about 4 to 5 km wide in N-S direction, and reaches an elevation of 900m in the W and 800m in the E (Fig. 1; Krainer 2006).

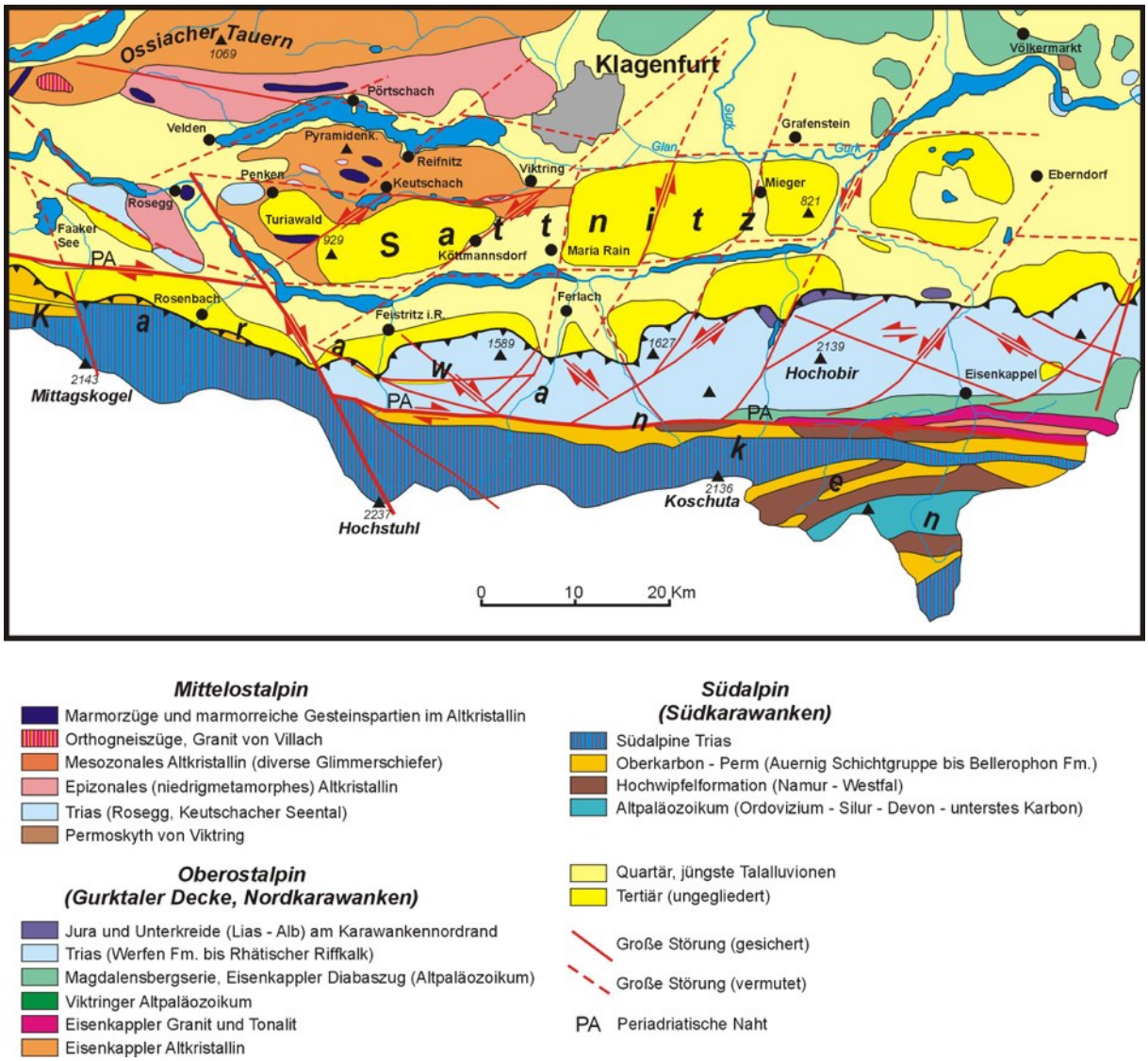

Figure 1: Geological overview map of the Klagenfurt Basin with the Karawanken chain in the S (simplified map from Krainer, 2006), which is based on geological maps from Kahler 1962 and Bauer 1981, 1985). Image courtesy of K. Krainer.

1 Previous Work

An early paper on the SC (Höfer, 1880) pointed out the widespread hollow carbonate- and dolomite-clasts dominating the clast composition by 80 to 90 percent, whereby the lighter colored carbonates are rounded, the darker are rather flat indicating bed load origin. The non-carbonate clasts are mainly silicified sandstones, quartz sandstones, schists, some quartzites, potential granulite and quartz-felsite. Höfer (1880) also pointed another peculiarity, that the clasts show notches at the contacts to each other, which could be classified now as pressure solution.

He describes the cement to be light-brown, including quartz grains, mica lamella and dolomitized carbonate in the matrix and in general to be an arkose arenite of low persistency. He found some beds with a high content of quartz boulders, which then reach cobble size of up to 0.2 m and contain remnants of granite and gneiss boulders. The matrix cements are rich in quartz.

He investigated the chemical composition of partly hollow boulders from the rim to the core and found that the carbonate and magnesia contents changed from the outside to the core, carbonate decreased from 64% to 56% and the magnesia content increased from 36% to 43% which implies that the solvent is acid-rich water and carbonate and magnesia were dissolved in a relation of 6.5 : 1 what caused an ongoing dolomitization over time due to the presence of water with dissolved CO_2.

Additional residuals of SC were located by (Dreger, 1909) about 8 km further E of Eberndorf. Dreger describes additional conglomerate spots in the Sattnitz area, which were formed in interglacial periods such as Pritschitz N of Wörthersee, a conglomerate quite similar to the Hollenburger Nagelfluh.

East of Carinthia, in southern Styria, Winkler-Hermaden (1914) found conglomerates deposited on coal-bearing sediments which developed under calm sedimentary conditions and indicate much stronger erosion, the Radel-, Remschnig-, Ehrenhausen, St. Egidi und Ehrenhausen conglomerates and those ‘Mediterranean’ conglomerates deposited in the lower part of the Styrian basin.

In his book about the area between the KW and the Wörthersee (Kahler, 1931) has made some interesting findings about the underlying formations of the SC, the Tertiary coal strata at Penken placed upon Tertiary potter's clay of marine origin, which must have been deposited latest in mid Miocene upon the old crystalline basement with some Triassic cover forming dolomite ridges. The Triassic strata are dominated by dolomite, the basement of which is a retrograded mica-schist containing marble lenses and layers. The Altkristallin basement is the same as the one underlying the Gurktal nappe in the N reaching up to the Alpine main ridge.

From Rosegg to Faaker See - there is no proof of Sattnitz Conglomerate. Worsch (1937) found that the ±170m thick Sattnitz Conglomerate at the Petelin could have been moved northwards by about 350 – 400m, and at the Tabor the SC is 120m high placed upon the red potter's clay, which is of the same type as the one at Penken.

The SC is the source of springs, which are drained by water tunnels. These are built at the boundary of the conglomerate to the fine-grained sediments underneath. These basal layers have been leached out by the fluids so that the cement was largely dissolved and the gravel has no more cohesion (Kahler, 1951).

The mammal fauna of the Penken coal field underlying the conglomerate was studied by Mottl (1955) who stated that due to the occurrence of the Mastodon longirostris-arvernensis the fauna of Penken indicates higher part of Lower-Pannonian to Upper-Pannonian (8 – 9.5 Ma).

Another coal-bearing layer under the SC was found in Stein in the Jaun-Valley situated 35km from Penken to the E (Weber and Weiss, 1983).

Griem et al. (1991) looked into the various component distributions in the western area of the SC, from Turiawald and the adjacent Tanzboden area to the E. The Tanzboden showed a higher carbonate content compared to Turiawald. At Wellersdorf, N of the Drau, these authors located an outskirt of Bärental Conglomerate (BC) and he named and they named it Wellersorf Conglomerate.

They assumed two braided rivers flowing into the sedimentation area as shown in Fig. 2, one from the W – Gailtal – and one from the NW – Drautal. They join at the

Petelin S of Villach. The drainage from the KW in the S created the KW gravel fans and conglomerates. The Triassic marble ridge stretching SE to NW, extending from the Drau Valley and going to Keutschacher See is not included but can be a candidate for a part of the enrichment of carbonate components at the lee side of the ridge – the Tanzboden area.

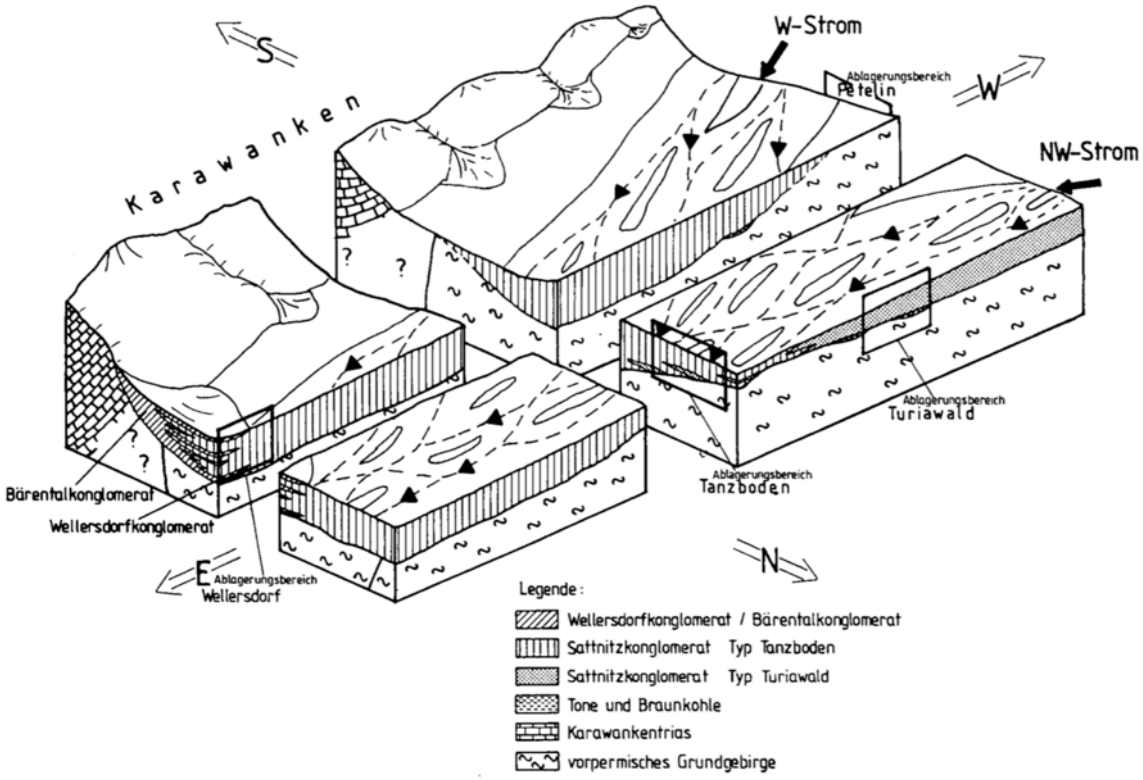

Figure 2: Model of the depositional environment of the Sattnitz Conglomerate (from Griem et al. 1991).

The tenor of the papers considers two mechanisms for the sediment accretion of the SC:

- The fluvial transport mechanism of the clasts, and
- the “upfolding” and uprise of the KW chain as the source of the matrix cement and of a part of the clasts.

Three Master Theses looked deeper into the hydrology of the SC and the discharge of water from the SC. Winkler (1997) investigated the hollow clasts in the SC in more detail. He found that the clasts and the surrounding micrite especially on top of the clasts were dissolved in parallel by water which is Ca-oversaturated and Mg-undersaturated. Staunig (2011) and Thalheim (2016) investigated the influence of the slope tectonics and the mass movements N of the SC on the hydrogeology of productive springs used for drinking water supply, the later put the conglomerate deposition into the Messinian.

2 Geological setting of the deposition and catchment area

2.1 Deposition and Orogenic Period

Based on available literature the time frame of the SC deposition is earliest at the Lower Pannonian (8 – 9,5 Ma) based on the mammal fauna of the Penken coal field dated by Mottl (1955) and latest until the early cool ages in Late Pliocene and/or early Ice Ages in Early Pleistocene (≤3 Ma) (Kuhlemann et al., 2002). At this time debris overlaying the conglomerate and gravel from gravel fans were removed.

The climatic situation before this period was warm, temperate and humid in Sarmatian (Lower Serravallian) with deciduous summer-green woodland (Kahler, 1955; van Husen, 1984) resulting in the coal deposits of the Penken coal field. During the Pannonian (Tortonian), humidity decreased, the climate became warm temperate. In the Pontian (Messinian) time, evergreen elements became scarce in the vegetation, which changed with the Dacian (Zanclean) showing again an increase in humidity (Kováč et al., 2006).

2.2 The Depositional Area

The depositional area is the KB, it stretches W – E from Villach to Bleiburg and the central-eastern Southern Alps, it ranges to the S until the KW thrust adjacent to the eastern Periadriatic fault (PAF) and to the N to Ossiacher Tauern and the

Magdalensberg. The first uplift of KW is dated as Late Sarmatian (± 12 Ma) (van Husen, 1984).

Towards the N the Altkristallin basement is overlain by the anchi- to epimetamorphic Gurktal nappe. To the W the Klagenfurt Basin stretches from ca. the combined Hochstuhl/Möll Valley fault crossing Villach to the E, where the Lavant Valley delimits the KB from the Koralpe. Fig. 3 shows a general map of the KB with the main faults and valleys with the three inflows and the outflow in the Messinian.

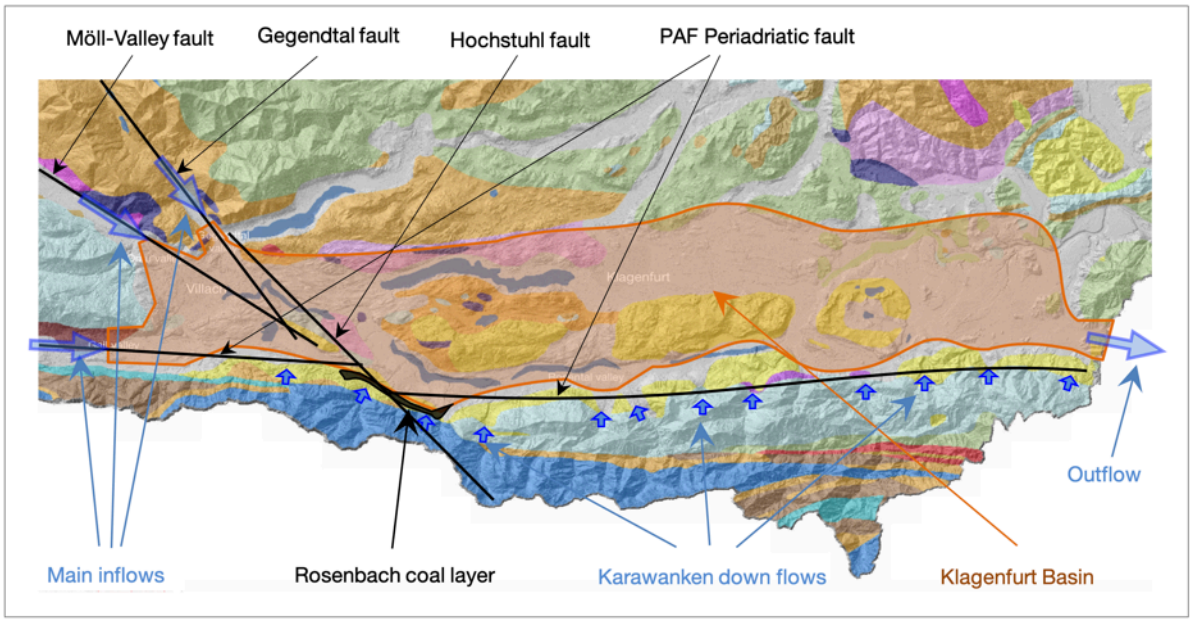

Figure 3: The Klagenfurt Basin with the main faults, the 3 main inflows from W and the slope down flows from the KW and the outflow during Messinian time. (Base map KAGIS: https://gis.ktn.gv.at/atlas/(S(uzdhqnobfu3zrascnrqoz0ds))/init.aspx?karte=atlas_basiskarten&ks=kaernten_atlas).

2.3 The Basement

The underground of the KB is the Altkristallin basement belonging to the Austro-Alpine unit (Steininger et al., 1989). The tectonics of the basin is dominated by dextral transpressive shearing against the north pushing and uplifting KW. Especially in the eastern part causing a bending and N dipping of the basin's basement and creating a flower structure of the KW along the Periadriatic fault (Nemes et al., 1997). In the western part, compressional shear dominates with more elevated old crystalline

basement as a buffer stop for the north pushing KW thus creating a multiple folded structure and a syncline directly north of the KW sustaining into the mountains S of the Wörthersee which are all steeply sloped imbricated old crystalline structures like the Pyramidenkogel, Friedelhöhe and Schrottkogel (Kahler, 1931).

On the Altkristallin, imbricates of Permian-Triassic strata are placed on top of this basement, which are even protruding through the SC to its surface at the border of Turiawald and Tanzboden. To the North the Gurktal nappe, which is mainly composed of a Paleozoic basement and is thrusted over the Altkristallin basement.

In the East the basin is quite deep, the base of the Sattnitz Conglomerate at Vellach Müllnernbrücke where a well was drilled did not reach the basement in 377 m below sea level (Nemes et al., 1997), the KW are thrusted over the sedimentary basin. More to the West the Drau River flows over bedrock at Rosegg at 475 m above sea level (a.s.l.) (Claasen et al., 1987) creating a pure compressional structure between the KW and the crystalline basement between Rosegg in the West and Ferlach to the East. In the far West at Villach with the bedrock seismically located at 400 m below sea level (Arndt and Bäk, 2005), the basin becomes flexural again and the KW form a flower structure protruding N over the sediments exposed in the surroundings of Faaker See.

The Altkristallin situated under the western SC shows already a mountainous structure. In the region N of Klagenfurt, the northern part of the SC rests on a base at Opferholz and Stifterkogel with altitudes of 700m a.s.l., in whereas in the N of the SC at Hollenburg the base is at 450 m a.s.l. (Arnold, 2012).

Looking at the basement altitude under the SC from N to S, the basement is prominent in the N at 600 – 700m whereas in the S adjacent to the Drau River it reaches 430 m a.s.l. Consequently the SC thickness increases from N to S.

2.4 The Catchment Area

There are three main faults corresponding to three valley systems joining at Villach and reaching out further, these are the PAF, the Mölltal- and the Gegental – Hochstuhl strike-slip faults.

These three valleys joining at Villach deliver inflow from the W by the Gail river, from WNW the by the Drau river and from NW out of the Gegendtal valley. Villach is the junction and the bottleneck of the rivers into the Klagenfurt Basin (Fig. 4).

The Gail River follows the Periadriatic Fault (PAF) – N of the Carnic Mountains, the watershed is in Kartitsch 100 km west of Villach in distance. The catchment of the Drau River is the SE area of the Tauern Window fed by two billabongs, the Lieser from the Tauern Window eastern domes and the Möll from its southern slopes. The Gegendtal catchment drains the Nock Mountains. Consequently, these three catchments represent longitudinal valleys, which drained into the KB.

Figure 4: The three longitudinal catchments of the KB joining at Villach.

To the S, the KW Mountains with elevations ranging from 1.500 to 2.000 m a.s.l. provide a rectangular catchment area stretching E - W, in the N the catchment are the Nock Mountains and the Noric area in the same range of altitude with rather small brooks flowing into the Klagenfurt Basin.

It is assumed that the outflow from the Klagenfurt Basin at the time of the Sattnitz Conglomerate's deposition was close to Bleiburg via the Velenje fault which is

10 km W of the recent outflow via Lavamünd. This change was most likely due to the about 500 m uplift of the Koralpe – Pohorje region, which started 6 – 5 Ma (Legrain et al., 2014)

3 Properties of the Sattnitz Conglomerate

3.1 Topology

The plateau-shaped mountain ridge is delimited by subvertical rock faces towards the Rosental Valley to the S and to the N towards the KB from Klagenfurt E to Greifenburg. A cross-section at Penken S of Schiefling is shown in Fig. 5 where the SC overlays a coalbed which is found only in the western section of it (Krainer, 2006).

The SC is delimited from the BC situated S by the Rosental valley and its elongation valley to the W to Faaker See and to the E from Annabrücke along the Vellach Valley via Bleiburg to the Mieß (Meze) Valley in Slovenia.

The BC fills the KW valleys and fanglomerates out of these valleys reach into the Rosental in several layers interleaving with the SC par exemple at Wellersdorf (Griem et al., 1991).

The Seental is situated N of the SC mountain ridge between Schiefling and Keutschach, where large slope areas in the S are covered by rockslide material of Turiawald and Tanzboden. To the N and in between the Seental and the Wörthersee there is an old crystalline mountain chain with Pyramidenkogel, Rauth, Friedelhöhe and Schrottkogel without any Sattnitz Conglomerate on top of it. There was never found any Sattnitz Conglomerate N of the Seental (Kahler 1931).

3.2 The Sattnitz Conglomerate

The SC is a poorly sorted conglomerate with sub-rounded cobbles and rounded pebbles. The clast diversity is dominated by carbonate/dolomite followed by crystalline phyllosilicates, vein quartz and arenite (Griem et al., 1991). The main components of the arenite matrix are quartz, phyllosilicates and carbonate cement (Griem et al., 1991).

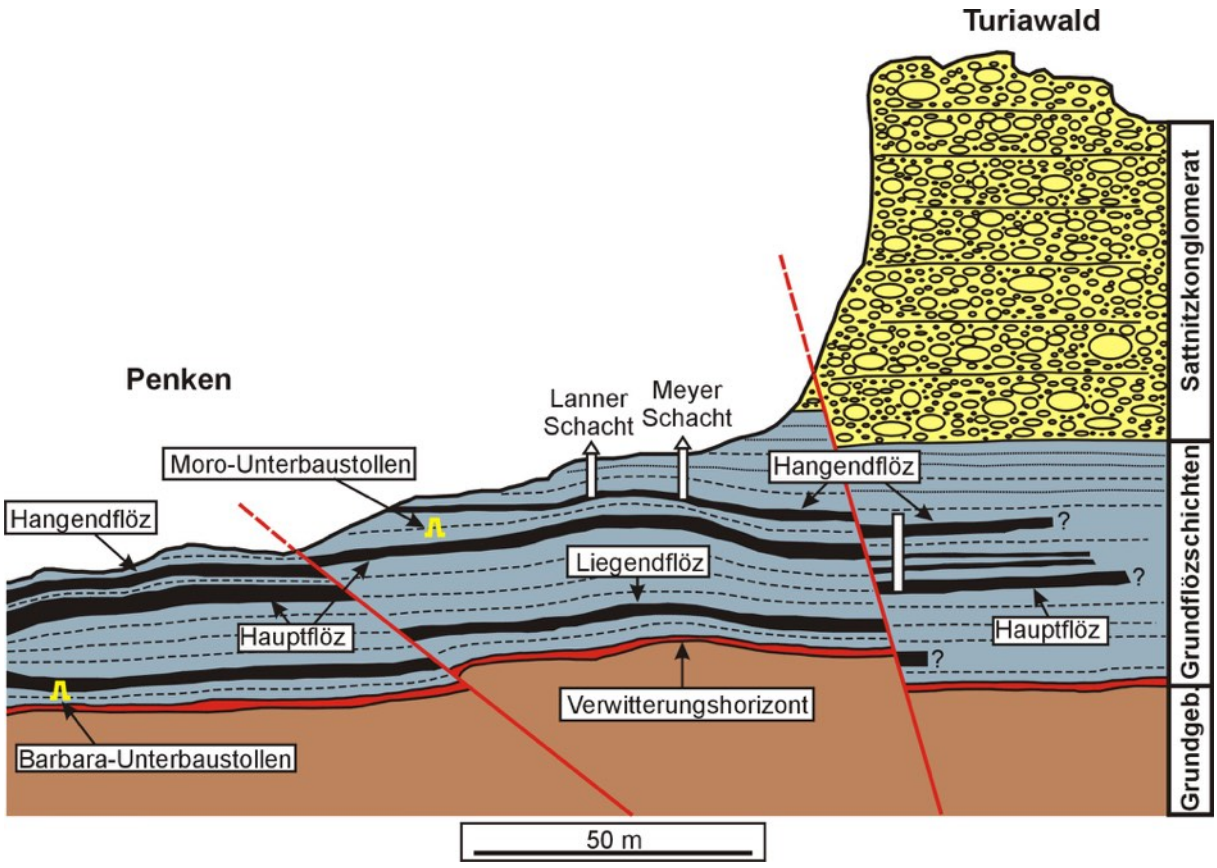

Figure 5: N-S cross section through the SC at Penken with the formerly mined coal seams (Krainer, 2006). Figure courtesy of K. Krainer.

There are cobbles with sizes up to 250 mm, thickly to very thickly bedded and at some places alternating with thin yellowish sandstone layers. The carbonate clasts are limestone and dolomite (Winkler, 1997).

Interstitial material is an ocher yellow arenite with non-uniform lime cement - sparitic and micritic with some embedded mica precipitated in a meteoric vadose environment (Winkler, 1997).

There are two conglomerate bodies in the KB, the BC on the northern calcareous slopes of the KW chain and SC on an old crystalline basement ridge bulged up in front of the PAF. Both are considered to represent Messinian freshwater sediments without any stratigraphic differentiation from bottom to top, thus the conglomerate formation must have been in “one go”.

In some areas, both conglomerates are placed on coal bearing horizons, the SC is placed on a base coal layer (Grundflöz), the BC is placed on a two layers, the Rosenbacher coal layers over the basal coal layer (Fig. 6) (Krainer, 2006).

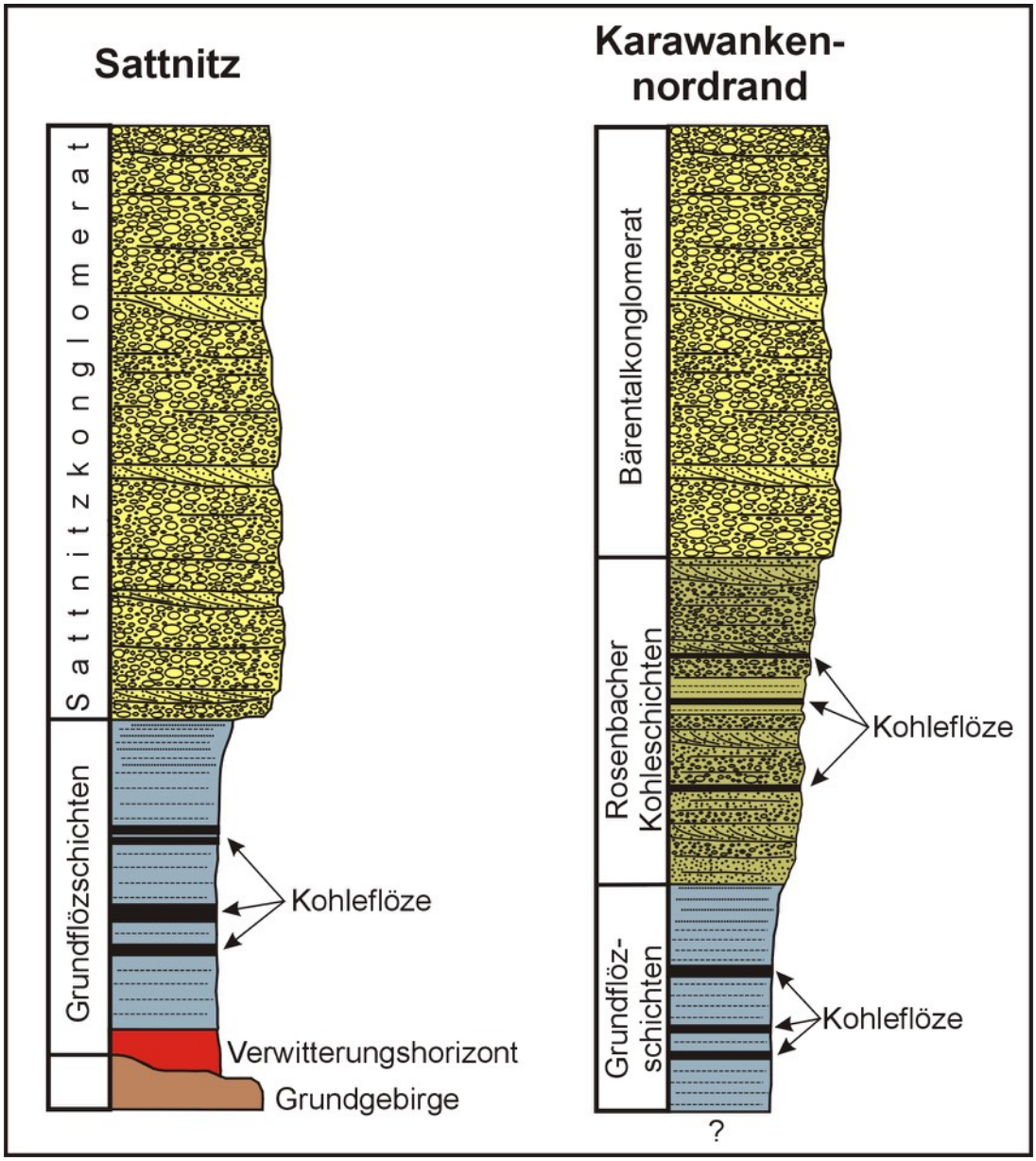

Figure 6: Schematic cross section through the SC and BC. Both conglomerates are placed on some places on coal seams, at some places the Rosenbacher Coal Seams from the basement of the BC (Krainer, 2006)*. Image courtesy of K. Krainer.*

3.3 Conglomerate structure

The outcrops show no visible variation over the entire SC, only fresh outcrops can be investigated as the older outcrops are covered by limestone agglomeration from limestone dissolved by weathering. Only the interglacial conglomerates depicted at the rear show a significant difference. Figures 7 – 10 show various outcrops.

Figure 7: SC at Bleiberg close to Villach *SC at Hojoutz S of Schiefling.*

Figure 8: SC at Dobein S of Keutschachersee at Rekagraben.

Figure 9: SC at Saager close to Annabrücke at Stein in Jauntal - Kirchberg.

3.3.1 Interglacial conglomerate outcrops

Interglacial conglomerates named “Nagelfluh” were available in the vicinity of the two main cities, Klagenfurt and Villach. The Hollenburg- and Köttmannsdorf-Nagelfluh (Fig. 10) situated straight S of the Klagenfurt and the Vinza Nagelfluh S of Villach at Faaker See.

Figure 10: Abandoned quarry NW of Hollenburg. *Quarry at Köttmannsdorf.*

4 Provenance analysis

To analyze the origin of clastics, several methods might be applied: (1) counting of gravels, particularly of unique clasts, which allow a direct link to the source, (2) quantitative analysis framework constituents of sandstones, (3) determination of the age of detrital mineral grains like zircons by the U-Pb method, white mica by the Ar-Ar method, or of apatite or zircon by fission track and (U-Th-Sm)/He methods.

In this study, we use a combined approach, namely counting of gravels, qualitative determination of framework constituents of sandstones combined with age dating of detrital white mica from the same samples. For sample locations and studied exposures, see Fig. 11.

Figure 11: Map of the SC from Faaker See in the W until Stein im Rosental in the E. Yellow pins indicate the sample locations for the mica age dating, red pins those of clast composition and gravel samples.

4.1 Provenance analysis of clasts in conglomerates

On several well-exposed fresh exposures of the Sattnitz Conglomerate, a provenance analysis of clasts with a diameter larger than 1 cm was performed.

All the clasts were well rounded indicating significant length of transport. In all cases, the composition is polymictic and includes a wide variety of rock types (Table 1, Fig. 12).

Sattnitz Conglomerate	share				count			
	Saager	**Hemma Felsen**	**Reka Graben 1**	**Reka Graben 2**	**Saager**	**Hemma-felsen**	**Reka-graben**	**Reka-graben 2**
a.s.l.	440 m	570 m	610 m	610 m	440 m	570 m	610 m	610 m
Micritic limestone, grey	13 %	17 %	25 %	13 %	12	17	22	8
Micritic/sparitic limestone, dark-grey/black	7 %	5 %	15 %	7 %	6	5	13	4
Micritic limestone, brownish	19 %	7 %		5 %	17	7		3
Micritic limestone, green								
Micritic limestone, red	2 %				2			
Sparitic limestone, light-brownish, fossil-bearing			5 %	3 %			4	2
Yellow dolomite	14 %			8 %	13			5
Yellowish cellular limestone	3 %	3 %		2 %	3	3		1
Yellowish marl	3 %	5 %	1 %		3	5	1	
Total carbonates	**62 %**	**38 %**	**46 %**	**38 %**	**56**	**37**	**40**	**23**
Conglomerate				5 %				3
Red quartz Sandstone/ subarkose (Gröden Sandstone			6 %	3 %			5	2
Light to grey quartz-sandstone		2 %		15 %		2		9
Carbonate (hybrid) sandstone	4 %				4			
Yellowish carbonate sandstone		7 %	1 %	2 %		7	1	1
Red carbonate sandstone								
Green sandstone		1 %		2 %		1		1
Red porphyroid	1 %			2 %	1			1
Total sandstone/conglomerate (and volcanics)	**6 %**	**10 %**	**7 %**	**28 %**	**5**	**10**	**6**	**17**
Vein quartz	26 %	16 %	14 %	28 %	24	16	12	17
Quartz-siderite vein			2 %				2	
Quartzitic micaschist	1 %	3 %	8 %		1	3	7	
Sericite quartzite	3 %				3			
Carbonate-phyllite	1 %		1 %		1		1	
Garnet-hornblende gneiss				2 %				1
Greenschist			2 %				2	
Carbonatic greenschist		4 %				4		
Orthogneiss	1 %		1 %		1		1	
Dolomite marble				2 %				1
Dark marble			1 %	2 %			1	1
Light-grey marble			17 %	2 %			15	1
White marble		29 %				28		
Total metamorphic clasts	**33 %**	**52 %**	**47 %**	**34 %**	**30**	**51**	**41**	**21**
Total clasts					91	98	87	61

Table 1: Composition of rock types at the counting locations

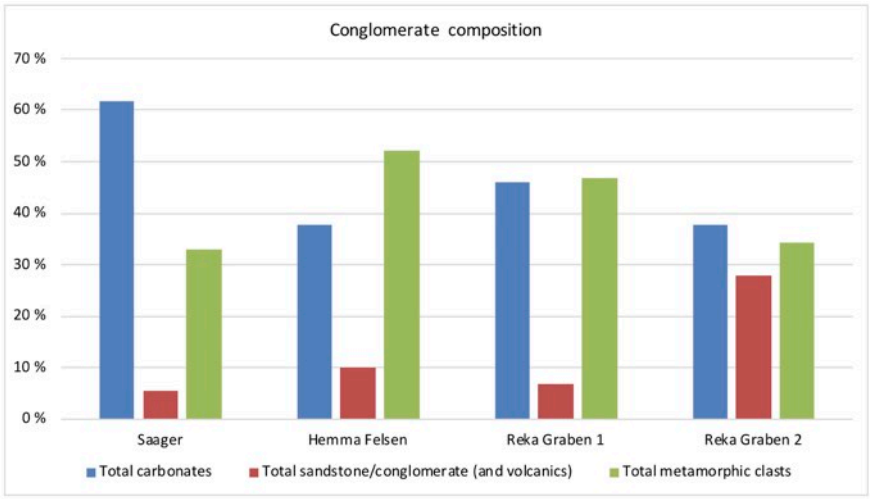

Figure 12: Composition of rock types pointing out the high carbonate yield at Saager situated close to the Drau river and Karawanken.

However, these rock types can be assigned to three major groups and some typical clasts from one exposure (Rekagraben 2) are shown in Fig. 13 as some of these have a typical source in limited areas:

(1) Unmetamorphic limestone, dolomites and marls. These are dominated by micritic, subordinate sparitic limestones of various colors ranging from grey (13 – 25 percent), via brownish to dark-grey/black to rare ones of red color. Light-brownish fossil-rich sparitic limestones are rare. Dolomites, dominantly of yellow color, are subordinate as well as yellowish cellular limestones (rauhwacke in the local literature) and marls.

(2) Various types of sandstones can also be distinguished by color (light-colored yellowish, red and green) and matrix, either a quartzose or calcitic one. Furthermore, rare acidic volcanic fragment (red porphyroid, Fig. 13) was found, too. The red sandstone is unique and represents the Permian Gröden sandstone of Drauzug and Southern Alps.

(3) The third group is represented by metamorphic clasts. These include dominant vein quartz (14 – 26 percent), rare siderite-quartz vein clasts, then quartzitic micaschist, sericite-phyllite, various types of greenschist, orthogneiss (from the Central Gneiss type of the Penninic Tauern window) and various types of marbles (dark-grey, light-grey and white in color). Among these, yellowish deformed dolomite marble clasts are common in the Tauern window.

Figure 13: Typical specific clasts of conglomerates.

4.2 Framework constituents of sandstones

The investigated sandstone samples are similar in composition of clasts and matrix and show a high amount of subangular framework clasts in a sparitic carbonate matrix. Interestingly and unexpected, siliciclastic clasts occur in similar amounts to carbonate clasts. The sandstones can be classified as hybrid arenites. A detailed description can be found in the chapter sandstone diagenesis.

Qualitatively, the following sand-sized components can be identified and these are here grouped into several populations:

(1) Monocrystalline siliciclastic grains, which include quartz, white mica, K-feldspar, which is often microcline, biotite and chlorite. Biotite is often partially degraded into hydro-biotite, respectively chloritized. White mica contains sometimes cleavage-parallel exsolutions of ore minerals. In a single case, resorption of quartz is observed arguing for a phenocryst from an acidic volcanic rock. Together, these monocrystalline, relatively large grains indicate that all these derived from plutonic, rare volcanic or metamorphic rocks, in the case indicating higher greenschist and/or amphibolite facies.

(2) Unmetamorphic siliciclastic rock fragments include mudstone, siltstone and polycrystalline quartz fragments likely derived from chert, then siltstone, fine-grained sandstone. Few grains of altered mafic volcanic rocks were detected, too, which are composed of microcrystalline feldspar and ore minerals in a matrix of chlorite.

(3) Very low-grade and low-grade metamorphic rocks include abundant polycrystalline metamorphic quartz, various types of chlorite schist respectively greenschist, slate, phyllite (sericite-phyllite), chlorite-phyllite, biotite-phyllite, and rare marble. Most of these fragments have in common that they are affected by late metamorphic, and less common, semi-brittle deformation postdating peak of low-grade metamorphism. These latter semi-brittle deformed clasts are uncommon and potentially record the preferred erosion of fault zones.

(4) Unmetamorphic carbonate rocks include sparitic and micritic limestone, sparitic and micritic dolomite (including peloid-bearing dolomite, cherty micritic limestone, and fine-grained hybrid carbonate-sandstone.

(5) Monocrystalline accessories also occur and include garnet, epidote and clinozoisite, rutile, sphene, zircon and opaque minerals.

4.3 Ar-Ar dating of detrital white mica

From three samples, detrital white mica of the grain size fraction 0.25 to 0.35 mm was separated by standard methods. Sample EM-1 is the lowest position and sample EM-4 the highest position within the Sattnitz Conglomerate (see Fig. 12, Table 1). The strategy was to reveal a potential change in the source region through time.

The Ar-Ar age determination were determined at the ARGONAUT Laboratory of the Geology Division of the University of Salzburg. The analytical procedure follows that

described in Kargaranbafghi et al. (2015) and Rieser et al. (2006). Some remarks on the methodology of Ar-Ar white mica dating can be found in Neubauer et al. (2007).

Total fusion experiments were carried out on together 56 grains of all three samples. The results are reported in Table 2. From these 56 grains, 52 grains gave a very small analytical error, whereas one grain of the intermediate sample EM-2 and three of the highest sample EM-4 show an ample error. As these grains had the same grain size, the low yield of radiogenic ^{40}Ar can be related to low potassium contents. The most likely explanation is that these four grains were paragonitic – Natron-Glimmer - white mica, and potentially an increase of the content of paragonitic white mica grains towards the top is likely.

EM-1		EM-2		EM-4	
age [Ma]	± [Ma] 1-σ abs.	age [Ma]	± [Ma] 1-σ abs.	age [Ma]	± [Ma] 1-σ abs.
82,9	2,8	228,5	1,6	94,1	5,4
83,9	3,0	79,8	1,1	84,1	2,9
328,8	1,1	87,2	2,2	301,0	18,9
31,9	1,6	92,5	1,8	59,1	17,4
323,0	1,5	41,3	2,3	85,6	1,7
326,3	1,7	252,4	2,0	57,8	2,9
202,3	1,5	79,4	2,9	28,3	3,3
322,0	2,6	86,0	1,2	69,5	3,6
233,0	1,2	122,6	1,8	36,2	4,2
89,9	3,8	313,2	1,6	235,6	5,2
87,1	2,5	98,8	2,2	103,2	5,4
321,4	2,4	299,6	16,1	114,4	5,2
301,7	2,5	85,2	2,1	98,8	2,6
159,1	1,5	81,6	1,6	86,4	13,2
86,2	3,4	324,2	1,5	89,1	3,9
247,6	1,8	319,1	2,0	80,8	4,4
341,9	5,1	317,5	1,3	44,9	1,6
86,5	2,1	221,6	3,2		
86,7	2,6	321,4	1,7		
		34,2	1,7		

Table 2: Results of total fusion experiments of single grain 40Ar/39Ar dating. Shaded ages likely result from paragonitic white mica.

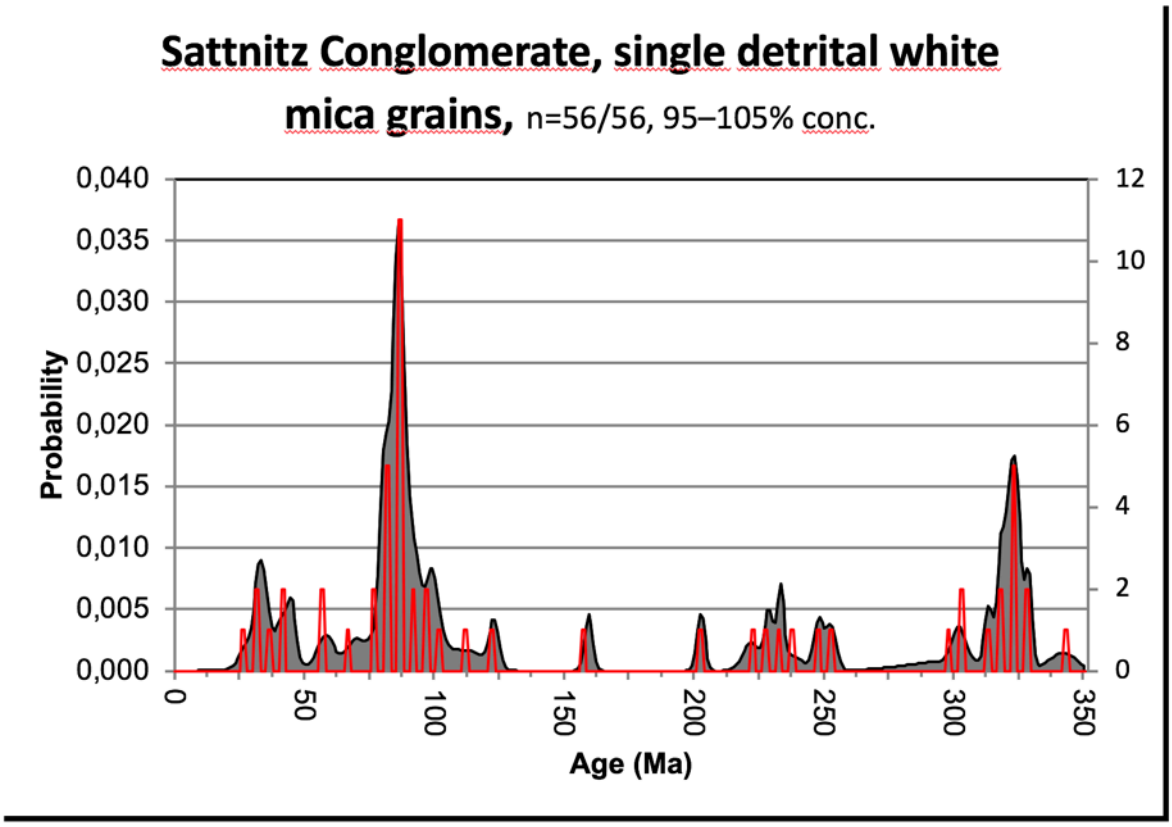

Figure 14: Ar/Ar age variation of detrital white mica.

The ages range between 28.3 ± 3.3. Ma to 341.9 ± 5.1 Ma (Fig. 14). Within the resulting ages, several populations can be distinguished from old to young. These include Variscan ages between 300 and 341 Ma typical for the Austroalpine basement ("Altkristallin") located south of the SAM line (Southern Limit of Alpine Metamorphism: Hoinkes et al., 1999), ages between 79 and 122 Ma also typical for the Austroalpine basement fully affected by the Early Alpine metamorphism typical for Austroalpine basement, too but located north of the SAM (Southern limit of Alpine Metamorphism) line (Fig. 15), and (3) ages between 28 and 50 Ma exclusively known within the Penninic units of the Tauern window ("Tauern Crystallization"). Subordinate single ages or small groups are an age of 159.1 ± 1.5 Ma in the lowermost sample EM-1, some ages between 202 and 252 Ma in the two deeper samples, and ages between 58 and 70 Ma in the uppermost sample.

These age populations allow a clear assignment to distinct well-known sources as well as a change of the erosion level through time (Fig. 15).

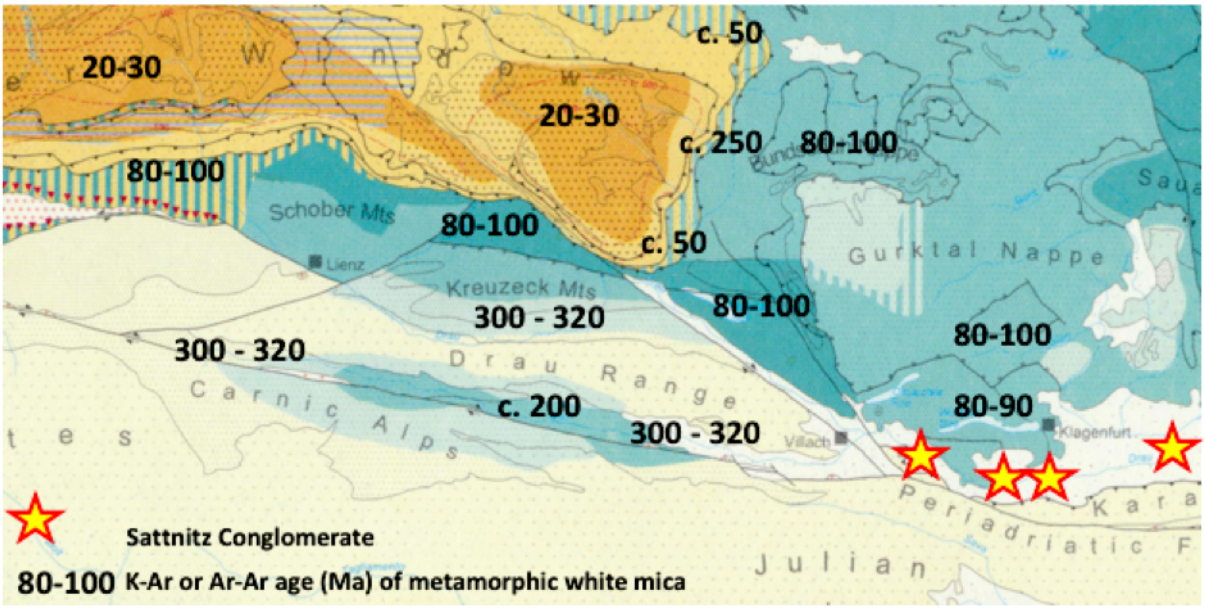

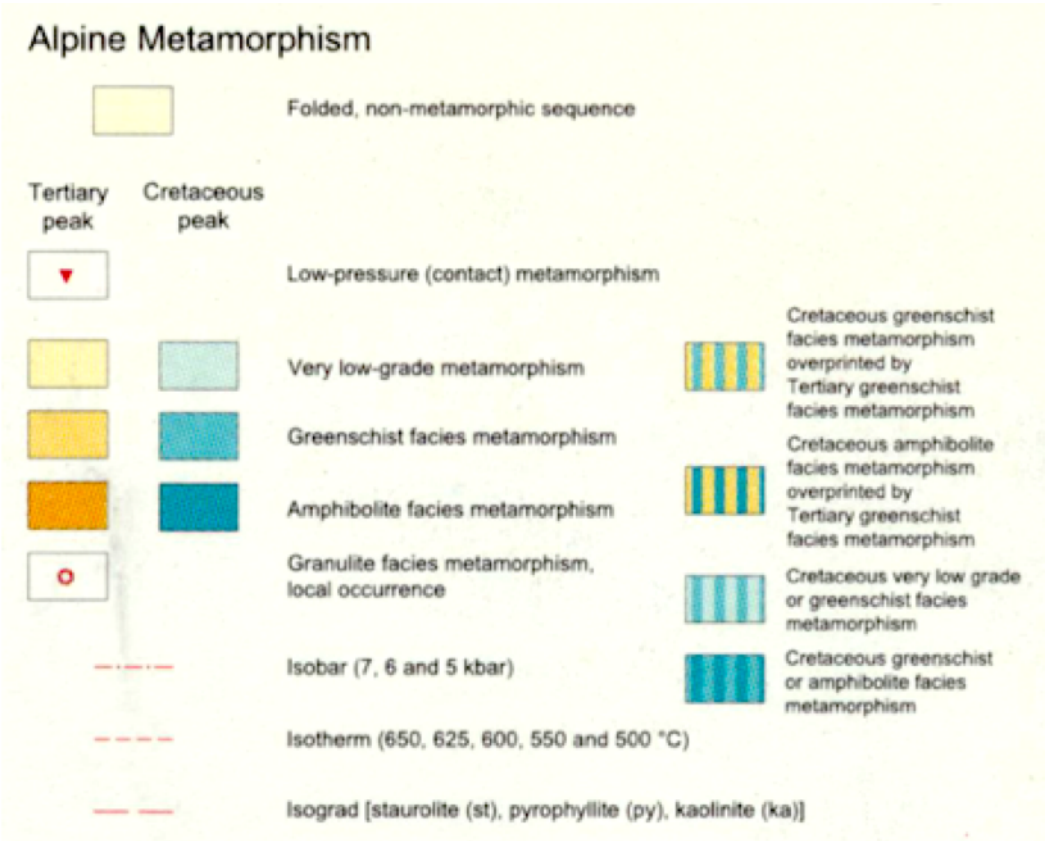

Figure 15: Age and degree of Alpine metamorphism with white mica K-Ar and Ar-Ar ages for explaining the origin of detrital white mica. Based on Frey et al., 1999 (Metamorphic maps of the Alps). Age data in the basement are compiled in (Frank et al., 1987; Liu et al., 2001; Thöni, 2006 *and references therein).*

The sources of the three major age populations is outlined above. Ages of the subordinate age group of about 202 Ma are representative for the Gailtal basement (Schuster et al., 2001) whereas ages of ca. 240 and 250 Ma are typical for the higher part Lower Austroalpine rim of the Tauern window (Liu et al., 2001). The age group of 58 and 70 Ma are known from the deeper part of the Lower Austroalpine rim of the Tauern window, too (Liu et al., 2001). Consequently, the age populations can be deduced from well constrained sources, which indicate longitudinal drainage from mainly the Drau Valley but also from sources located in the northwest and subordinately from the Gail Valley. Not good constraints are from the “Altkristallin” basement complexes exposed along the Periadriatic fault in the south.

In respect to the temporal evolution, several constraints can be deduced.

(1) Already the lowermost sample contains a single age of 32 Ma, which argues that the Penninic rocks of the Tauern window were already exposed. As the age of erosional unroofing of Penninic rocks is constrained of Pannonian stage, at ca. 8 Ma (Spiegel et al., 2001), this gives a similar Pannonian age constraint as mammalia fossils (Mottl, 1955).

(2) The increasing amount of “Tauern window ages” towards the uppermost sample indicates the importance of the Drau Valley catchment by draining the Tauern window area.

5 Diagenesis

The investigated sandstone and conglomerate samples are well cemented by carbonate cement and the porosity is low. In a few cases, open vugs were observed, which are decorated by sparry crystals growing into the cavity. Between larger clasts, two types of carbonatic (mostly calcite) cement can be observed (Fig. 16a, b): An earlier generation is growing from clast carbonate crystals (cement A), whereas another type is represented by fine-grained inclusion-rich cement A. The remaining cavity is filled up by sparry/blocky cement B with grain sizes ranging from 0.1 to maximum ca. 1 mm. cement A and B grains show some deformation fabrics including grain boundary migration and twinning (Fig. 16 c, d).

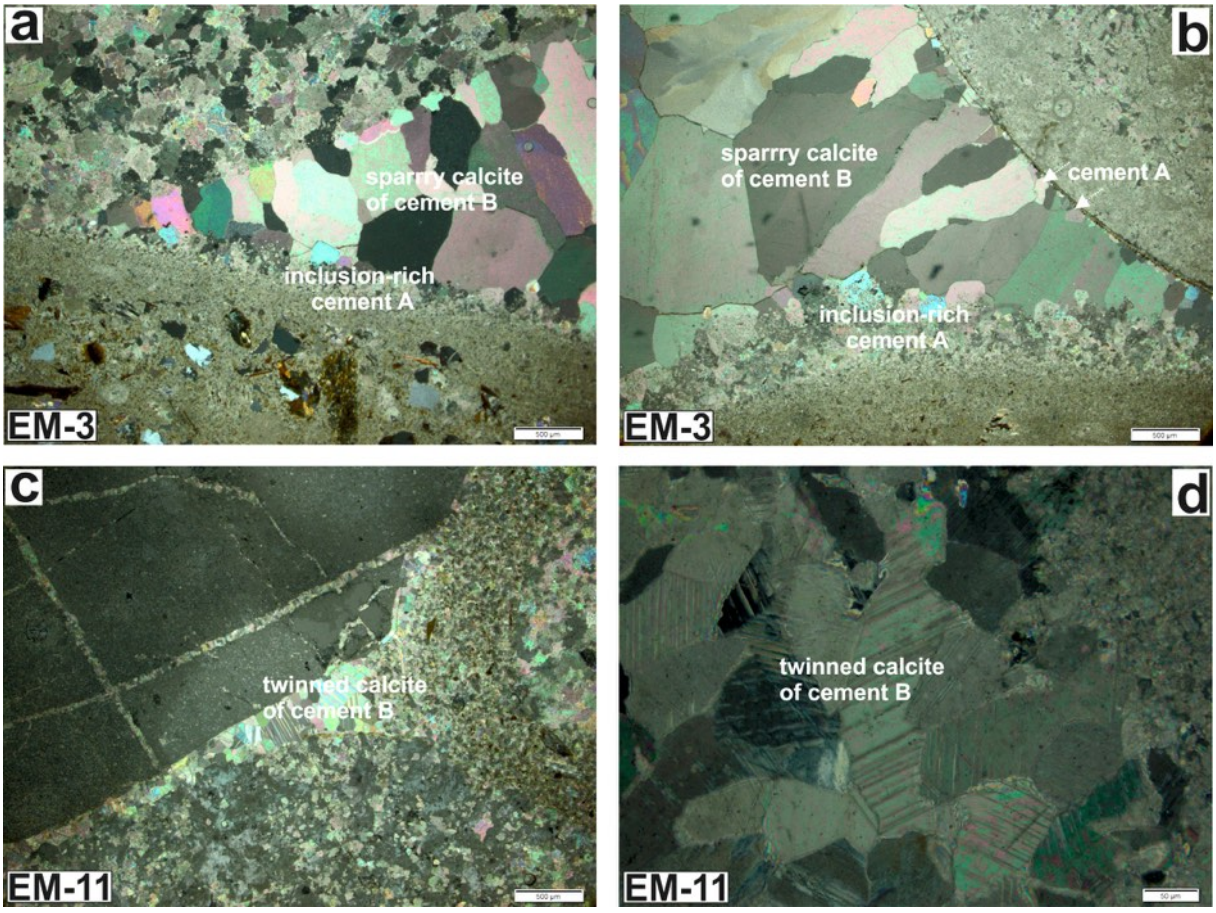

Figure 16: Diagenesis of sandstones and conglomerates. (a) and (b) Two cement generations in conglomerate. Note sutured grain boundaries in (b) indicating grain boundary migration. (c) Twinned calcite forming cement B along margins of a clast. (d) Twinned calcite.

The chemical analysis of the cement composition was analyzed by the Scanning Electron Microscope JEOL-8530F at the University Graz in microprobe mode and the elements were determined by the characteristic X-rays (EDX). Single element maps were generated out of which “Compo” maps combining the major elements showing the phase distribution.

For orientation, single points were selected, and the element spectra were scanned (Fig. 17). Then at of each of the 3 samples an interesting area was selected and then the element-maps were scanned, and the compo-maps were optimized to map the mineral/element compositions (Figs. 18, 19, 20).

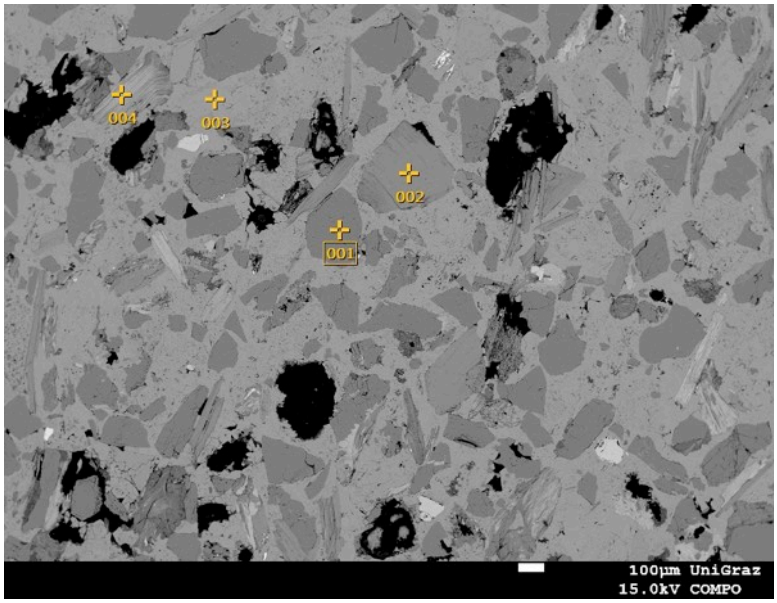

Volt : 15.00 kV

Mag. : x 40

Date : 2018/11/05

Pixel : 1280 x 960

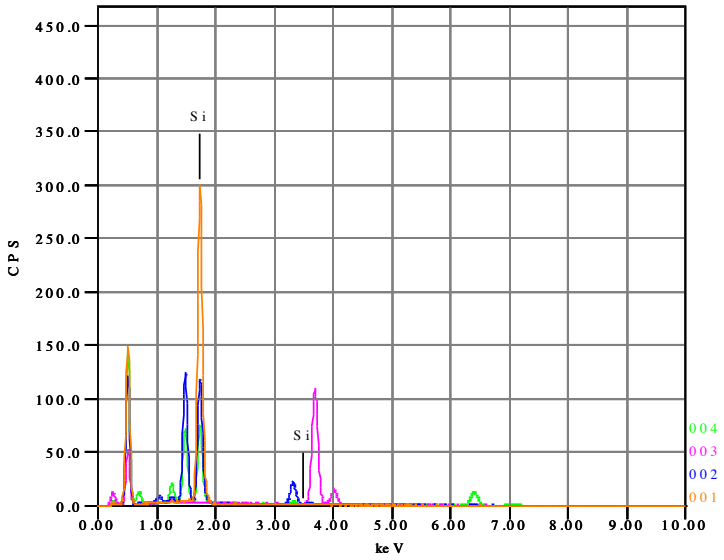

Acquisition Condition

Instrument : 8530F

Volt : 15.00 kV

Current : ---

Process Time : T2

Live time : 30.00 sec.

Real Time : 48.23 sec.

DeadTime : 38.00 %

Count Rate : 3294.00 CPS

	CaO	Na2O	MgO	Al2O3	SiO2	K2O	TiO2	FeO
001					100.00			
002		1.55	1.35	36.38	49.82	10.02	0.87	
003	100.00							
004			6.35	26.57	36.36	1.29		29.43
Average	100.00	1.55	3.85	31.48	62.06	5.66	0.87	29.43
Deviation	0.00	0.00	3.54	6.94	33.54	6.17	0.00	0.00

Figure 17: Sample EM-13 - single point analysis.

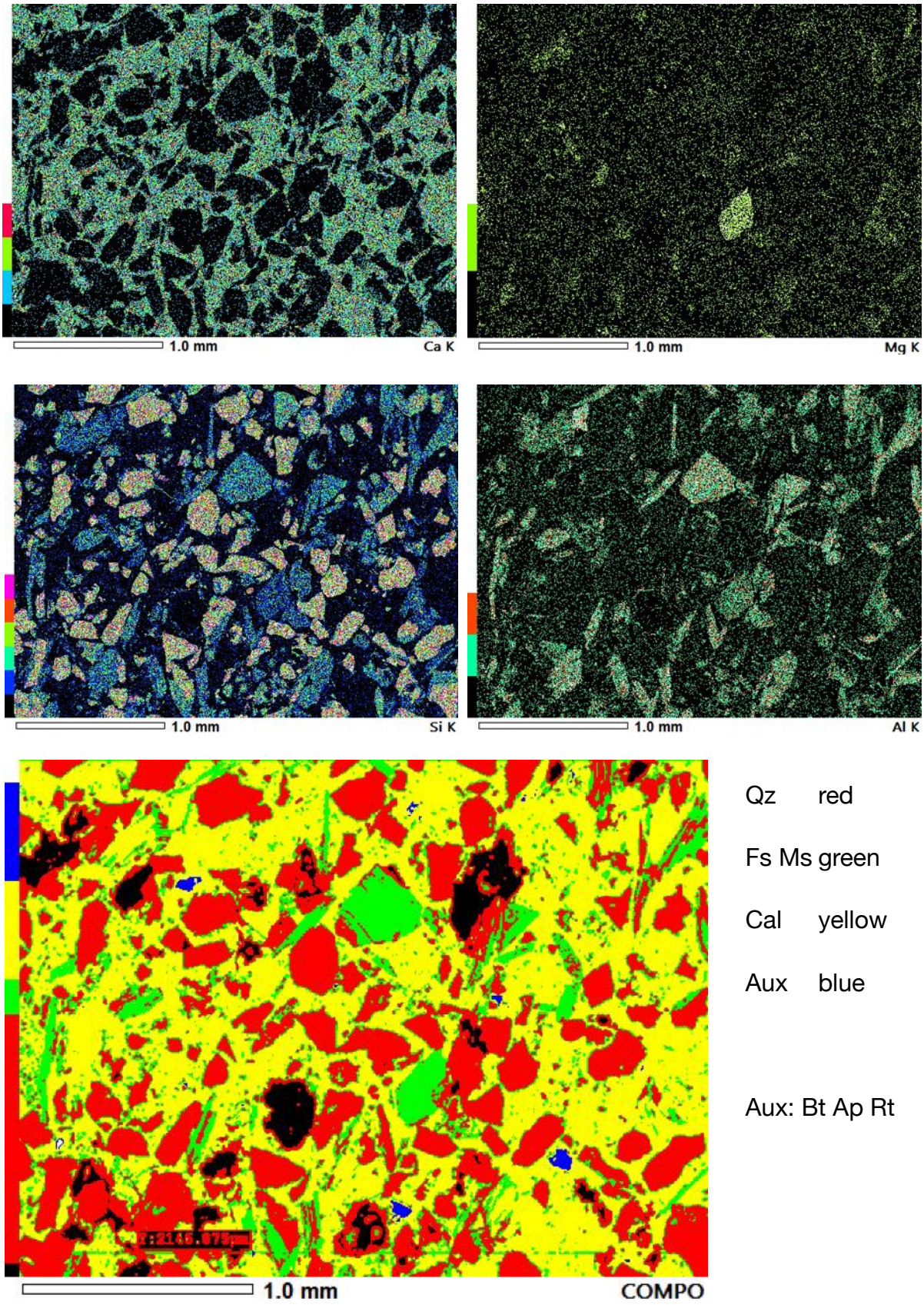

Figure 18: Sample EM-13 element- and compo- maps

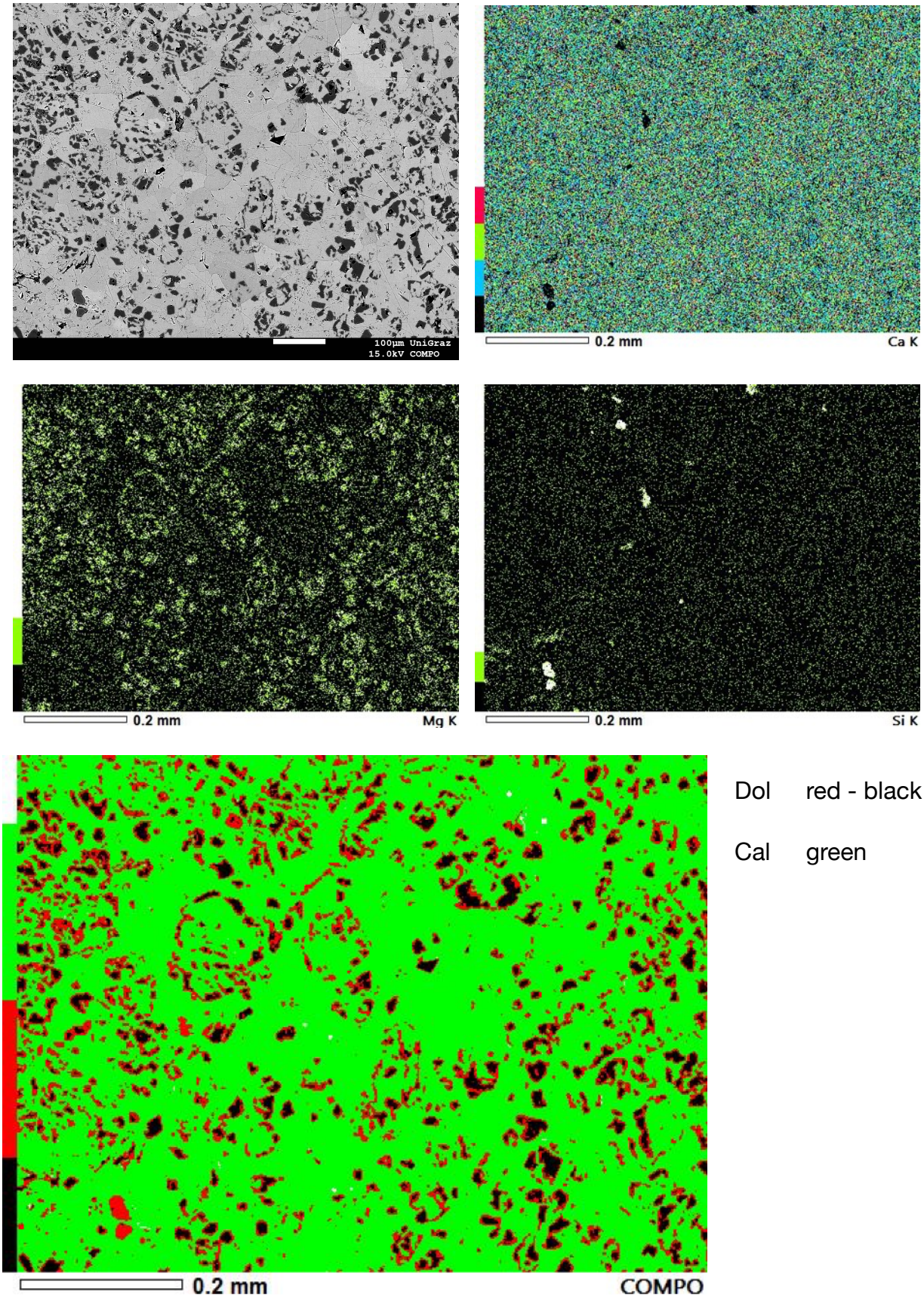

Figure 19: Sample EM-11 element- and compo-maps

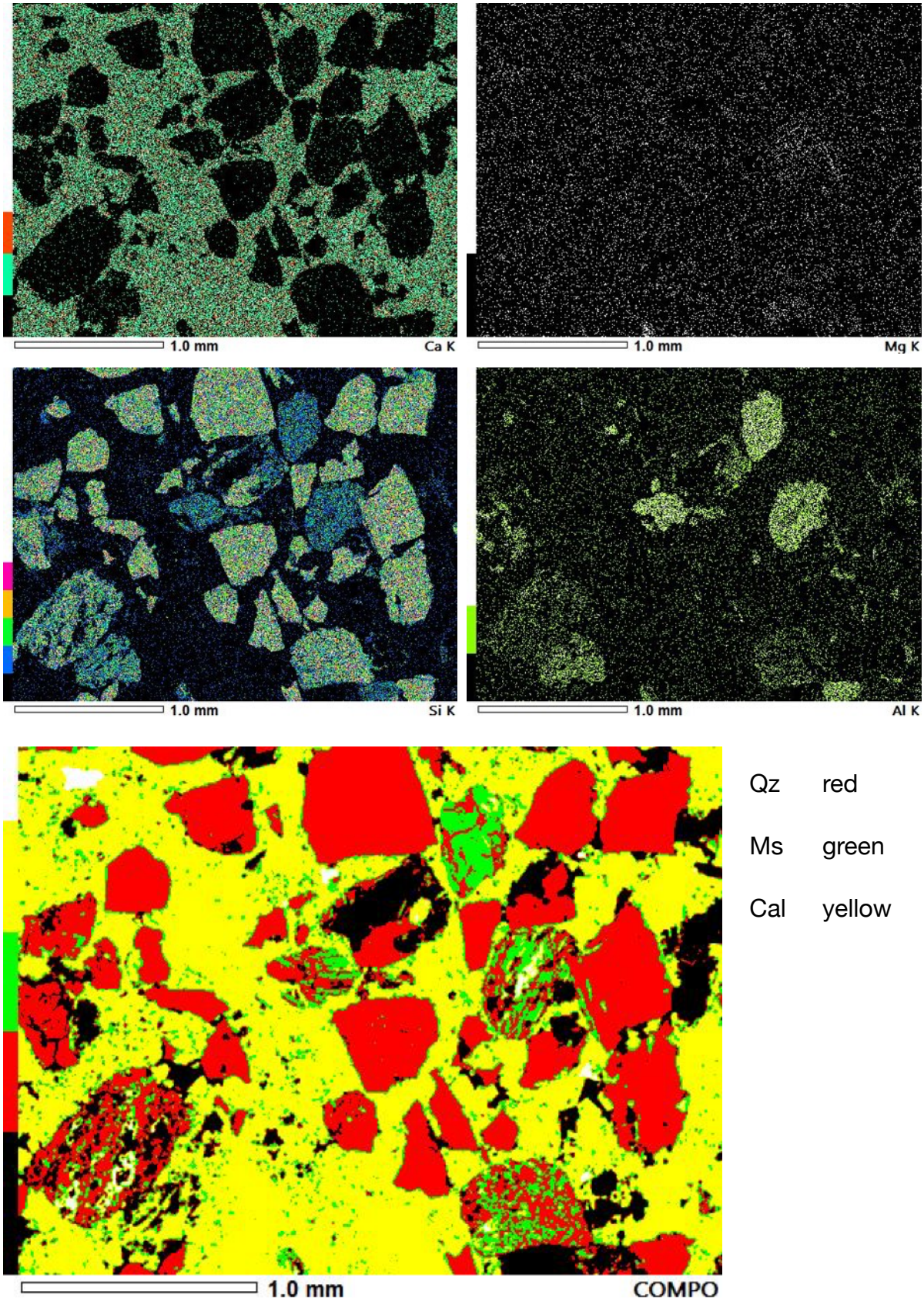

Figure 20: Sample EM-2 element- and compo-maps

Out of the compo maps the quantitative mineral composition was assessed dominated by calcite but with a large variety of silicate content within (Table 3).

EM13		
Cal	50%	Matrix
Fs Ms	5%	Clasts
Bt Rt Ap	5%	Clasts
Other silicates	40%	Clasts
EM11		
Cal	85%	Matrix
Dol	10%	Matrix
Rt Ap	2%	Clasts
Other silicates	3%	Matrix
EM2		
Cal	60%	Matrix
Dol	5%	Matrix
Ms	5%	Clasts
Other silicates	30%	Clasts

Table 3: Bulk mineral composition – both framework and matrix, assessed from composite element maps.

From the three samples, sample EM-11 shows an interesting feature: Coating of detrital calcite grains by a thin layer of dolomite (Fig. 19), whereas the main stage of cement is calcite. This could be interpreted in the following way: In a first diagenetic stage fine-grained dolomite formed preserved as coating on calcite grains, and potentially the dolomite was later partly removed. In a subsequent stage, fibrous calcite A and then sparry cement B was precitated. This means, that the brine and external physico-chemical conditions changed during the diagnesis. However, the preservation of dolomite cement should be proofed by more samples.

To clarify this further, point analyses were made from sample EM-11, particularly from the tiny fine-grained dolomite coating detrital calcite grains (Q1). The results are shown in the Appendix. The detrital calcite grain in Q 1 (Appendix) contains a low amount of Mg, consequently this is a Mg-calcite. The coating dolomite contains some Mn but low amounts of Fe, typical for early diagenetic dolomite. The other measured points show a similar result except Q4, which shows an elevated FeO content. Consequently, an early diagenetic origin of the coating fine-grained dolomite coating detrital Mg-calcite grains during early diagenetic formation is likely.

5.1 Post diagenesis

The freshly deposited and cemented conglomerate was quite tight with low porosity. The post-diagenetic deformation by twinning of the cement caliche led to an increase in porosity and water permeability. The SC has only marginal surface water, the percolated precipitation feeds some springs abounding in water which supply the region from Velden to Klagenfurt with drinking water.

6 Climate & Precipitation Impact

6.1 Climate

The climate before diagenesis created coal layers originating from summer green woodland. So what dramatic climate change was the dominant factor for a change to the forth-bringing of enormous gravel fields cemented by carbonate sandstone with thicknesses up to a couple of hundred meters?

The transport of the gravel volumes with these cobble/pebble sizes requires extreme rainfall floods and a significant topographic gradient and on the other hand there must have been longer evaporation periods in between the individual flood events to give the carbonate milk – the lime wash - time to desiccate and crystallize, so the extreme rainfall floods were sporadic.

Long dry periods interrupted by extreme thunderstorms creating sheet floods are a typical precipitation pattern for semiarid climates such as par example nowadays SE Spain (Eberle et al., 2017) or in Las Vegas where the floods swept motor vehicles from parking lots away before protection dams were erected. Sheet flood events move heavyweight blocks – up to tons - and the floods are not only flooding along depression lines but as well wide on the surrounding terraces leading to wide span river surfaces (Eberle et al., 2017).

6.2 Messinian Salinity Crises

In the deposition and orogeny period under consideration between Lower Pannonian and Pliocene an exceptional event in the proximity in the S happened, the Messinian salinity crisis (MSC; 5.97–5.33 Ma) (Hsü et al., 1973; Vasiliev et al., 2017). In Late Messinian the MSC led to massive gypsum deposits which indicates a couple of long-term desiccation events of the Mediterranean Sea to at least 25% of the original water volume.

Detailed investigations by (Krijgsman et al., 1999) found that the isolation from the Atlantic Ocean was established between 5.59 and 5.33 million years ago causing a

large fall in Mediterranean water level. In the period 5.50 - 5.33 million years ago, deposition of non-marine sediments were found in the ‘Lago Mare’ basin. Cyclic evaporite deposition is almost entirely related to circum-Mediterranean climate changes driven by changes in the Earth's precession, and not to obliquity-induced glacio-eustatic sea-level changes’ (Krijgsman et al., 1999).

Gargani and Rigollet (2007) found repeated desiccations in the later MSC, which differ slightly for the western and eastern basin of the Mediterranean Sea. “Mediterranean water level variation for the Western (green line) and the Eastern basins (red line) (Fig. 21). The uplift rate $U_{threshold}$ is of (a) 0.30 mm/yr and (b) 0.667 mm/yr (1 km in 1.5 Ma) [Duggen et al., 2003] for the area between the Atlantic Ocean and the Mediterranean Sea. We consider a small rate of uplift (30 m/Ma) for the Sicily threshold during the MSC [Patriat et al. 2003]. A calibrated insolation curve calculated at 65°N, July 1st, is used to simulate the glacio-eustatic variations of amplitude comprised between -50 m and +50 m, during the MSC [Miller et al., 2005], due to global climate change. We also use the insolation curve to simulate the hydrological flux [Gargani et al. 2006]. The geometry of the two basins is taken into account as in the study of Meijer and Krijgsman [2005]. We assume a bathymetry Zinit = ±380 m for the threshold between the Mediterranean Sea and the Atlantic Ocean, and of ±35 m for the threshold between the Western and the Eastern Basins. This model allows an interpretation of the existence of 3–5 cycles in the sediments, as well as the observable lowstands in rivers profiles” Description and Fig. 21 by (Gargani and Rigollet, 2007).

Investigation of sedimentation in the Nijar Basin (SE Spain) showed a persistent sequential pattern of eight Lago–Mare cycles, which are interpreted as precession-controlled variations in regional climate (Fortuin and Krijgsman, 2003).

A coincidence between the rate of erosional flux to accretionary flux with an increase of sediments coming down from the Alps was found by Willett et al. (2006) and additional, that this change occurred synchronous with the last phase of the MSC starting 5.55 Ma ago, which coincides with the Lago Mare phase of the MSC. At this stage, the ice volumes expanded, the Atlantic warmed up, leading to the change in

water budget for the Mediterranean (Willett et al., 2006). The fresh water for the Lago Mare situation in the Mediterranean derived from the Paratethys which was at that time an epicontinental sea connected to the Mediterranean during the late Miocene and Pliocene (van Baak et al., 2017).

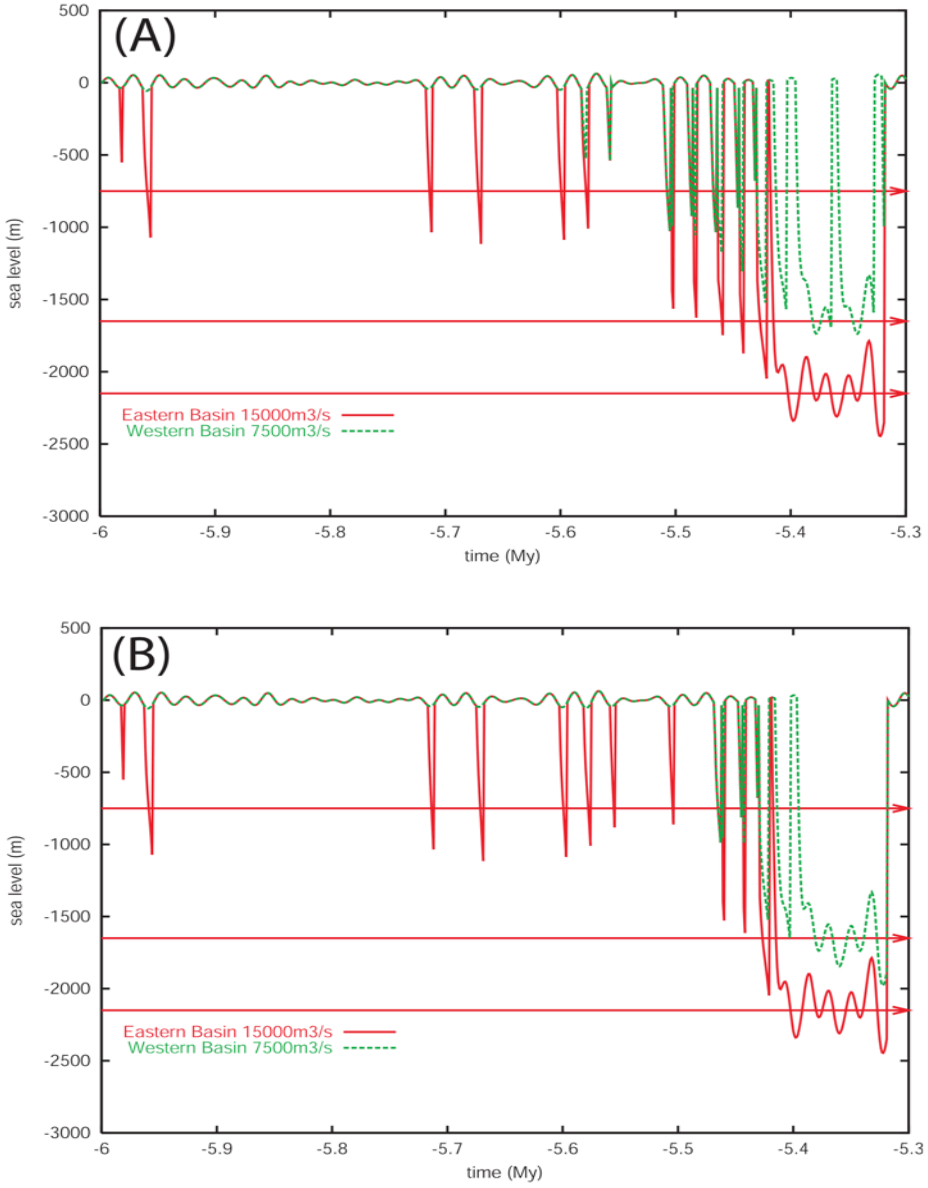

Figure 21: Mediterranean water level variation for the Western (green line) and the Eastern basins (red line) (Gargani and Rigollet 2007)

An examination by Meijer et al. (2004) on the circulation and water properties of the Mediterranean Sea in Late Miocene was using an ocean circulation model. In order to take the paleo-geographical model of the Mediterranean at that time they

reconstructed the sub-basins to their Late Miocene shape where the Apennine was not yet fully developed (Fig. 22). The Adriatic and Ligurian Sea were exposing a much greater water surface area S of the Alps and an intense deep-water circulation moved waters in the Mediterranean (Fig. 23).

The processes of desiccation and re-filling was investigated by (Meijer et al., 2005) with the result that desiccation and re-filling are fast; desiccation occurs on a time scale of 3–8 Ka, re-filling probably even faster showing what enormous amounts of humidity were emitted into the atmosphere at that time. This suggests that the Mediterranean at that time was unlikely to attain stable intermediate water levels.

The climatic situation during the MSC was checked by pollen data (Fauquette et al., 2006), in particular in the southwestern area where the climate was very dry and warm before, during and after the event, a weak decrease in precipitation at the beginning of the crisis in the Black Sea region, increasing precipitation and decreasing temperatures at the end of the Messinian at Maccarone – Sicily, so no big change.

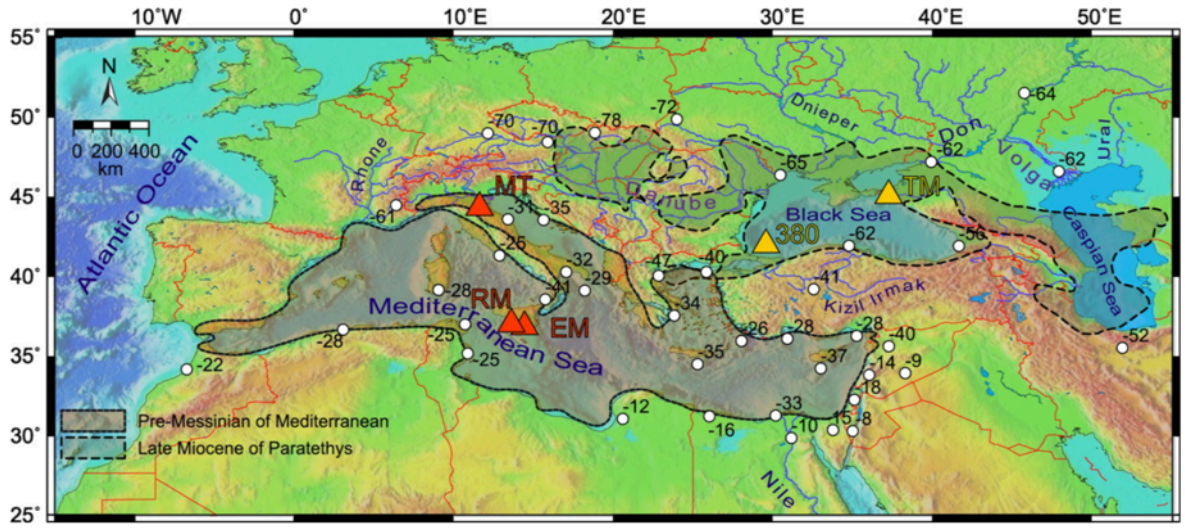

Figure 22: Palaeogeographic map of the late Miocene, showing the Mediterranean and Paratethys areas. The difference in precipitation value at Late Miocene to the present-day values (according to IAEA (2001)) and their locations are marked by the white circle. The yellow triangles indicate the locations of Taman peninsula (TM) and Deep Sea Drilling Project 42B (Hole 380A), the red triangles are the points where δD isotopes were measured on long chain C29 and C31 n-alkanes from Monto Tondo (MT) and Eraclea Mino (EM) and Realmonte (RM) (Vasiliev et al., 2017).

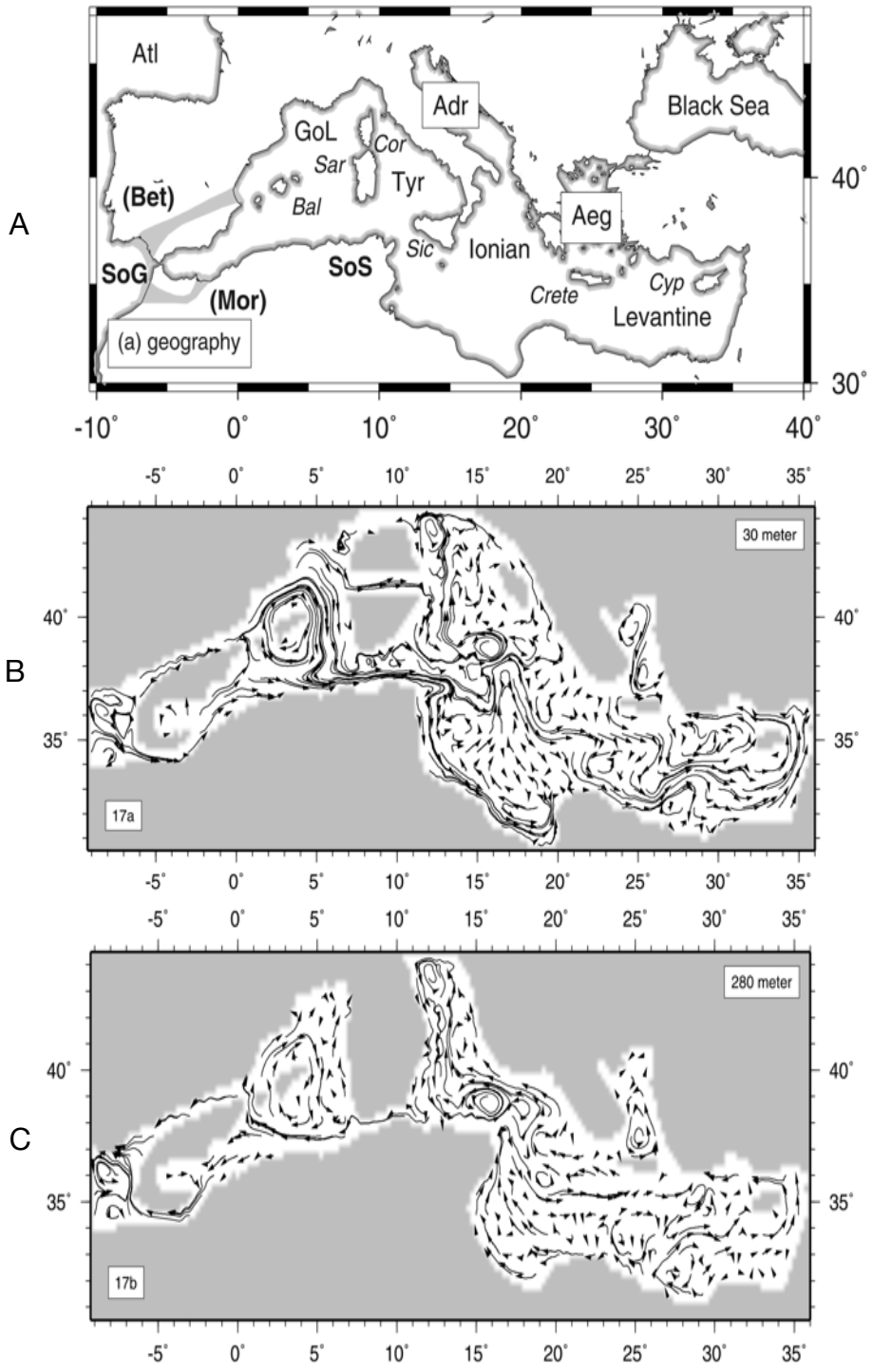

Figure 23: A) Geography of the recent Mediterranean and B) & C) the late Miocene landscape with modeled water circulations therein (P. T. Meijer, Slingerland, and Wortel 2004).

6.2.1 The climate during the MSC

Schneck, Micheels, and Mosbrugger (2010 and papers cited therein) looked into the pollen record from southern Italy and found that dry climatic conditions prevailed before and during the deposition of the Messinian evaporites, whereas, in contrast, the northern part of Italy was relatively humid at that time. From a climatic point of view, a transition from subtropical/warm - temperate conditions during the Messinian to warm - temperate/temperate conditions during the Zanclean is recorded (Bertini, 1994).

Fauquette et al. (2006) investigated pollen pattern in the MCS time. They suggested that no significant climatic change occurred during this time, an inference confirmed by climate modelling in the same paper.

Kuhlemann et al. (2002 and citations therein) stated that according to palaeoflora proxy-data, the average annual palaeo-temperatures in the northern East-Alpine foreland were in the range of 11 to 12 °C in Miocene times which is about 4 C higher than in modern times. This means that the tree line on the northern flank of the Eastern Alps was located about 600 m above the recent tree line, at around 2,400 m, assuming a standard temperature decrease of 0.7 °C per 100 m altitude the snow line would have ranged at around 3,400 m a.s.l.

If we add to this exceptional temperature increase of 4 °C the standard temperature increase of a falling sea level of 1,200 m, assuming something between a dry adiabatic lapse rate of 9.8 °C/km and a moist adiabatic lapse rate of 6.5 °C/km we add 8 to 12 °C for 1,200 m sea level fall. Adding up Mediterranean summer temperature maxima of 40°C to 46°C nowadays, 4 °C temperature increase in the Messinian and 8 – 12 °C from the 1,200 m adiabatic lapse rate results in air temperatures of 52 – 62°C at sea level during the MSC. The additional warming up of the top water layer by sun irradiation must have resulted in a surface water temperature in the 65°C range!

6.3 The MSC's Influence on the Climate of the Catchment- and Depositional Area

The Friuli region in the Southern Alps is even nowadays exposed to weather situations leading to extreme rainfalls causing heavy debris flows effecting mainly the northern slopes. A recent example with extreme flash flood occurred on August 29th, 2003 on the eastern Italian Alps where rainfall intensity up to 100 mm/h over 15-min time step was recorded during the explosive growth phase of the storm (between 14:00 and 18:00 CET). A synoptic weather situation of quasi-stationary convective banded structures occurred, some of which persisted in the same locations for the duration of the event (Sangati and Borga, 2009). The storm rainfall intensity reached 100 mm/h measured over 15-min. time step totaling more than 300 mm between 14:00 and 18:00 CET. At Ugovizza giant rock masses were swept out of unconsolidated rockfall fans hitting the village.

"Rainfall produced by the August 2003 storm resulted in severe flooding throughout the Fella river basin. The storm produced catastrophic flooding at drainage areas up to 80–90 km^2. The flash flood of the Fella catchment on 29 August 2003 occurred at the end of a climatic anomaly of a dry and hot summer. The extreme rainfall from the August 2003 storm was produced by quasi-stationary convective banded structures. Some of the bands persisted in the same locations for the duration of the event. The steadiness of these rain bands led to highly variable precipitation accumulations and runoff" (Sangati and Borga 2009 and papers cited therein).

Out of the data of Sangati and Borga (2009) the calculated water flow of the Fella river at Moggio was 4.580 m^3/sec under the assumptions of 80% rainfall in the top 4 hours and 70% run off and a catchment of 623 km^2. The Fella valley at Moggio is 500 m wide and assuming an average flow speed of the water and gravel mix of 3 m/sec the level raises by 3 m over the 500 m valley width – a sheet flood in the flat braided river bed (Table 3). These floods are caused by a weather situation with an extended throw, an upper low-pressure zone over the Adriatic Sea leading to extreme rainfalls causing heavy floods and debris flows. These heavy rainfalls reached the Julian and eastern

Carnic Alps with the main drainage Fella valley and the Friulan Dolomites and the western Carnic Alps which fed the Tagliamento, the largest braided river in Europe.

During the MSC this kind of situation was exaggerated due to the semiarid climatic conditions over the Southern Alps. Gigantic floods from torrential downpours were frequently generated not only in the Friuli region but also further north in the catchment of the three valleys Lesach-Gail, Drau and Gegental joining at the Villach cross-way, a 10km wide plane at the western end of the Klagenfurt Basin, which supplied the gravel for the Klagenfurt Basin fill and the debris and cement for the SC. All the southern slopes being in the luv of the moving rain clouds up to the alpine main ridge were exposed to the torrential downpours out of relief rainfalls. On the KW's north slopes along the PAL, the BC and the adjacent SC parts were formed by the weather fronts, so precipitation must have been heavy even on northern slopes which indicates that the northern flanks were a substantial catchment and not always on the lee side.

The KB deposition area was shielded by the KW from the south and with 4 °C warmer temperatures must have been relatively arid at the time of deposition.

Monitored rainfall of the Fella basin August 29th 2003

No.	Basin (catchment)	Catchment area	Total rainfall 1 km resolution	Total rainfall volume	80% of total volume 14:00 - 18:00	14:00 - 18:00 4 hours; m³ per hour	Net flow with 70 % run off	Net flow m³ per sec.	Valley width	**assumpted avg. flow speed**	**Water level**
1	Rio degli Uccelli at Pontebba	10,5 km²	353 mm	3.706.500 m³	2.965.200 m³	741.300 m³/h	518.900 m³/h	140 m³/s	100 m	**3 m/sec**	**0,5 m**
2	Rio Bianco at S. Caterina	17,5 km²	307 mm	5.372.500 m³	4.298.000 m³	1.074.500 m³/h	752.150 m³/h	210 m³/s	100 m	**3 m/sec**	**0,7 m**
3	Uque at Ugovizza	24 km²	287 mm	6.888.000 m³	5.510.400 m³	1.377.600 m³/h	964.320 m³/h	270 m³/s	100 m	**3 m/sec**	**0,9 m**
4	Aupa at Moggio Udinese	50 km²	301 mm	15.050.000 m³	12.040.000 m³	3.010.000 m³/h	2.107.000 m³/h	590 m³/s	100 m	**3 m/sec**	**2,0 m**
5	Pontebbana at Pontebba	71,2 km²	246 mm	17.515.200 m³	14.012.160 m³	3.503.000 m³/h	2.452.100 m³/h	680 m³/s	100 m	**3 m/sec**	**2,3 m**
6	Fella at S. Caterina	139 km²	241 mm	33.499.000 m³	26.799.200 m³	6.699.800 m³/h	4.689.860 m³/h	1.300 m³/s	300 m	**3 m/sec**	**1,4 m**
7	Fella at Pontebba	165 km²	247 mm	40.755.000 m³	32.604.000 m³	8.151.000 m³/h	5.705.700 m³/h	1.580 m³/s	300 m	**3 m/sec**	**1,8 m**
8	Fella at S. Rocco	250 km²	253 mm	63.250.000 m³	50.600.000 m³	12.650.000 m³/h	8.855.000 m³/h	2.460 m³/s	300 m	**3 m/sec**	**2,7 m**
9	Fella at Dogna	329 km²	237 mm	77.973.000 m³	62.378.400 m³	15.594.600 m³/h	10.916.220 m³/h	3.030 m³/s	500 m	**3 m/sec**	**2,0 m**
10	Moggio (basin outlet)	623 km²	189 mm	117.747.000 m³	94.197.600 m³	23.549.400 m³/h	16.484.580 m³/h	4.580 m³/s	500 m	**3 m/sec**	**3,1 m**

Table 4: Flow and flow level of the flood event in the Fella catchment on August 29th, 2003

7 Discussion

7.1 The Formation of the Sattnitz Conglomerate

The SC is a freshwater conglomerate with a carbonatic–dolomitic matrix. The deposited debris clasts show a continuous grain size spectrum from 0.2mm - middle grained sand - to cobbles up to 250 mm. The conglomerate is mainly clast-supported and transits at some places to matrix supported and finally to sandstone in form of lenses and ribbons (Winkler, 1997), with a W-E extension of 56km, and a N–S width of 3 to 5 km, its main ridge stretches 25 km W–E. The top elevations in the W are 900m, the top elevations in the E are 800m resulting in a very low slope gradient of 0.23°, $S = \Delta h/h = 0.004$.

The orogenesis of the Sattnitz freshwater conglomerate required three criterions:

a. abundant supply of gravel in the volumes and composition deposited delivered;

b. carbonatic – dolomitic brine delivered for cementing the conglomerate;

c. a limate to expose the brine to evaporative concentration with the dissolved calcite and dolomite to form the caliche cementing the clasts.

With respect to items a. and c. of the above-mentioned requirements short-period flash floods out of the three catchments joining at Villach flushed an abundant supply of coarse gravel, brine and suspension over floodplains into the Klagenfurt Basin. When short-period flash floods ceased the brine disappeared into the gravel beds provided there was sufficient porosity between the gravel. In order for the brine to desiccate only a shallow layer of debris close to the top of the gravel flood plain was able to hold the brine close to the surface and exposed it to evaporative concentration. The long anticlinal bulge of the crystalline basement along the north side of the Rosental provided this setting.

Item b. concerning the carbonatic – dolomitic brine supply is best fulfilled by the Gail valley coming through the Schütt area where frequent large to gigantic rockfalls form the north wall of the carbonatic Dobratsch were washed away by the sheet floods.

Additional debris and brine came down from the KW northern slopes leading to an interleaving pattern of layers from both sources.

7.2 Supply of Gravel

7.2.1 Basin fill and denudation in catchment

The assessments of the KB fill and the catchment and its denudation rate are (Table 4):

- Debris fill volume 300 km³
- Catchment area 4.800 km²
- Denudation rate is 370 mm/Ka under the premise that all debris from denudation was deposited in the Klagenfurt basin.

Klagenfurt Basin				
Length EW	Width NS	Area	mean height	Basin Volume
65 km	12 km	748 km²	0,4 km	300 km³

Catchment Area				
Length EW	Width NS	Area	Basin Volume	Denudation
120 km	40 km	4.800 km²	300 km³	62.500 mm

Denudation in catchment				
Denudation	From	To	Duration	per 1000y
62.500 mm	5,50 My	5,33 My	0,17 My	370 mm/Ky

Table 5: Assessment of KB basin volume and denudation

This is well in the current denudation range of the Alps of 700 - 800 mm/Ka at an altitude of ± 1000 m. (von Blanckenburg, 2005). If we assume that the denudation rate at the time of the MSC was higher or at least at the current level, up to 50% of the sediments were deposited in the Klagenfurt Basin.

7.2.2 Provenance of the clasts

Out of the clast composition the gravel supply can be allocated to catchment of the three valleys joining at Villach and the KW north slopes, out of Villach the Gail supplied carbonate and dolomite from the Southern Calcareous Alps (Drauzug), the Gegental's catchment supplies crystalline basement rocks, phyllites and quartz, the catchment of the Drau which includes the south-eastern dome of the Tauern Window delivers both, however the Drau- and Gail-valley dominated.

The deposited gravel clasts show a continuous grain size spectrum from 0.2mm - middle grained sand - to clasts up to 250 mm – blocks/boulders.

7.3 The Formation of the Bärental- and Sattnitz-Conglomerate

In the literature both conglomerate formations are linked to the emergence of the Karawanken chain without a deeper assertion of the conglomerate formation. Griem et al. (1991) describes the interleaving of the BC and SC at Wellersdorf which is indicating a coeval deposition (Fig. 2). The BC is deposited on the relative steep northern flank of the KW whereas the SC lies flat on a bulge of the Altkristallin basement in front of the KW chain.

The brine for forming conglomerate's caliche comes together with the gravel from the same origin or at least direction. The clasts and the brine for the BC came mainly from the southern Karawanken chain down the northern slopes, the last exhumation pulse of the Karawanken was in Late Miocene (Heberer et al., 2017) whereas those of the SC must have come out of the Villach feeding channels. The brine for the SC was dominated by the inflow channel from the Gail valley via Villach, however the thunderstorms from the Mediterranean discharged as well above the KW so the interleaving of BC and SC described (Griem et al., 1991) indicates that sheet floods from the KW stretched out over the Sattnitz. The high carbonate share in the rock composition at Saager in the SE of the Sattnitz is a further indicator (Fig. 13).

7.3.1 Origin of the Carbonatic–Dolomitic caliche of the Sattnitz Conglomerate

From where could the brine be supplied? The best candidate is the Gail valley where a couple of kilometers west of Villach the Schütt area (Schütt means rockfall) is the deposit of large rockfalls down the north wall of the Dobratsch in historic times. The Dobratsch mountain, one of the main summits of the “Drautal Zug” or “Drauzug”, is situated north of the vertex of the Fella – Sava fault which pushes north directly against the Drautal Zug range including the Dobratsch mountain. The Lesach – Gail valley has a catchment of 1.000 km² and is very exposed to relieve rainfall from the Adriatic Sea similar to or exceeding the catastrophic flood 2003 in the Fella catchment.

A major landslide in historic time (1348) and some interglacial landslides from the Dobratsch into the Schütt area are reported by Lenhardt (2007) (Fig. 24), further up the Gail valley an interglacial – between Riß- and Würm-glacial) landslide from the Spitzegel is documented by (van Husen, 1985).

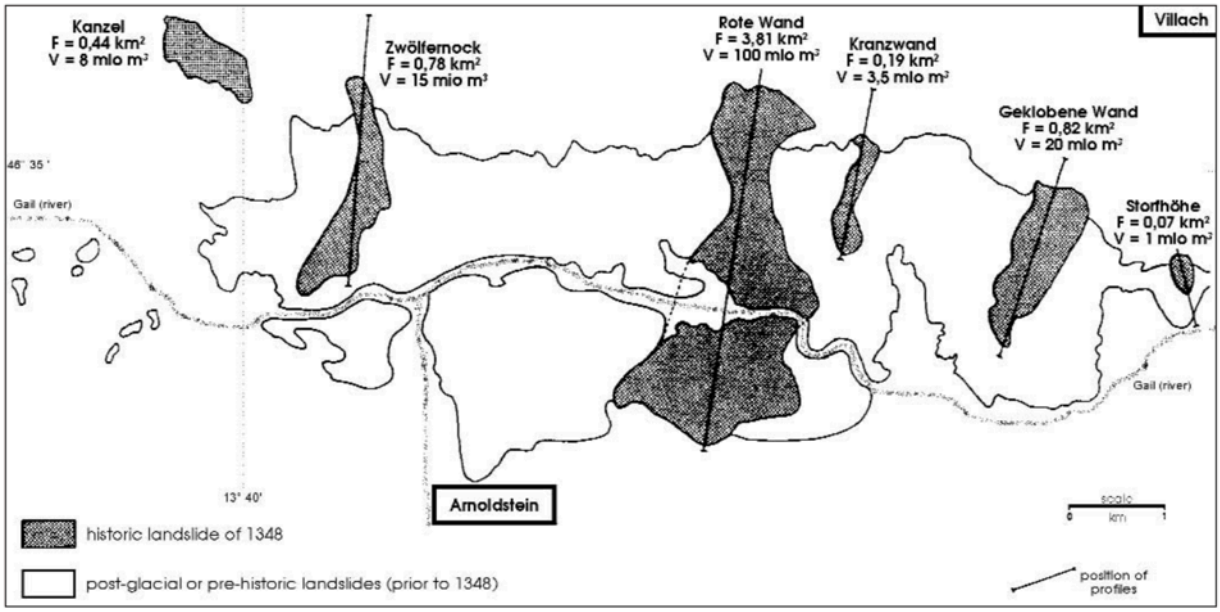

Figure 24: Location of six landslides associated with the earthquake of 1348 and some post glacial landslides in the Schütt area (Lenhardt, 2007 and authors cited therein)

Nickel (1985) suggests “that the distribution of carbonates in alluvial-fan systems, in front of alluvial fans and in the adjacent fluvial regimes is also due to the hydrological pattern. Acquisition of the different ions by solutions (groundwater and surficial runoff) will largely depend on the lithologies and the climate in the source area and on the mineralogical composition of the fan-detritus. Following the principle of brine evolution, groundwater and, to a lesser degree, surface water, which both are generated by weathering solutions in the source area, would be prone to evaporative concentration when flowing down-fan from the apex to the fan-edge.” The fan is in the case of the Sattnitz conglomerate the gravel plain out of Villach. The high Mg content in the caliche could have developed along the enrichment model for Mg in carbonate-sulfate brines from Eugster and Hardie (1978 cited in Nickel, 1985) (Fig. 25).

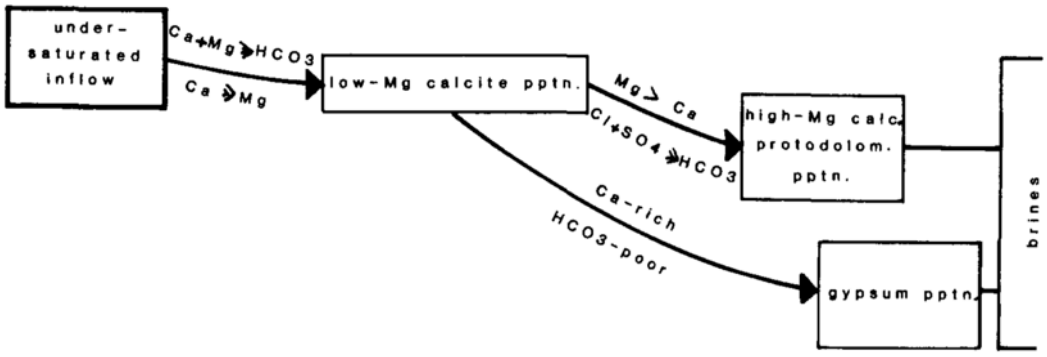

Figure 25: Conceptual model of the evolution of carbonate-sulfate brines from proximal to distal areas in an alluvial-fan system the brine evolution pathways (Eugster and Hardie 1978)

7.4 Sheet floods and the morphology of the deposits

We have already considered the semiarid climate with occasional torrential downpours during the MSC. These torrential downpours out of relief rainfalls augmented on the southern slopes were hitting the valleys at one spot at the time. These torrential downpours out of relief rainfalls are caught in the valleys and produce there the sheet floods from the spot on down the valley. These sheet floods are capable of encasing a lot of unstratified and unsorted, angular to sub-angular, pebble to boulder rock-avalanche deposit containing moderate matrix content (Blair and McPherson, 1994).

Torrential downpour deposited a matrix-poor debris-flow lobe in the range of meters the valley up acting as a buffer stop for the flood so that the vast bulk of the flood with the encased gravel was jetting the valley down. Due to these buffer-stop lobes the valleys needed not to be filled up with sediments all up to the valley head.

A plano-convex cross-profile is inherent in sheet flood depositions, which is the inverse of the through-like cross-sectional form of a river system. This results in sheet flood deposits with surface parallel, planar-stratified or low-angle anti-dune sequences (Blair and McPherson, 1994).

There are not too many papers on the topic of morphing debris surfaces available, a climatic situation like the one during the MSC is recently obviously not known. A paper of Wells and Dohrenwend (1985) describe sheet flood deposits of the Mojave Desert of southeastern California during latest Pleistocene to middle Holocene: “The majority of meso-bed forms occur on fan segments several kilometers away from the mountain front and commonly near the intersection points between Pleistocene and Holocene alluvial fans. Macro-bed forms occur on fan and pediment remnants that extend from within the mountain complex to well over 3 km down-piedmont. These larger forms, as well as some meso-bed forms, also occur locally on deeply dissected surfaces near mountain fronts” (Wells and Dohrenwend, 1985) (Fig. 26).

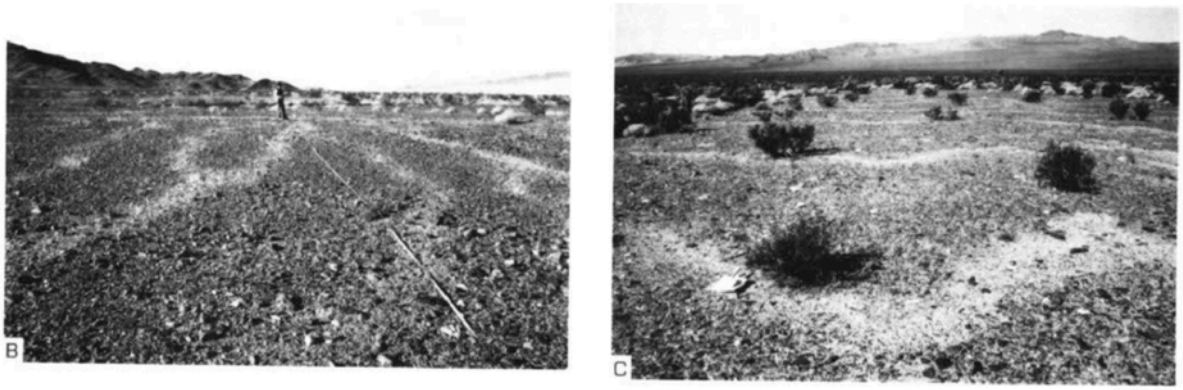

Figure 26: Ground view of sheet-flood meso-bed forms on late Pleistocene fan surface on Silver Lake-Soda Mountains piedmont. B: Ground view of sheetflood meso-bed. C: Sinuous in-phase plan forms of meso-bed forms on North Providence Mountains piedmont of eastern California. Note uniformity in bed-form width. (Wells and Dohrenwend, 1985).

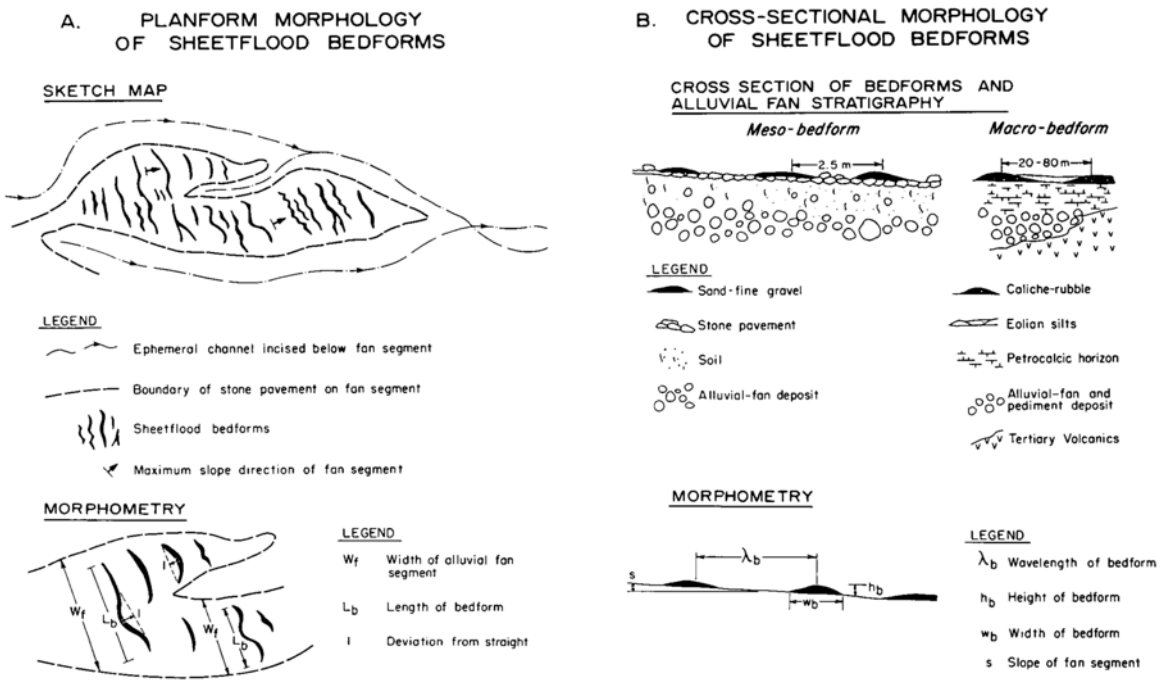

Figure 27: Plan form morphology and definitions of parameters for meso- and macro-bed forms. B: Cross-section morphology and definitions of parameters for meso- and macro-bed forms; note different cross-sectional sketches for meso- and macro-bed forms (Wells and Dohrenwend, 1985)

Both scales of bed forms occur on inactive fan surfaces from 1 to as much as 10 m above active ephemeral drainageways. These surfaces are gently sloping (0.020-0.067) and are characterized by well-varnished, well-developed interlocking stone pavements that typically have less than 0.15 m of microrelief. Some meso-bed forms occur on surfaces having up to 0.3 m of relief related to individual clasts or degraded longitudinal depositional bars.

The sketches on morphology and the photographs give an impression on the extremely flat spreading of the debris as a consequence of sheet floods. Bed forms are characterized by light-colored, finer grained material on darker, varnished stone pavement. Note bifurcation and straight plan form (Fig. 27) (Wells and Dohrenwend, 1985).

7.5 The floods at the Villach cross-way

Fig. 28 shows the three catchments feeding the debris into the KB. As the Southern Alps are mainly exposed to humidity from the south – humidity from the north is coming down as relief rainfall onto the slopes north of the Alps. The catchment areas for the calculations are encompassing only the south slopes of the valleys.

Out of peak rainfall per hour and catchment, the catchment area of the south slopes, a runoff ratio of 70% and the valley widths the flow level and the average flow speed are calculated using a transformed Manning-Strickler equation (Chaudhry, 2008). The flood levels at Villach are in the range of some meters, the Drau up to 20 meters and the average flow speeds range from 1 to 3.7 m/sec (Table 5).

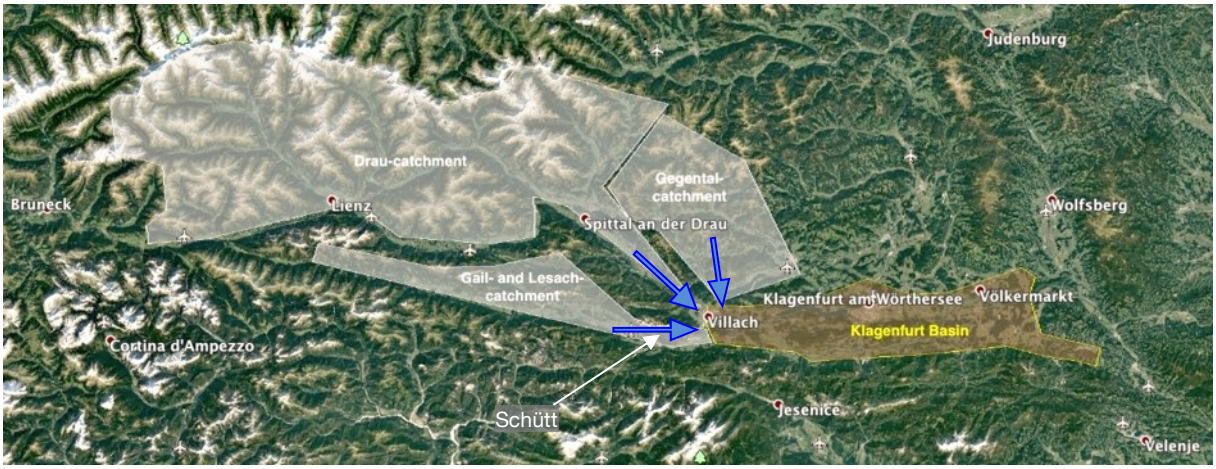

Figure 28: The three catchment areas, the sheet flood channels towards Villach with the main rock fall area Schütt and the Klagenfurt Basin

Flow and Flow Level calculation by the transformed Manning-Strickler equation

$$H = \left(\frac{k_s^{1/3} q_w^2}{\alpha_r^2 g S} \right)^{3/10}$$

	Peak rainfall onto catchment's south slopes	Catchment Area - South slopes	Total rainfall volume per hour	Runoff ratio	Runoff flow per sec.	Flow width	Valley length	Valley decline	Slope	Flow per m valley width		Roughness m^1/3/sec		range 8 - 9 gravel bed -> 8,1		**flow level**	**avg. flow speed**
									S	qw	qw^2	ks	ks^1/3	αr	αr^2	**H**	**vm**
Gail valley	100 mm/h	560 km²	56.000.000 m³/h	70%	10.890 m³/s	1.600 m	30 km	63 m	0,0021	7 m³/s	46,33	20	2,714	8,1	65,61	**3,9 m**	**1,7 m/sec**
Gail valley	50 mm/h	560 km²	28.000.000 m³/h	70%	5.440 m³/s	1.600 m	30 km	63 m	0,0021	3 m³/s	11,56	20	2,714	8,1	65,61	**2,6 m**	**1,3 m/sec**
Gail valley	25 mm/h	560 km²	14.000.000 m³/h	70%	2.720 m³/s	1.600 m	30 km	63 m	0,0021	2 m³/s	2,89	20	2,714	8,1	65,61	**1,7 m**	**1,0 m/sec**
Gail valley at Schütt	100 mm/h	560 km²	56.000.000 m³/h	70%	10.890 m³/s	800 m	30 km	63 m	0,0021	14 m³/s	185,30	20	2,714	8,1	65,61	**5,9 m**	**2,3 m/sec**
Gail valley at Schütt	50 mm/h	560 km²	28.000.000 m³/h	70%	5.440 m³/s	800 m	30 km	63 m	0,0021	7 m³/s	46,24	20	2,714	8,1	65,61	**3,9 m**	**1,7 m/sec**
Gail valley at Schütt	25 mm/h	560 km²	14.000.000 m³/h	70%	2.720 m³/s	800 m	50 km	50 m	0,001	3 m³/s	11,56	20	2,714	8,1	65,61	**3,2 m**	**1,1 m/sec**
Drau valley	50 mm/h	3.250 km²	162.500.000 m³/h	70%	31.600 m³/s	1.500 m	50 km	50 m	0,001	21 m³/s	443,80	20	2,714	8,1	65,61	**9,6 m**	**2,2 m/sec**
Drau valley	25 mm/h	3.250 km²	81.250.000 m³/h	70%	15.800 m³/s	1.500 m	50 km	50 m	0,001	11 m³/s	110,95	20	2,714	8,1	65,61	**6,3 m**	**1,7 m/sec**
Drau valley before Villach	50 mm/h	3.250 km²	162.500.000 m³/h	70%	31.600 m³/s	400 m	50 km	50 m	0,001	79 m³/s	6.241,00	20	2,714	8,1	65,61	**21,2 m**	**3,7 m/sec**
Drau valley before Villach	25 mm/h	3.250 km²	81.250.000 m³/h	70%	15.800 m³/s	400 m	50 km	50 m	0,001	40 m³/s	1.560,25	20	2,714	8,1	65,61	**14,0 m**	**2,8 m/sec**
Gegendtal valley	50 mm/h	900 km²	45.000.000 m³/h	70%	8.750 m³/s	750 m	8 km	60 m	0,0075	12 m³/s	136,11	20	2,714	8,1	65,61	**3,7 m**	**3,2 m/sec**
Gegendtal valley	25 mm/h	900 km²	22.500.000 m³/h	70%	4.380 m³/s	750 m	8 km	60 m	0,0075	6 m³/s	34,11	20	2,714	8,1	65,61	**2,4 m**	**2,4 m/sec**

Table 6: Flow and flow level out of the valleys joining at Villach.

7.6 The role of the basement onto the conglomerate genesis

As indicated before, the genesis of a conglomerate requires a fluviatile environment to allow for evaporative concentration of a brine, so when the altitude of underlying basement supports this, a conglomerate body will be built up.

Coming from N the old crystalline basement is bent down towards the KW to a flexural basin forming the Rosental Valley. The bending down forms a bulge north of the basin on top of which ridges of Triassic carbonates, marbles and dolomites are cropping out.

On some spots the SC is placed on clay layers containing coal seams – Penken, Keutschach, Stein, Oberloibach, etc. otherwise it is placed directly on the old basement and the overlaying Triassic limestones and dolomites.

The SC is placed on the southern limb of an anticlinal shaped basement caused by a compressive regime which is folded and not only representing the bulge under the Sattnitz Conglomerate but as well the ridges lining up to the N:

- the Seental valley,
- the Pyramidenkogel, Rauth, Friedelhöhe and Schrottkogel,
- the Wörthersee is the next synclinal to the north, followed by
- the Ossiacher Tauern mountain and
- the Ossiacher Lake, the Gerlitzen mountain

in a full spectrum of concertina folds stretching ca. E - W.

The compressive tectonic regime originates from the situation at the Tauern Window East Dome where the Adriatic plate begins to subduct under the European plate and the orogen is pressure-forged around this corner giving rise to the pronounced surface uplift of the Julian Alps and the Dobratsch and builds the Fella-Sava fault zenith. This compressive regime extends to the E until the Pyramidenkogel north of the Sattnitz main ridge.

Between the two Tauern Domes the two plates collided frontally resulted in the upfolding respectively uprising Tauern Window. W of it, the European Plate is subducted under the Adriatic Plate, E of it the Adriatic Plate is subducted under the European Plate (Fig. 29) (Lippitsch et al., 2003; Schmid et al., 2004; Luth et al., 2013; Brückl and Hammerl, 2014; Handy et al., 2014).

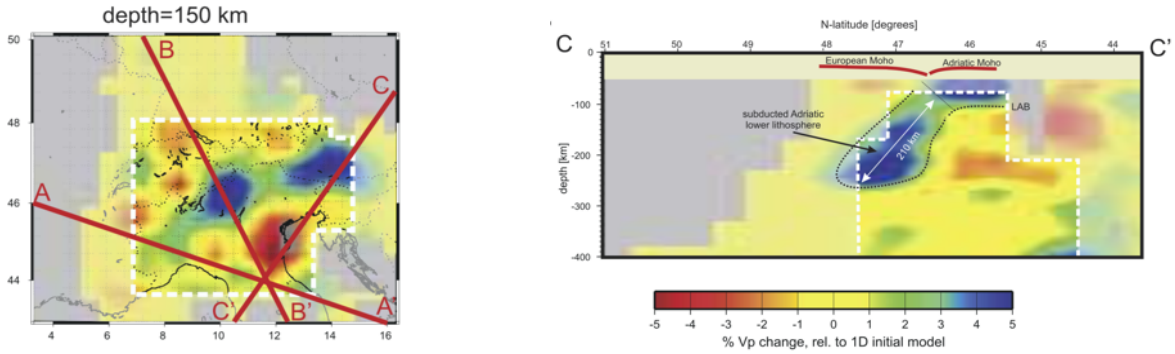

Figure 29: Location map (left) and (right) cross section through the upper mantle model crossing (C) the Eastern Alps. Velocity variations are plotted from red to blue relative to the 1-D global reference model. Extent of lithospheric slab bodies is tentatively outlined by dotted lines (from Lippitsch et al. 2003)

The altitude of the old crystalline basement at the southern rim is 470 m a.s.l.. at Rosegg, 430m at Hollenburg whereas at the northern flank the basement comes up to 600 – 700 m a.s.l. at Opferholz and Stifterkogel situated west and east of the Viktring to Maria Rain valley. South of the Seental valley, the basement is covered by SC rockslides with some outcrops of the Hafner Lake and east of the Rauschele Lake.

7.7 The Klagenfurt Basin fill at the time of the conglomerate orogenesis

The sheet floods from the three valleys joined at the 10 km wide intersection at Villach becoming the apex of the fan stretching out over the entire KB. The short-period flash floods with the duration of hours brought large volumes of a water-gravel-suspension-composite as sheet floods onto the flood plains.

In contrast to rivers these lobes form at the end of the individual sheet flood events, there are no chutes out of these lobes. If the lobe stops on the flood plain a slightly elevated rim can be heaped up on top of the delivering flood plain (Fig. 31).

When the floods come to an end they have deposited gravely, matrix-rich debris flow lobes. These lobes ad up to an entire fan out of the apex covering the whole basin over time. The fan radii extend from the apex in all directions at a relatively similar slope forming an arc – Figure 30 - into the basin with the apex as center (Blair and McPherson, 1994).

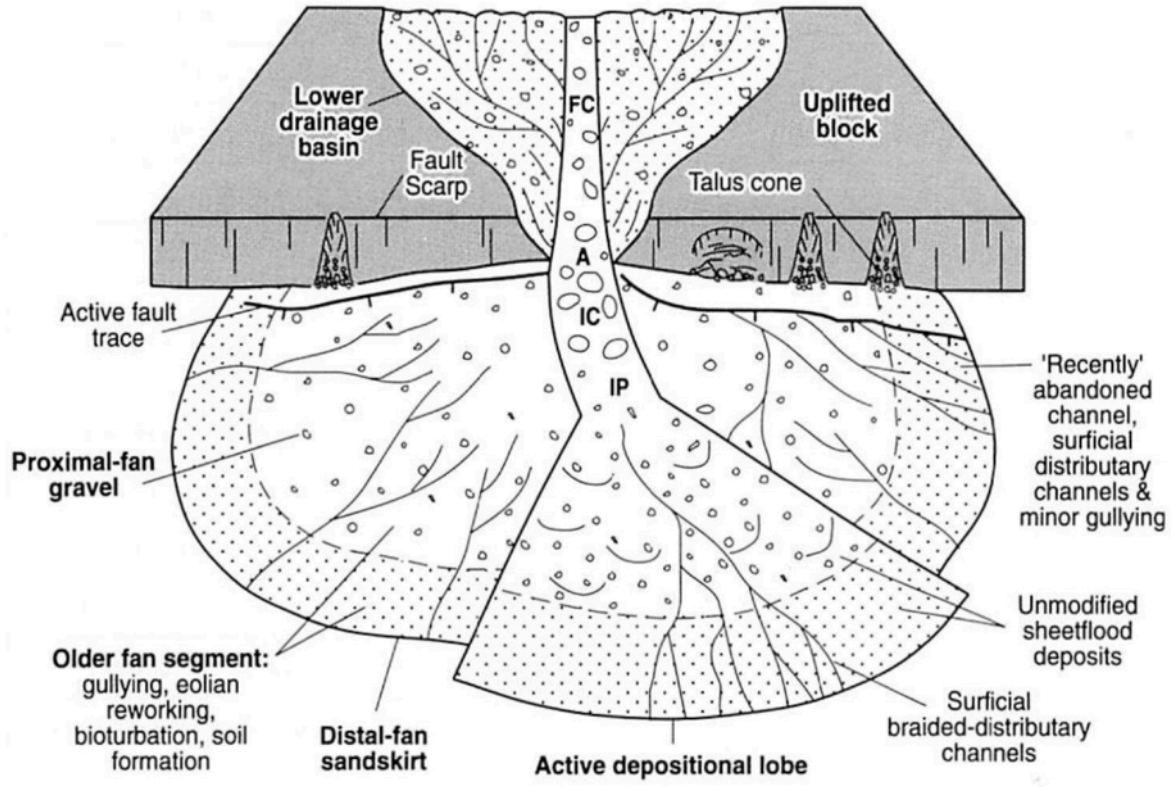

Figure 30: Lower drainage basin, and primary and second- arc depositional features of alluvial fans by sheet flood processes. Abbreviations: A = fan apex; FC = drainage- basin feeder channel; IC = incised channel on fan; IP = fan intersection point (Blair and McPherson, 1994).

The majority of sheet flood fans develop at mountain fronts to some kilometers down-piedmont. The debris is washed out from a drainage basin in the mountain slopes above, an apex is cut into the lower end of the slope resulting in a slope of 2 – 3° (S = 0.034 – 0.05) in these morphological situations. An equilibrium is established

between the bottom level to which delivery area is carved out and the top level of the fan – the apex.

The fan of the KB fill is coined by the combination of two flows:

- The main inflow from the Villach apex, and
- floods coming down the Karawanken incisions

So, theoretically the W–E slope of the Sattnitz Conglomerate from its highest elevations W and E is only 0.23° (S = 0.0034) over a length of 37km which can be explained with the additional floods down from the Karawanken.

Here the situation is that the apex is on bedrock and the floods cannot cut in the debris was stapled already in the apex and valley up to that the actual apex height was above the valley base and the debris flow was fanning out flat over larger distances.

Some conglomerate formations reach far down to a low altitude basement. The mechanism for this mode of structure formation could well be that when a new debris-brine flood reached the edge of the existing flood plain it slumped down the slope and, the debris being on the slope surface, so the brine was exposed to evaporative concentration over large vertical slopes.

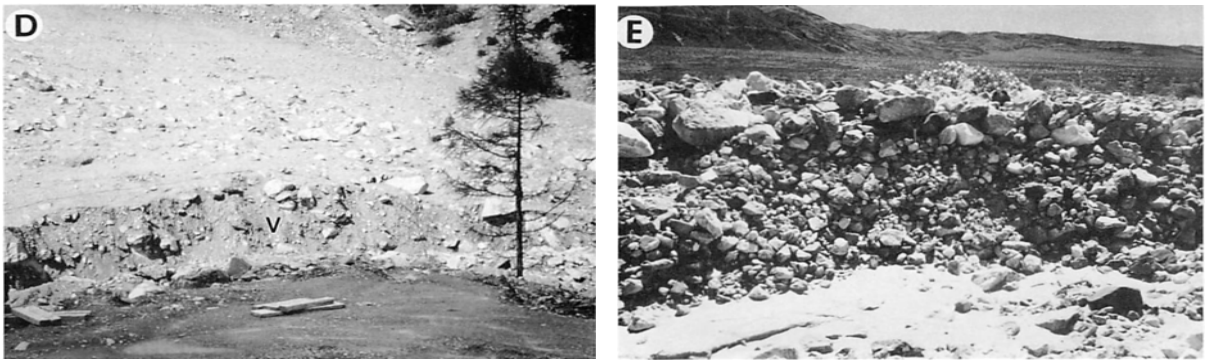

Figure 31: Sample lobe rims: D) Close-up of a 4 m high vertical cut (V) of the distal part of the Herbriggen avalanche revealing an unstratified, unsorted, matrix-rich clayey pebble to boulder gravel texture. E) One-meter high vertical section of a clast-rich, matrix-poor debris flow lobe deposited on the Panamint Canyon fan in Panamint Valley during August of 1984. Photographs and text from Blair and McPherson (1994).

The alluvial fan of Fig. 32 from the Taklamakan Desert, Xinjiang Province (China) gives an idea on the fan covering the KB out of Villach.

Figure 32: Alluvial Fan, Taklamakan Desert, Xinjiang (China). Photo Credit: University of Maryland

7.8 Gravel fill and conglomerate side by side

Due of the characteristics of sheet flood deposits the fan out of Villach filled the whole Klagenfurt Basin with a slope of 0.02 to 0.04. Conglomerates out of this period are only found on the northern slopes of the Karawanken mountain chain, the Bärental Conglomerate and the Sattnitz Conglomerate (Fig. 35).

There are more conglomerates deposited in the Klagenfurt Basin, these are much younger and prevailing of interglacial origin: Vinza Nagelfluh, Hollenburg Nagelfluh, Straschitz Conglomerate, Pritschitz Conglomerat (Krainer, 2006), Augsdorf Nagelfluh (Kahler, 1931).

Sheet-floods out three valleys arrive at the Klagenfurt Basin at Villach, from South to Nord these are the Gail, Drau and Gegendtal valleys (Fig. 30). Floods from the Gail valley supply calcareous debris and as they have flooded the rock avalanches from the Dobratsch and other mountains north of the valley they supply additionally the calcareous brine cementing the conglomerate. Floods from the Drau valley deliver crystalline debris with a minor calcerous fraction, the Gegendtal valley furnishes crystalline material (Fig. 33).

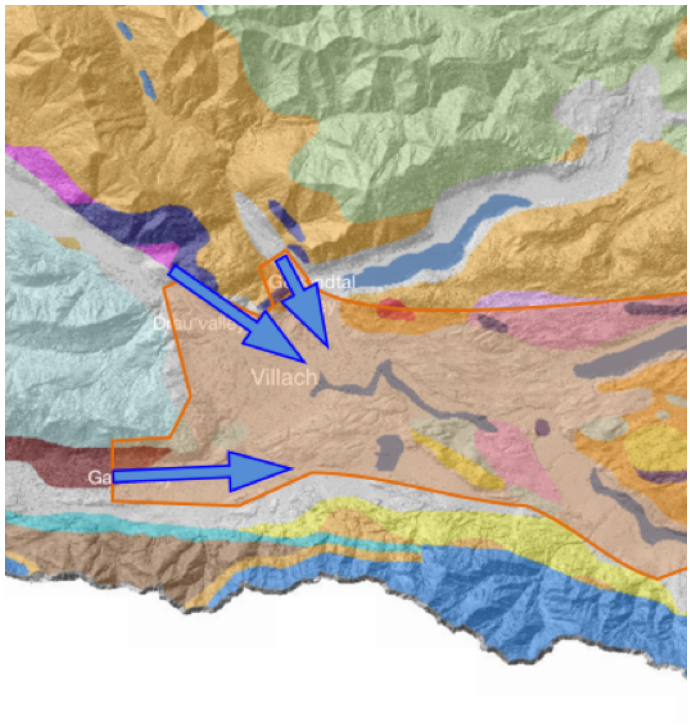

Figure 33: The three inflow channels of sheet floods towards Villach (Base map: KAGIS https://gis.ktn.gv.at/atlas/(S(myehat42arbmamqueulp0jnb))/init.aspx?karte=atlas_basiskarten&ks=kaernten_atlas)

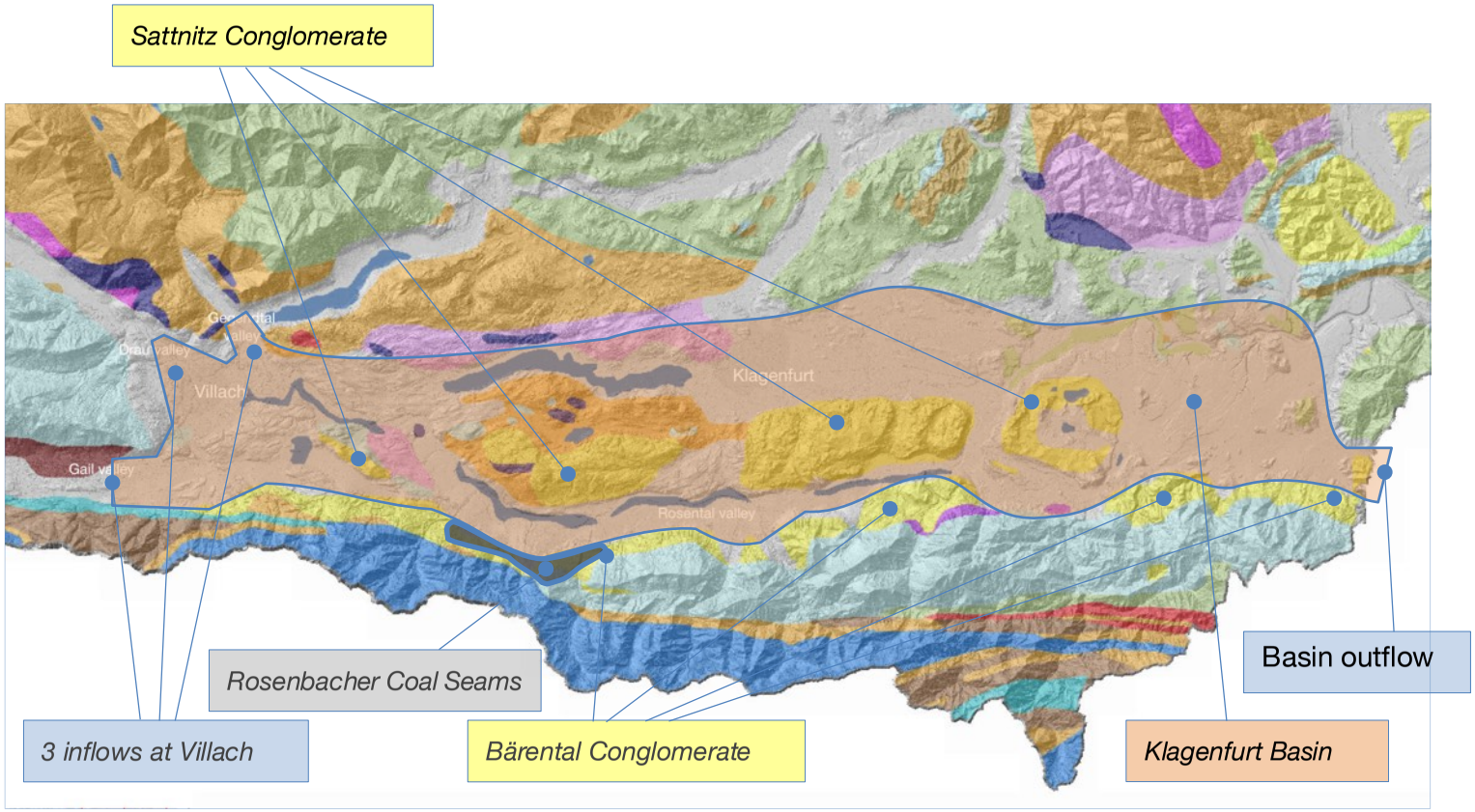

Figure 34: The Klagenfurt Basin with the apexes of the Gail-, Drau- and Gegendtal- valleys and the Sattnitz- and Bärental-Conglomerate. (Base map: KAGIS https://gis.ktn.gv.at/atlas/(S(myehat42arbmamqueulp0jnb))/init.aspx?karte=atlas_basiskarten&ks=kaernten_atlas)

An overview of the Klagenfurt Basin is given in Fig. 34.

The BC on the northern slopes of the KW consists of calcareous debris and brine originating from the KW uplift.

The Sattnitz Conglomerate situated on the southern side of the Klagenfurt Basin is exposed to the sheet floods from the Gail Valley and from the Drau Valley. The debris is dominated by calcareous material, the cement is dominated by calcite, at some locations filled with angular fine sand particles of quartz. The sheet floods spread out in a vadose regime, the brine was exposed to evaporative concentration and the conglomerate was cemented layer by layer. Distal fan sand skirts (Blair and McPherson, 1994) became the source of sandstone beds.

The Rosental valley with only marginal conglomerate deposits is situated in between the Sattnitz- and Bärental- Conglomerate. This valley follows the flexural basin between the KW and the Altkristallin basement under the Sattnitz Conglomerate and has existed at the time of conglomerate deposition. The sheet floods were splashing over the alluvial fans and went over the current Rosental but in contrast to the Sattnitz range the waters and brine percolated down the crevasses in the gravel where it reached a phreatic zone and subsequently this brine was not exposed to evaporative concentration.

The water flows out of the northern part of the Villach apex did obviously not contain sufficient calcareous brine to cement a conglomerate which is proofed by the absence of conglomerate north of the Sattnitz range. A second proxy for this concept is the massive rock breakoffs and -slides on the southern rim towards the Seental valley showing a decline in cementing strength, potentially by post-diagenetic secondary processes by influence of meteoric water.

The basin outflow (Fig. 34) was in the direction Miess-valley, the current outflow at Lavamünd is much younger as the southern part of the Koralpe, and the Pohorje were uplifted by 400 – 600 m the last 5 Ma (Fig. 35) (Legrain et al., 2014). This is indicated by conglomerates north and south of the outflow from the basin suggesting its outflow at the time of the formation of the conglomerates.

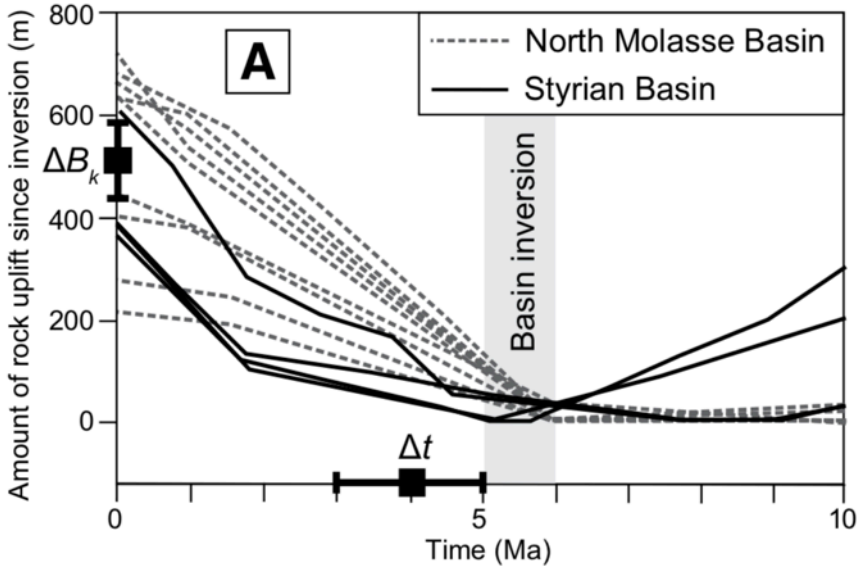

Figure 35: Comparison between total amount of base-level fall calculated for Koralpe and amount of rock uplift allocated to the subduction of Adriatic Plate – Adriatic Indenter - since inversion of basin. Total relative base-level fall (⊿Bk) and time (ΔT) from the beginning of an incision into the Koralpe (Legrain et al., 2014)

The total length of the two conglomerates from Faaker Lake to Miesstal is 75km. In his book on sedimentary basins Einsele (1992) gives an overview on transport distances for various flows and deposits, for debris flows and mud flows (of Lahars) he indicates several 10 to 100 km (Fig. 36) and shows as an example the volcanoclastic sediments deposited in Miocene at Washington with massive clast supported conglomerates at a length of more than 120 km (Fig. 37).

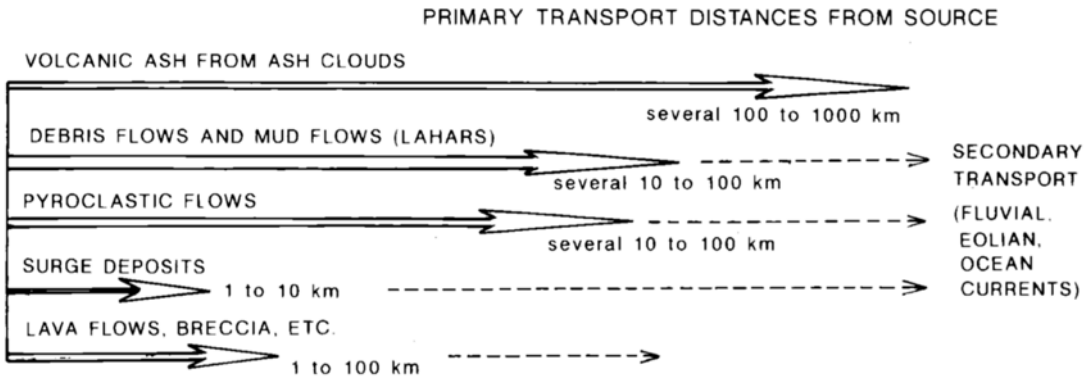

Figure 36: Frequent ranges of primary transport distances of various tephra (Einsele 1992).

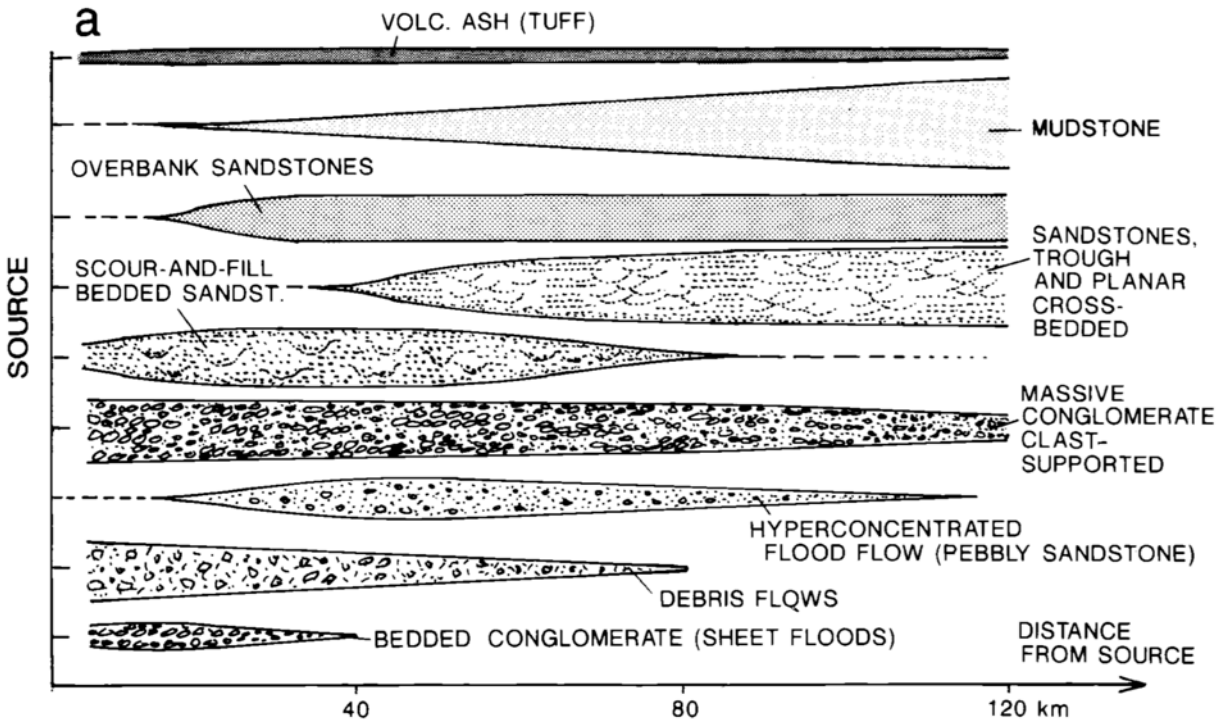

Figure 37: Illustration of proximal to distal facies changes in a Miocene fluvial to lacustrine environment in Washington which was episodically affected by volcanic eruptions (Einsele 1992).

For the altitude of the alluvial fan, the terraces in and around the KB give some indications. The highest elevations of the western Sattnitz on Tanzboden at 910 m – 920 m a.s.l. seems to be above the original accretionary fan surface due to an uplift of the Tanzboden relative to Turiawald where the top elevation is 870 m a.s.l. Terraces at 700 m a.s.l. are prevalent in the eastern Sattnitz. The residual terraces between 660 m and 630 m and 570 m a.s.l. respectively are rather of erosional origin. Indicators of the fan level height are in the Villach area a rim at the Dobratsch at 950 m a.s.l. SW of the Villach town and a 1.000 m level at Singerberg close to Ferlach (Winkler-Hermaden, 1957).

Parallelization of these altitudes with the SC is a hint for an advanced denudation of the SC. The levels at circa 750 m and 650 m a.s.l. could be the uppermost Pliocene level, the lower one could represent the pre-glacial niveau. At the Ossiacher Lake this

level is at 700 – 740 m a.s.l. At Lienz, 90 km above Villach in the Drau valley, the pre-glacial level is at 1050 m a.s.l. which is 200 – 300 m above the valley ground (Winkler-Hermaden, 1957 and papers cited therein).

7.9 The Pliocene impact on the Klagenfurt Basin fill

When the Mediterranean desiccation ended, the short sheet-flood events with their short distance transport capability had accumulated large amounts of debris in the valleys and basins of the Alps. With the climate becoming more humid the enormous debris deposits in the Alpine basins and valleys were transported into the seas.

In the paper *"Messinian climate change and erosional destruction of the central European Alps"* Willett et al. (2006) state that "an increase in sediment yield both north and south of the Alps provides strong circumstantial evidence that these events are causally related, and are diagnostic of an increase in erosional flux from the Alps. This increase may have initiated with the base-level fall associated with the MSC, but the persistence of high sediment yield into the Pliocene (Fig. 38) suggests a wetter, more erosive climate that initiated with the end of the late Miocene glacial period and is marked by the Lago Mare conditions in the Mediterranean."

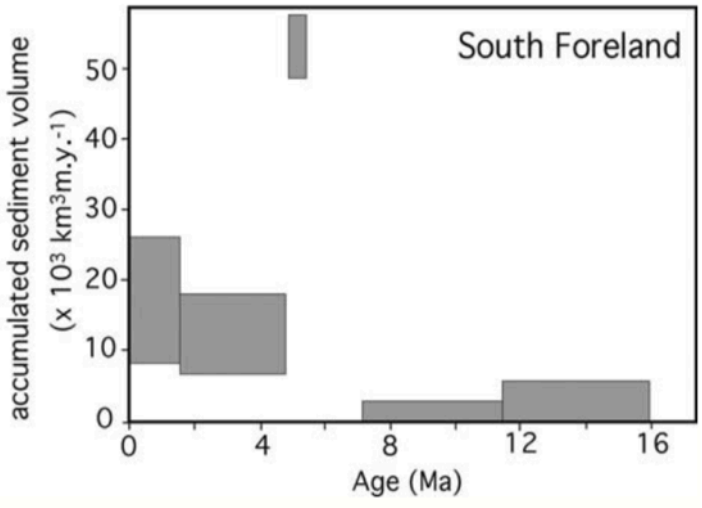

Figure 38: Sediment yield from southern Alpine drainages (Willet et al. 2006).

Kuhlemann et al. (2002) comes to the point that “The basic reason for this drastic increase of sediment discharge is not clear. The event is not yet recorded in the surface cooling pattern of large parts of the Alps, except for the external massifs and the Lepontine dome in the Swiss and Western Alps.” The large amounts of debris accumulated in the valleys and basins of the Alps by the sheet flood appear to be likely.

So, we can assume that the alluvial fan was carved out by rivers cutting into the alluvial fan and that quite a share of the unconsolidated debris was transported out of the KB via the Miess valley and already the Drau valley via Lavamünd.

7.10 The Pleistocene morphogenesis of the Sattnitz Conglomerate

Around the previous Neogene/Quatemary boundary, at about 1.8 Ma, the drainage pattern of the Eastern Alps was fully developed. At present, the Pliocene/Quaternary boundary is set at 2.6 Ma (www.stratigraphy.org) and the Quaternary is considered as part of the Neogene. The transition to a different climatic regime with more extreme glaciations than the previous period started at about 0.9 Ma which explains that no glacial deposits older than the Günz Glaciation have been found in the Eastern Alps (van Husen, 2004). The fluvial erosion of the unconsolidated material was dominant over a period of 4.4 Ma, so most of the material accessible by fluviatile erosion was gone.

The extent and flow direction of the glaciations which covered the KB until Griffen in the E is shown in Fig. 39. The glaciations formed overdeepened tongue basins in the ablation area where the higher ice velocity increases the basal debris load and where basal meltwater drainage under hydrostatic pressure occurs. They were shaped successively during each glaciation because the tongue areas always developed more or less in the same positions. The base in the Gail and Drau valleys was found at an elevation of 200-240 m. This investigation and a similar study in the Salzach area shows that the overdeepening may be limited to about 400 m in this part of the Austrian Alps (van Husen, 2004).

The overdeepened valley parts in the catchment and deposition area of the KB are shown in Fig. 40. In the catchment areas, the Drau and Gail valleys were affected, in the depositional area the Wörthersee with the present-day KB (Jaunfeld) and the Rosental.

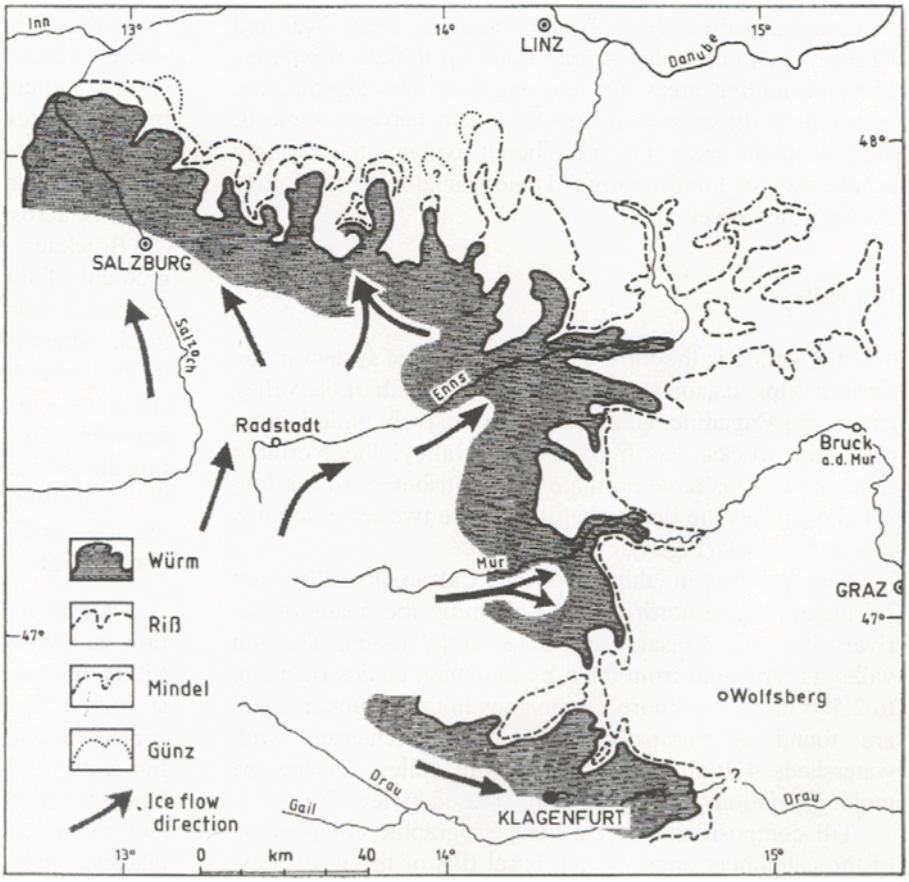

Figure 39: Extent of the glaciers of the four glaciations known in Austria. Theice flow direction is similar during each glaciation (van Husen, 2004)

The Würm glaciation maximum height over the SC was in the W above Tabor 1,350 m and declined to the E to 1,100 m at Klagenfurt to 900 m a.s.l. above Stein im Drautal (van Husen, 1987). This means an overburden thickness of about 300 m over Turiawald and Tanzboden resulting in a pressure impact of 3 Mpa on the SC surface.

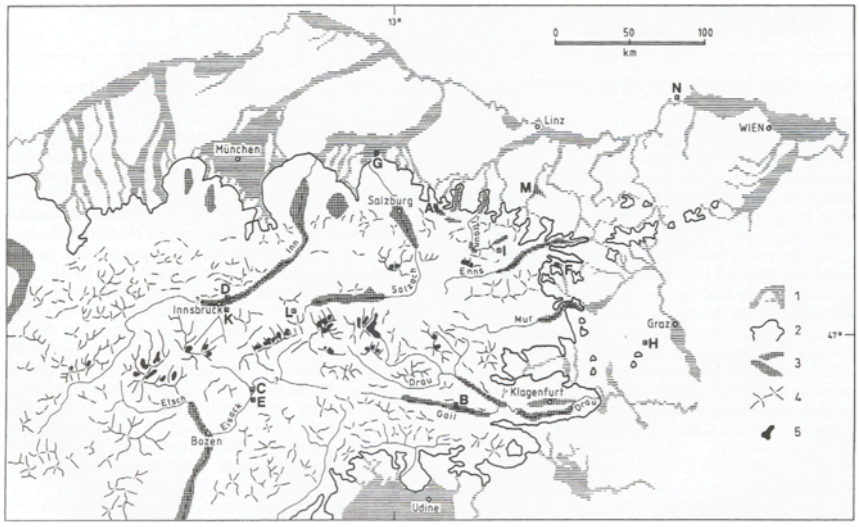

Figure 40: Figure 37: Sketch map of the Eastern Alps during the Würmian glaciation; 1 terrace; 2 maximum extent of glaciers; 3 overdeepened parts of the valleys; 4 Nunatak; 5 glacier extent of the Holocene. Localities in the Gail catchment: B: Nieselach (van Husen, 2004).

The SC range is cut by several faults (Fig. 1), which have developed in Plio- and Pleistocene times, unconsolidated material in the area of these faults was removed by fluviatile erosion and later and much stronger by glacial fining down.

The glacial erosion of the BC and SC top layers formed the secondary conglomerates, around Faaker Lake this is the Vinza Nagelfluh and the Hollenburg Nagelfluh around the name-giving castle. Severe striation marks, e.g., on the limestone ridge separating Turiawald and Tanzboden (Fig. 41) give proof of glaciation and an indication of the thickness of the glacial overburden at the top of the ridge.

Figure 41: Striation marks on limestone ridge separating Turiawald and Tanzboden.

7.10.1 The Sattnitz mesa mountain structure after the ice ages

The flanks of the SC show impressive walls especially towards the S and E (Fig. 42). These are shaped by the glaciers at the end but the stability of the consolidated material in contrast to the unconsolidated one which was grinded away. What mechanisms could have created such a contrasting stability?

Figure 42: Southern wall of the SC at Kohldorf close to Annabrücke

In the chapter on conglomerate orogenesis, the evaporative concentration of the brine explained the difference of unconsolidated debris and conglomerate where the layer thickness of fresh debris holds the brine and is transformed to cement by the sunrays. This mechanism works similar to a 3D laser printer, which solidifies the laser exposed areas of a layer of powder whereas in the unmachined areas the powder stays at it was and is removed.

8 Use of Conglomerates as Building Material

8.1 Klagenfurt Basin Conglomerates

In the KB a couple of conglomerates and sandstones are on hand which were used as building material in historic times. Currently all the quarries are out of operation. From the genesis the conglomerates can be classified into such of Neogene or interglacial age. The Neogene conglomerates are:

- Sattnitz Conglomerate (SC)
- Bärental Conglomerate (BC)

Part of the BC was deposited at the same time as the SC because of the interleaving of the two (Griem et al., 1991). A part of the BC was pushed northwards by the progressing KW and became steeply inclined (Krainer, 2006).

Two main areas of interglacial conglomerates and sandstones were exploited:

- Vinza Nagelfluh
- Hollenburg Nagelfluh

Both Nagelfluh stones were called “smooth stones” by the chiselers and stone cutters and they favored them over the conglomerates as they were easier to work on. Like all the porous limestones they are soft in the moisty state when freshly quarried and harden thereafter considerably. For the use as construction stone the cleavability and the high porosity (Fig. 43) were extra benefits as the later reduced the thermal conductivity of the walls and avoided the “sweating” of the walls due to condensation (Kieslinger, 1956).

The Vinza Nagelfluh is a thin layer fining downwards to a more sandstone habitus, in the range up to meters on the Vinza Ridge S of Faakersee. It is likewise the underground of the Faak village and is exposed on the island within the Faak Lake. Numerous quarries along the ridge were delivering the building material which are closed by now. This stone was widely used in the Villach area up to north of Klagenfurt.

A similar conglomerate/sandstone mix was found further to the W in the southern edge of the Gail Valley between Feistritz in the Lower Gail Valley and Arnoldstein (Anderle, 1953).

The Hollenburg Nagelfluh has a similar habitus but with a much greater thickness in the range of 10 m and big blocks were exhausted there. The Hollenburg castle was built of this material and as the sovereigns of Hollenburg were endowing the church of Maria Saal commenced in the 15th century (Jakl, 2017) and were engaged in the building of the main church of Maria Wörth (Fig. 54) which was at that time built on an island (until 1770) of the Wörthersee. The Hollenburg Nagelfluh deployed there was most likely transported by boats over the lake.

Figure 43: Sample of Vinza Nagelfluh photographs of both sides (Zirkl, 1985).

The Bärental Conglomerate was used as a locally available material when building the railway through the Rosental for passages underground and railway stations.

The Sattnitz Conglomerate was difficult to quarry but numerous erratic blocks were used as building material. In a recent building (1980) the Main Communications Building of Klagenfurt was cladded with Sattnitz Conglomerate (Fig. 44).

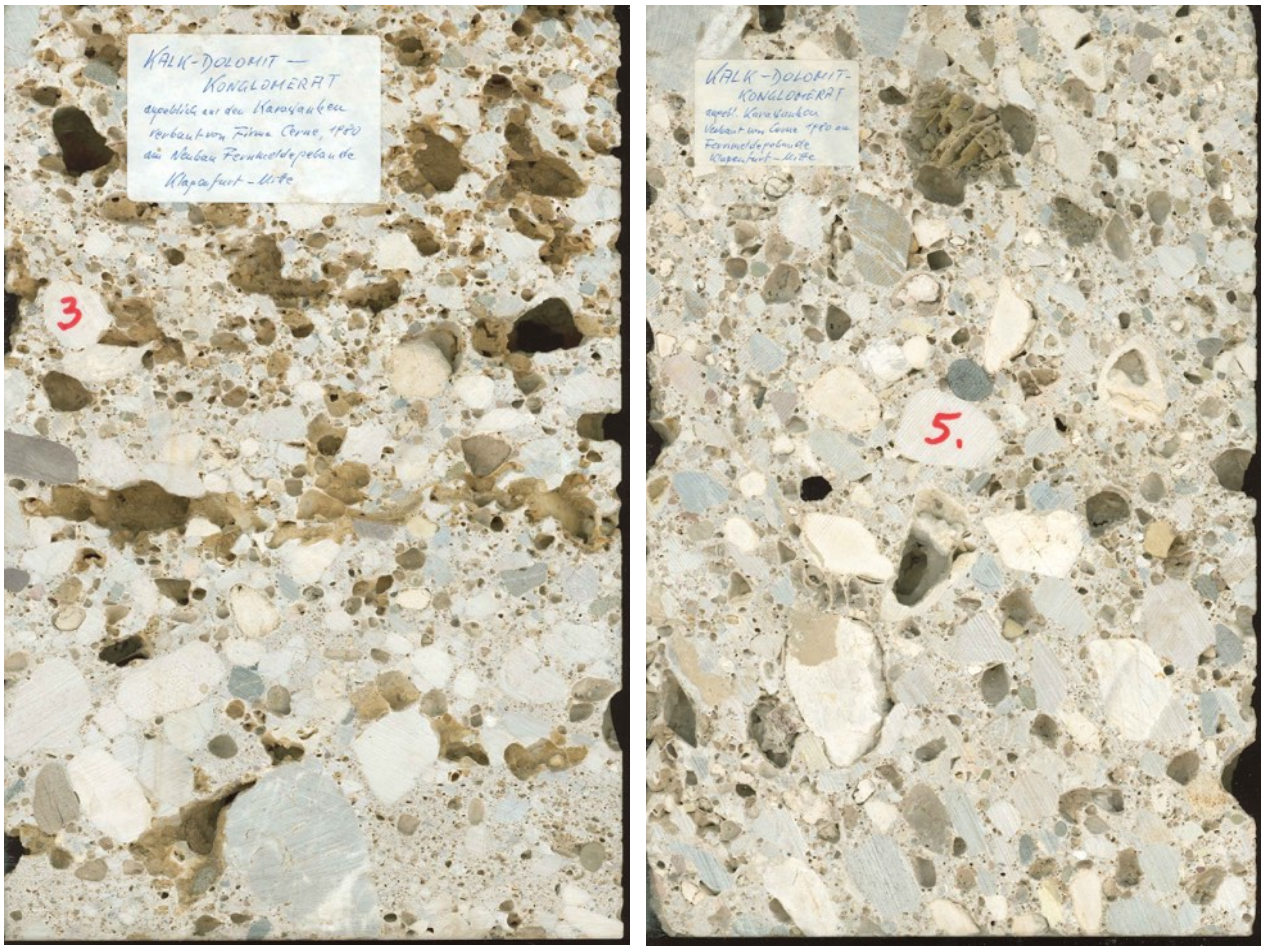

Figure 44: Sample of Sattnitz Conglomerate - photographs of both sides - used for the Main Communications Building of Klagenfurt (Zirkl, 1985).

8.2 Use of conglomerates in the construction of buildings

The soft conglomerates were in some cases used for:

- complete structures p.e. the cathedral of Maria Saal, more often as main construction material p.e. the church of Maria Wörth, Maria Gail, the castle Alt-Finkenstein, the tower of the main church of Villach

and frequently for

- construction elements such as wall corners in long and short works, pillars, buttresses, wall rips, rip faults, door- and window- garments (Kieslinger, 1956).

The same author presents an extensive list of examples where these conglomerates were deployed (pages 115-118).

8.2.1 Major Buildings complete with conglomerate

8.2.1.1 Dome of Maria Saal

The present-day church of Maria-Saal was built in a Late Gothic style between 1430 and 1459, later partly refurbished with a Baroque interior in the 17th century (Fig. 45). The dominant construction material is Hollenburger Nagelfluh, which was also used for the vault, the interior works like pillars and ribs (Figs. 46 and 47).

Figure 45: Maria Saal Cathedral, left-hand Dome (Photograph by Johann Jaritz, CC BY-SA 4.0), right-hand Nave.

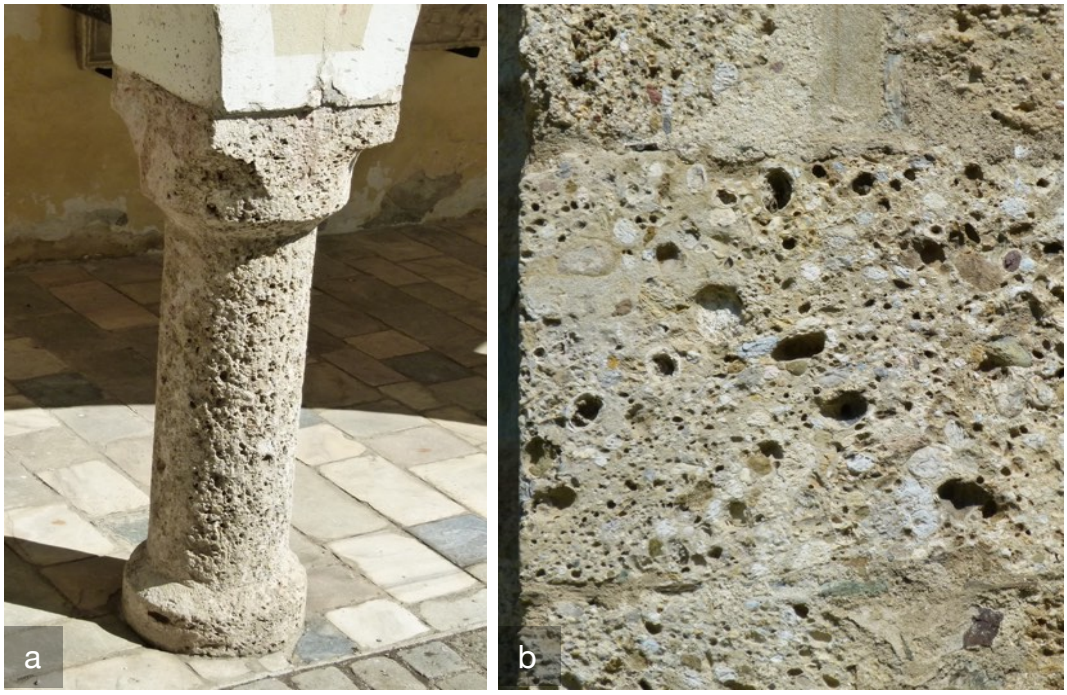

Figure 46: (a) and (b) show the structure of the disposed conglomerate.

Figure 47: Archway with holes due to fallen out pebbles.

8.2.1.2 Hollenburg

The castle dates back to ~ 1100 by the Margraves of Styria and gained strategic importance when the road over the Loiblpass was expanded in the 13th century. Due to the earthquake of 1348, the castle was partially destroyed, but immediately rebuilt (Fig. 48 – 50).

Figure 48: Fortress Hollenburg from the south out of the Rosental

Figure 49: SC base of the fortress

Figure 50: Details of the courtyard, Top: Balustrade at the inner courtyard, Bottom: porticos.

8.2.1.3 Church of Stein im Jauntal

The St. Lawrence Church (Fig. 51) is said to have been donated in the 11th century but shows different construction times for the individual parts. The church rises on a steeply sloping hill to the south and east, all main constructive parts are built from the locally available alluvial conglomerate (Fig. 52).

Figure 51: St. Lawrence Church of Stein in the Jaun Valley.

Figure 52: St. Lawrence Church: left-hand Wall aside the main portal, right-hand Outcrop along the Way of the Cross up from the ground.

8.2.1.4 Parish – and Winter church of Maria Wörth

The main church of Maria Wörth, first documented in 894, was built under Bishop Waldo von Freising. The second smaller church, the Winter-Church, consecrated in 1155 by Bishop Roman von Gurk, was used for the ongoing parish service (Fig. 53).

In 1399, the collegiate and parish church on the island became a robbery of flames. Although both churches were rebuilt, the work was very slow. Only around the year 1420, the small parish church was rebuilt, but with gothic windows. Several decades later, the provost's church was restored, this time in gothic style. Later, this historic pilgrimage church received a beautiful baroque décor (Community Maria Wörth, 2018, (https://www.maria-woerth.info/en/the-history/ retrieved 11-09-2018)

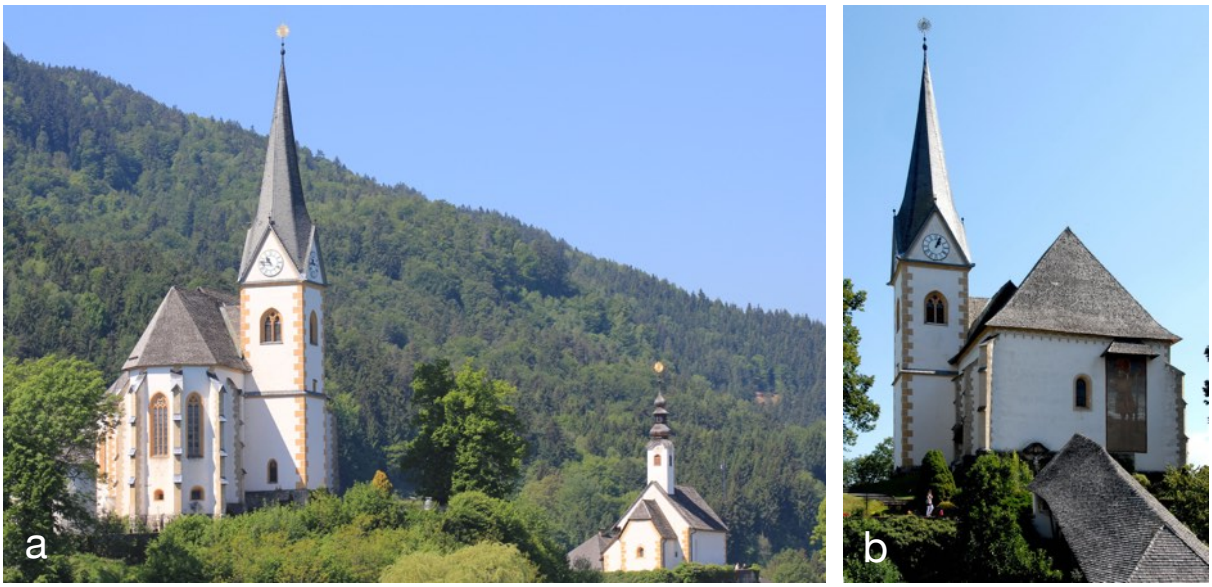

Figure 53: (a) Parrish- (left-hand) and Winter-church (right-hand), (https://de.wikipedia.org/wiki/Kirchenanlage_Maria_Wörth) (b) Parish church (https://commons.wikimedia.org/wiki/Kirchen_von_Maria_Wörth?uselang=de).

Figure 4: Entrance door from the covered stairway to the Parish Church

The entrance door from the stairway (Fig. 54) and the Parish church's main construction elements on the outside are all made of Nagelfluh (Fig. 55), the Nagelfluh is uncovered, in the interior all Nagelfluh- pillars and ribs are color painted (Fig. 56).

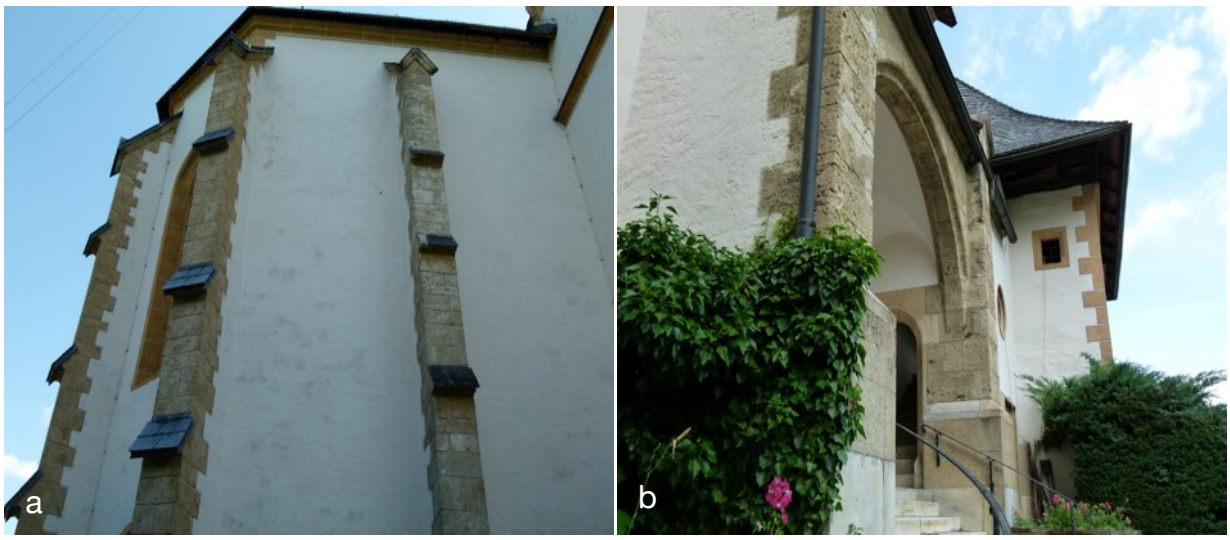

Figure 54: Buttress construction (a) and portal (b), both in Nagelfluh.

Figure 55: Parish church - ribbed vault, ribs in Nagelfluh — painted.

The portal of the Winter church is built in Nagelfluh, the doorsill is made of coarse conglomerate, the Lord's Table is a cube made of Nagelfluh blocks (Fig. 57).

Figure 56: Winter Church, left-hand Doorsill, right hand Lord's Table.

8.2.2 Major Buildings with construction elements out of conglomerate

8.2.2.1 Main Communications Building of Klagenfurt

Built in 1980, the Main Communications Building of Klagenfurt was cladded with original Sattnitz Conglomerate (Fig. 58).

Figure 57: Main Communications Building cladded with SC.

8.2.2.2 Old city houses in Klagenfurt

The old city around the Old Place was erected in the 13th century but a fire destroyed Klagenfurt in 1514 and 4 years later a canal was dug connecting the city to the Wörthersee Lake as a supply route to rebuild the city. So the old city houses originate from the 15th to 16th century. The Hollenburg Conglomerate was the construction material for pillars, door garments etc. (Fig. 59)

Figure 58: Pillars and door garments of old city houses in Klagenfurt.

CONCLUSION

- The Sattnitz Conglomerate is interpreted to have been deposited by gigantic sheet floods out of three valleys joining at Villach and as well pouring down the Karawanken slopes. The floods likely originated from an extreme semiarid climatic situation originating from the partly desiccated Mediterranean Sea during the Messinian Salinity Crisis.
- In the Sattnitz Conglomerate the enormous debris deposits in the basins and valleys of the Alps caused by sheet-floods with their inherent short distance transport capability during Messinian Salinity Crisis are cemented. These deposits led to an increase of debris flow out of the Alps into the Pliocene.
- Out of Villach the water with encapsulated debris flushed out as sheet floods into the Klagenfurt Basin where the mostly dry climate desiccated the brine and cemented the conglomerate sheets, potentially in two diagenetic stages (first in a poorly preserved dolomitic stage, then by calcite).
- From the well-known date of this event the deposition and diagenesis can be interpreted to date between 5.59 and 5.33 Ma.
- The provenance analysis by Ar-Ar dating of white mica and projecting these ages onto the known exhumation dates of the catchment areas yields the contribution of the catchments of the three valleys and the Karawanken.
- As mentioned above, there are some hints for a two-stage diagenesis: A first diagenetic stage formed in some cases fine-grained dolomite preserved as coating on calcite grains, and potentially later largely removed. The full cementation was then by calcite.
- Conglomerates were widely used as construction material of buildings and construction elements. This thesis presents some outstanding exsamples from the Wörhersee region.

APPENDIX

EM11 SCOPE MAP

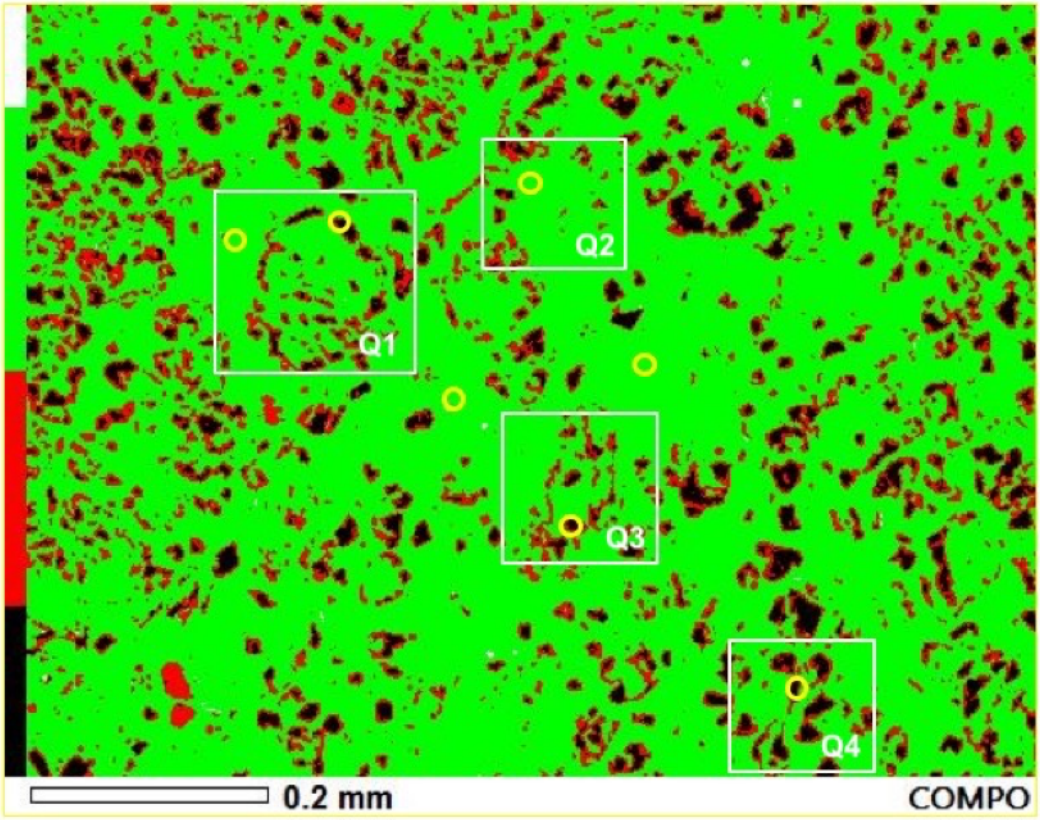

Q1 MAPS

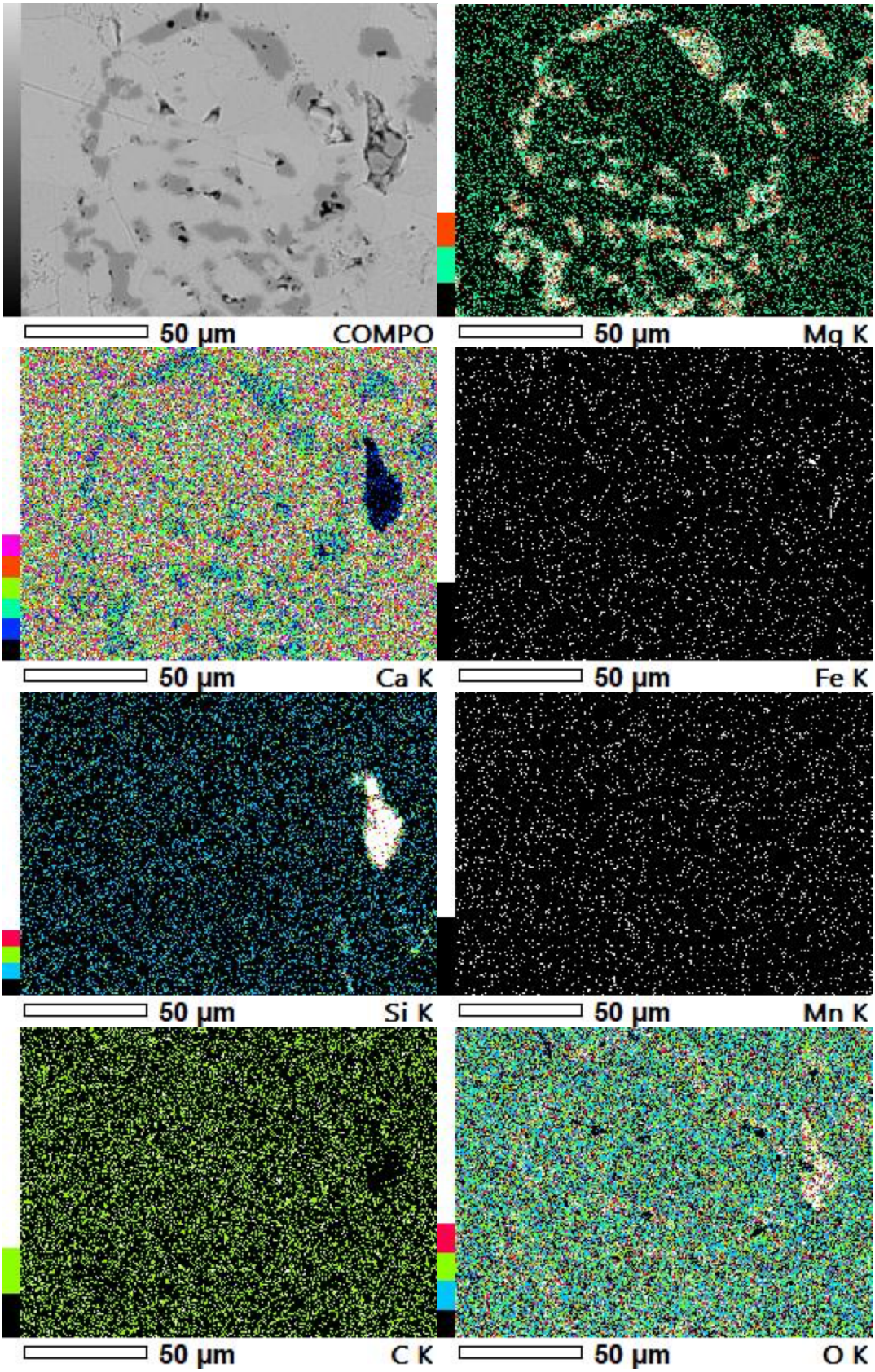
50 µm
COMPO
50 µm
Mg K
50 µm
Ca K
50 µm
Fe K
50 µm
Si K
50 µm
Mn K
50 µm
C K
50 µm
O K

Q1

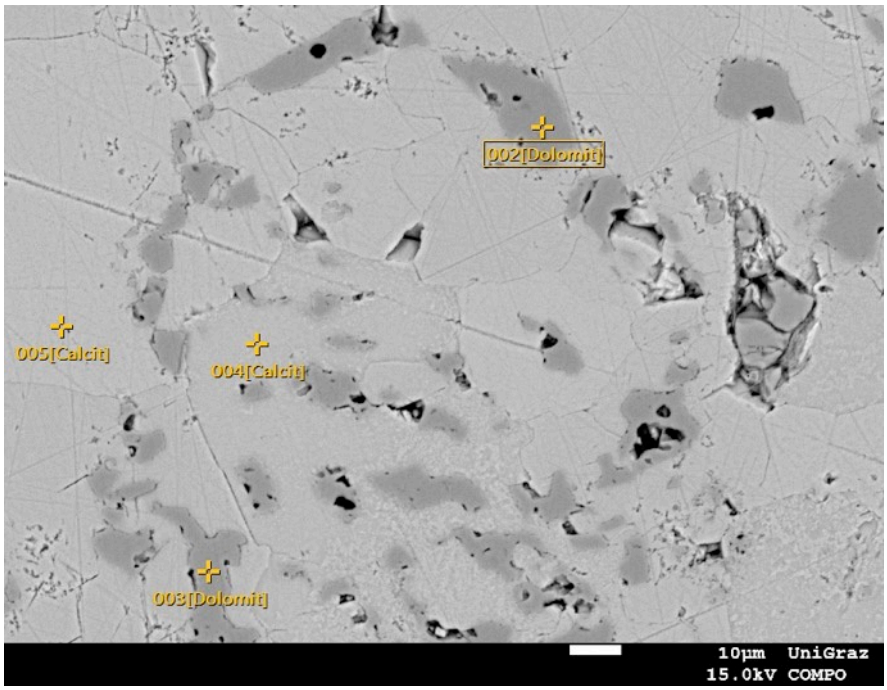

Volt : 15.00 kV

Mag. : x 700

Date : 2018/11/08

Pixel : 1280 x 960

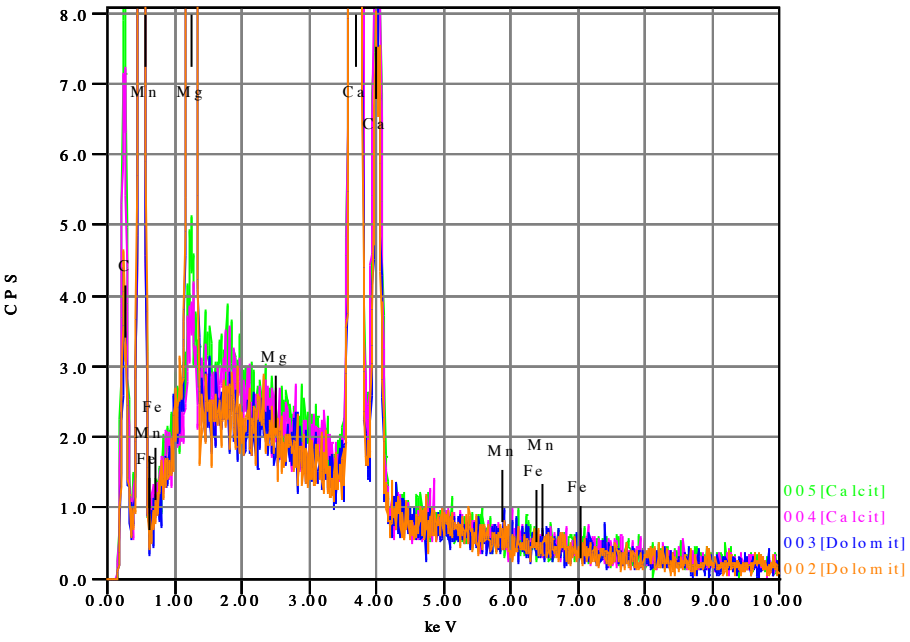

Acquisition Condition

Instrument : 8530F

Volt : 15.00 kV

Current : ---

Process Time : T2

Live time : 30.00 sec.

Real Time : 47.51 sec.

DeadTime : 37.00 %

Count Rate CPS : 1395.00

	Fe	CaO	C	MgO	MnO	Mn	FeO
002[Dolomit]		61.51	2.42	35.27	0.63		0.18
003[Dolomit]	nd	64.29		35.50	0.21		
004[Calcit]		99.21		0.60	0.04		0.14
005[Calcit]	nd	99.32		0.68		nd	
Average	0.00	81.08	2.42	18.01	0.29	0.00	0.16
Deviation		21.03	0.00	20.06	0.30		0.02

Q2

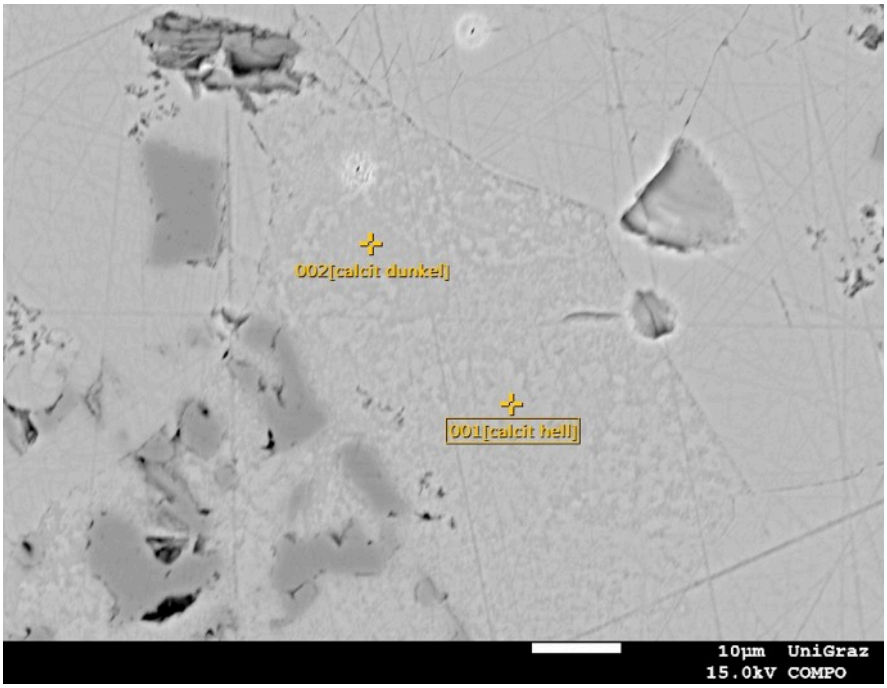

Volt : 15.00 kV

Mag. : x 1,200

Date : 2018/11/08

Pixel : 1280 x 960

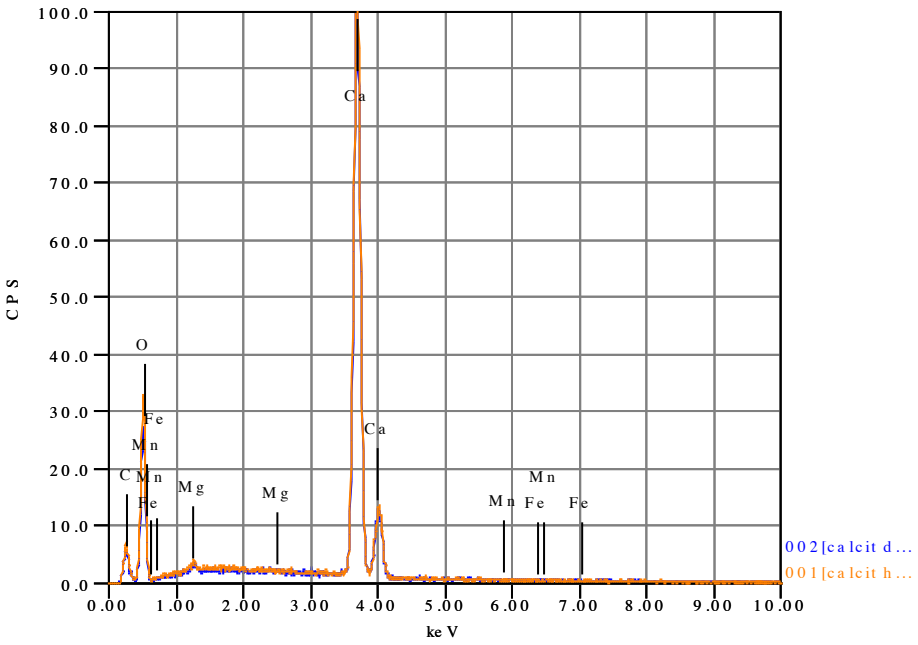

Acquisition Condition

Instrument : 8530F

Volt : 15.00 kV

Current : ---

Process Time : T2

Live time : 30.00 sec.

Real Time : 47.88 sec.

DeadTime : 38.00 %

Count Rate : 1725.00 CPS

	Fe	CaO	O	C	MgO	Mn	FeO
001[calcit ..	nd	96.61	0.00	2.88	0.51	nd	
002[calcit ..		99.16	0.00		0.61	nd	0.23
Average	0.00	97.88	0.00	2.88	0.56	0.00	0.23
Deviation		1.80	0.00	0.00	0.07		0.00

Q3

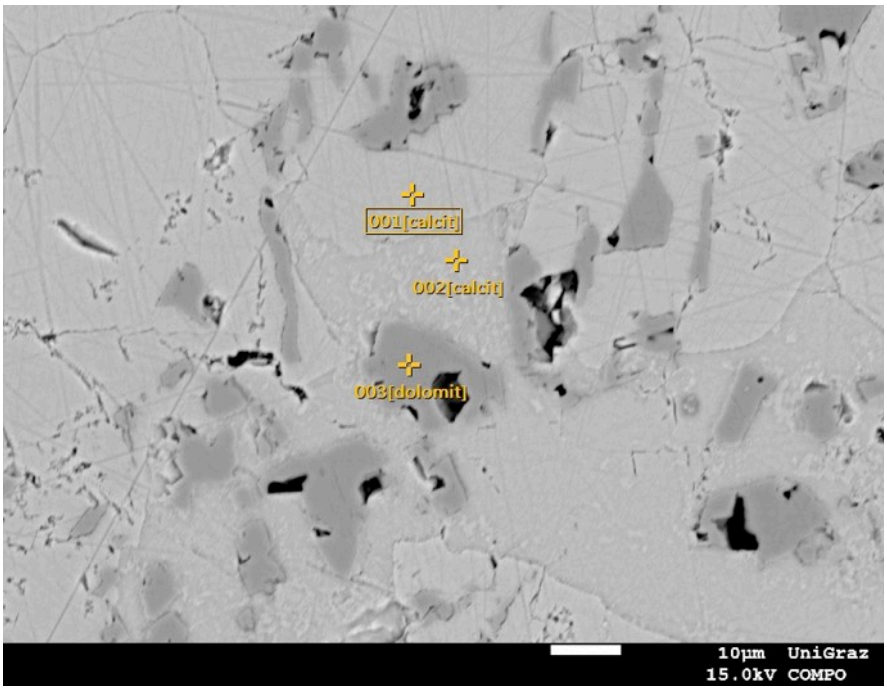

Volt : 15.00 kV

Mag. : x 950

Date : 2018/11/08

Pixel : 1280 x 960

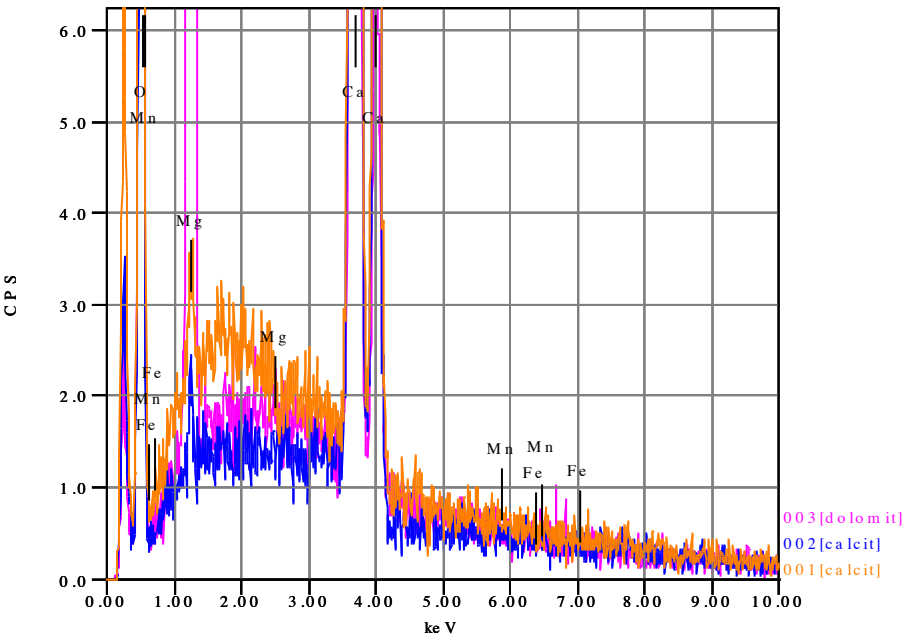

Acquisition Condition

Instrument : 8530F

Volt : 15.00 kV

Current : ---

Process Time : T2

Live time : 30.00 sec.

Real Time : 47.91 sec.

DeadTime : 37.00 %

Count Rate : 1744.00 CPS

	Fe	CaO	O	MgO	Mn	MnO
001[calcit]	nd	99.50	0.00	0.50	nd	
002[calcit]	nd	98.90	0.00	0.70		0.40
003[dolomit]	nd	70.14	0.00	29.39		0.47
Average	0.00	89.52	0.00	10.20	0.00	0.43
Deviation		16.78	0.00	16.62		0.05

Q4

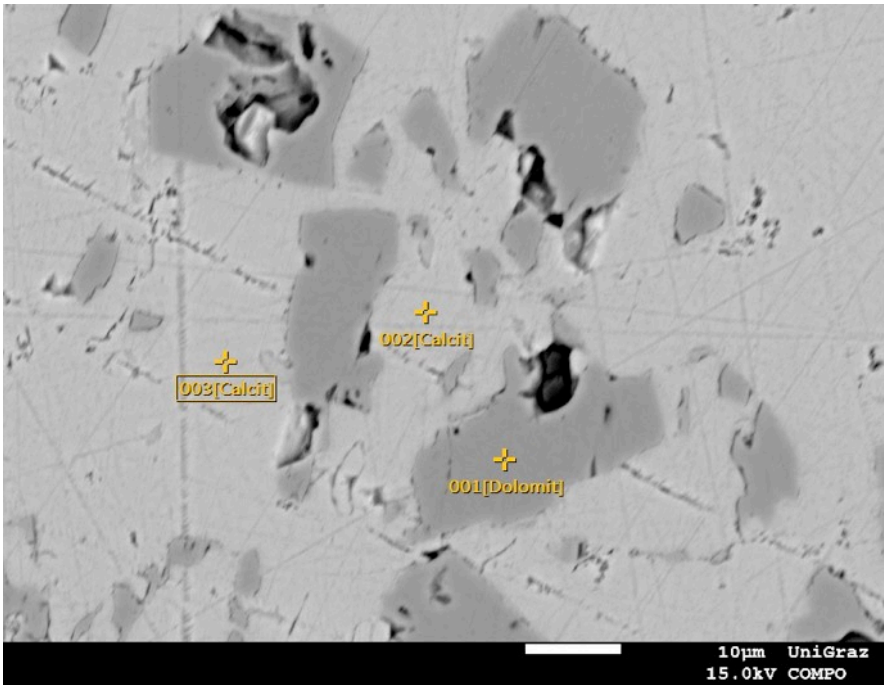

Volt : 15.00 kV

Mag. : x 1,300

Date : 2018/11/08

Pixel : 1280 x 960

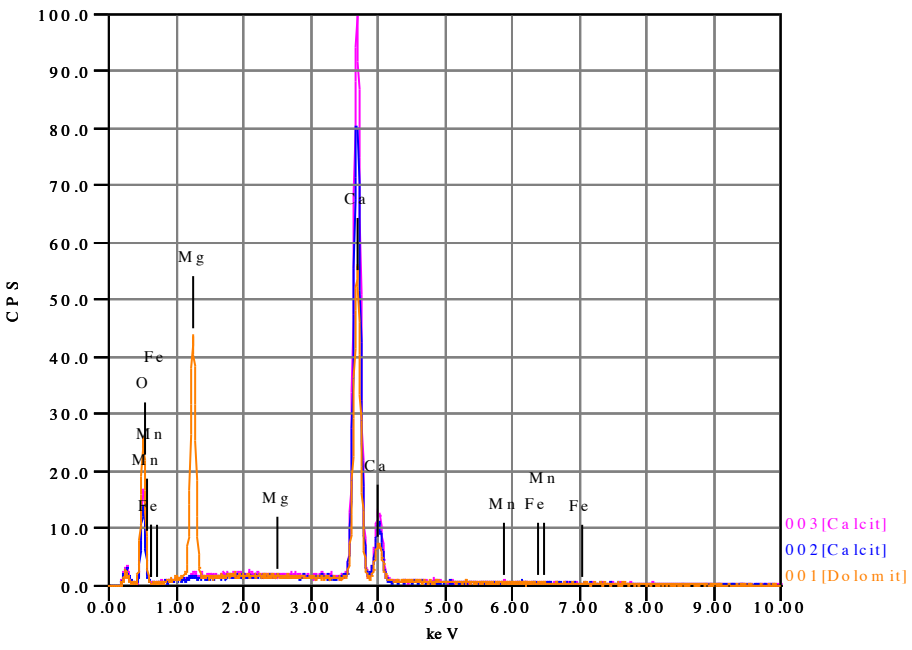

Acquisition Condition

Instrument : 8530F

Volt : 15.00 kV

Current : ---

Process Time : T2

Live time : 30.00 sec.

Real Time : 47.90 sec.

DeadTime : 38.00 %

Count Rate : 1651.00 CPS

	Fe	CaO	O	MgO	Mn	MnO	FeO
001[Dolomit]		72.01	0.00	27.41	nd		0.59
002[Calcit]	nd	99.70	0.00	0.30	nd		
003[Calcit]	nd	99.21	0.00	0.65		0.14	
Average	0.00	90.31	0.00	9.45	0.00	0.14	0.59
Deviation		15.85	0.00	15.55		0.00	0.00

LIST OF FIGURES

List of tables

Anderle, N., 1953. Aufnahmen 1952 auf dem Blatt Villach-West und -Ost. Verhandlungen Der Geologischen Bundesanstalt 64–66.

Arndt, R., Bäk, R., 2005. Geophysik im Drautal – Ergebnisse und Erkenntnisse. Arbeitstagung Der Geologischen Bundesanstalt 103–115.

Arnold, K.P., 2012. Die geologischen und morphologischen Grundstrukturen. Die Östliche Sattnitz - Bergbauern Vor Den Toren von Klagenfurt. 56–70.

Bertini, A., 1994. Messinian-Zanclean vegetation and climate in North-Central Italy. Historical Biology 9, 3–10. https://doi.org/10.1080/10292389409380483

Blair, T.C., McPherson, J.G., 1994. Alluvial fans and their natural distinction from rivers based on morphology, hydraulic processes, sedimentary processes and facies assemblages. Journal of Sedimentary Research A64, 450–489.

Brückl, E., Hammerl, C., 2014. Eduard Suess' conception of the Alpine orogeny related to geophysical data and models. Austrian Journal of Earth Sciences Jan 2014, 94–114.

Chaudhry, H.M., 2008. Open-Channel Flow. Springer Science+Business Media.

Claasen, T., von Gosen, W., Sylvester, H., Thiedig, F., 1987. Die Permotrias und ihr Grundgebirge zwischen Faaker See und Turiawald südöstlich von Villach (Kärnten/Österreich). Jahrbuch Der Geologischen Bundesanstalt 130, 391–413.

Community Maria Wörth, 2018. Maria Wörth [WWW Document]. URL https://www.maria-woerth.info/en/the-history/

Dreger, J., 1909. Bemerkungen über das Sattnitzkonglomerat in Mittelkärnten und die darin vorkommenden hohlen Geschiebe. Verhandlungen Der Geologischen Bundesanstalt 46–57.

Eberle, J., Eitel, B., Blümel, W.D., Wittmann, P., 2017. Deutschlands Süden – vom Erdmittelalter zur Gegenwart. Springer. https://doi.org/10.1007/978-3-662-54381-8

Einsele, G., 1992. Sedimentary Basins Evolution, Facies and Sediment Budget.

Eugster, H.P., Hardie, L.., 1978. Saline lakes. Lakes-Chemistry, Geology, Physics. 356pp.

Fauquette, S., Suc, J.-P., Bertini, A., Popescu, S.-M., Warny, S., Bachiri Taoufiq, N., Perez Villa, M.-J., Chikhi, H., Feddi, N., Subally, D., Clauzon, G., Ferrier, J., 2006. How much did climate force the Messinian salinity crisis? Quantified climatic conditions from pollen records in the Mediterranean region. Palaeogeography, Palaeoclimatology, Palaeoecology 238, 281–301.

https://doi.org/10.1016/j.palaeo.2006.03.029

Fortuin, A.R., Krijgsman, W., 2003. The Messinian of the Nijar Basin (SE Spain): sedimentation, depositional environments and paleogeographic evolution. Sedimentary Geology 160, 213–242. https://doi.org/10.1016/S0037-0738(02)00377-9

Frank, W., Kralik, M., Scharbert, S., Thöni, M., 1987. Geochronological data from the Eastern Alps. Geodynamics of the Eastern Alps, Flügel, H.W., Faupl, P. (Eds.), Deuticke, Vienna. 372–379.

Gargani, J., Rigollet, C., 2007. Mediterranean Sea level variations during the Messinian salinity crisis. Geophysical Research Letters 34, 1–5. https://doi.org/10.1029/2007GL029885

Griem, W., Wolf, S., Sylvester, H., Thiedig, F., 1991. Sedimentologie und Sedimentpetrographie des tertiären Sattnitzkonglomerats zwischen Villach und Klagenfurt (Kärnten, Österreich). Jahrbuch Der Geologischen Bundesanstalt 134, 27–36.

Handy, M.R., Ustaszewski, K., Kissling, E., 2014. Reconstructing the Alps–Carpathians–Dinarides as a key to understanding switches in subduction polarity, slab gaps and surface motion. International Journal of Earth Sciences 104, 1–26. https://doi.org/10.1007/s00531-014-1060-3

Heberer, B., Reverman, R.L., Fellin, M.G., Neubauer, F., Dunkl, I., Zattin, M., Seward, D., Genser, J., Brack, P., 2017. Postcollisional cooling history of the Eastern and Southern Alps and its linkage to Adria indentation. International Journal of Earth Sciences 106, 1557–1580. https://doi.org/10.1007/s00531-016-1367-3

Höfer, H., 1880. Die hohlen Gerölle und Geschiebeeindrücke des Sattnitz-Conglomerates bei Klagenfurt. Mineralogische Und Petrographische Mitteilungen 2, 325–349. https://doi.org/https://doi.org/10.1007/BF0299609

Hsü, K.J., Ryan, W.B.F., Cita, M.B., 1973. Late Miocene Desiccation of the Mediterranean. Nature 242, 240–244. https://doi.org/10.1038/242240a0

Jakl, I., 2017. Der Dom darf nicht zerbröckeln. Kärntner Kirchenzeitung - „Sonntag" 1–3.

Kahler, F., 1955. Urwelt Kärntens-Eine Einführung in die Geologie des Landes.pdf. Naturwissenschaftlicher Verein Für Kärnten 18. Sonder, 1–107.

Kahler, F., 1951. Über das Kohlenvorkommen des Turiawaldes südlich Velden am Wörther See. Naturwissenschaftlicher Verein Für Kärnten 45–55.

Kahler, F., 1931. Zwischen Wörthersee und Karawanken. Naturwissenschaftlicher Verein Für Steiermark 83–145.

Kargaranbafghi, F., Neubauer, F., Genser, J., 2015. The tectonic evolution of western

Central Iran seen through detrital white mica. Tectonophysics 651–652, 138–151. https://doi.org/10.1016/j.tecto.2015.03.019

Kieslinger, A., 1956. Die nutzbaren Gesteine Kärntens.pdf. Carinthia II 1–356.

Kováč, M., Baráth, I., Fordinál, K., Grigorovich, A.S., Halásová, E., Hudáčková, N., Joniak, P., Sabol, M., Slamková, M., Sliva, Ľ., Vojtko, R., 2006. Late Miocene to Early Pliocene sedimentary environments and climatic changes in the Alpine–Carpathian–Pannonian junction area: A case study from the Danube Basin northern margin (Slovakia). Palaeogeography, Palaeoclimatology, Palaeoecology 238, 32–52. https://doi.org/10.1016/j.palaeo.2006.03.015

Krainer, K., 2006. Geologie des Sattnitz-Höhenrückens. Aufbau, Zusammensetzung und Entstehung der tertiären und quartären Ablagerungen des Sattnitz-Höhenrückens. Die Sattnitz. Konglomerat Der Natur Im Süden Kärntens, Naturwiss. Verein Für Kärnten, Klagenfurt. Golob, B. & Zwander, H. (Hrsg.). 93–108.

Krijgsman, W., Hilgen, F.J., Raffi, I., Sierro, F.J., Wilson, D.S., 1999. Chronology, causes and progression of the Messinian salinity crisis. Nature 420, 652–655.

Kuhlemann, J., Frisch, W., Székely, B., Dunkl, I., Kázmér, M., 2002. Post-collisional sediment budget history of the Alps: tectonic versus climatic control. International Journal of Earth Sciences 91, 818–837. https://doi.org/DOI 10.1007/s00531-002-0266-y

Legrain, N., Dixon, J., Stüwe, K., von Blanckenburg, F., Kubik, P., 2014. Post-Miocene landscape rejuvenation at the eastern end of the Alps. Lithosphere 7, 3–13. https://doi.org/10.1130/L391.1

Lenhardt, W.A., 2007. Earthquake-Triggered Landslides in Austria – Dobratsch Revisited. Jahrbuch Der Geologischen Bundesanstalt. 193–199.

Lippitsch, R., Kissling, E., Ansorge, J., 2003. Upper mantle structure beneath the Alpine orogen from high-resolution teleseismic tomography. Journal of Geophysical Research 108, 5 1, 5 15. https://doi.org/10.1029/2002JB002016

Liu, Y., Genser, J., Handler, R., Friedl, G., Neubauer, F., 2001. 40 Ar/ 39 Ar muscovite ages from the Penninic-Austroalpine plate boundary, Eastern Alps. Tectonics 20, 526–547. https://doi.org/10.1029/2001TC900011

Luth, S., Willingshofer, E., Sokoutis, D., Cloetingh, S., 2013. Does subduction polarity changes below the Alps? Inferences from analogue modelling. Tectonophysics 582, 140–161. https://doi.org/10.1016/j.tecto.2012.09.028

Meijer, P., Krijgsman, W., Wortel, M.J.R., 2005. A quantitative analysis of the desiccation and re-filling of the Mediterranean during the Messinian Salinity Crisis. Earth and Planetary Science Letters 240, 510–520. https://doi.org/10.1016/j.epsl.2005.09.029

Meijer, P.T., Slingerland, R., Wortel, M.J.R., 2004. Tectonic control on past circulation of the Mediterranean Sea: A model study of the Late Miocene. Paleoceanography 19, n/a-n/a. https://doi.org/10.1029/2003PA000956

Mottl, M., 1955. Neuer Beitrag zur Säugetierfauna von Penken bei Keutschach in Kärnten.pdf. Naturwissenschaftlicher Verein Für Kärnten 60–91.

Nemes, F., Neubauer, F., Cloetingh, S., Genser, J., 1997. The Klagenfurt Basin in the Eastern Alps: an intra-orogenic decoupled flexural basin? Tectonophysics 282, 189–203.

Neubauer, F., Friedl, G., Genser, J., Handler, R., Mader, D., Schneider, D., 2007. Origin and tectonic evolution of Eastern Alps deduced from dating of detrital white mica: a review. Austrian Journal of Earth Sciences 100, 8–23.

Nickel, E., 1985. Carbonates in alluvial fan systems. An approach to physiography, sedimentology and diagenesis. Sedimemtary Geology 42, 83–104.

Rieser, A.B., Liu, Y., Genser, J., Neubauer, F., Handler, R., Friedl, G., Ge, X.-H., 2006. 40Ar/39Ar ages of detrital white mica constrain the Cenozoic development of the intracontinental Qaidam Basin, China. Geological Society of America Bulletin 118, 1522–1534. https://doi.org/10.1130/B25962.1

Sangati, M., Borga, M., 2009. Influence of rainfall spatial resolution on flash flood modelling. Natural Hazards and Earth System Sciences 9, 575–584.

Schmid, S.M., Flügenschuh, B., Kissling, E., Schuster, R., 2004. Tectonic map and overall architecture of the Alpine orogen. Eclogae Geologicae Helvetiae 97, 93–117. https://doi.org/10.1007/s00015-004-1113-x

Schuster, R., Scharbert, S., Abart, R., Frank, W., 2001. Permo-Triassic extension and related HT/LP metamorphism in the Austroalpine - Southalpine realm. Mitt. Ges. Geol. Bergbaustud. Österr. 45, 111–141.

Spiegel, C., Kuhlemann, J., Dunkl, I., Frisch, W., 2001. Paleogeography and catchment evolution in a mobile orogenic belt: the Central Alps in Oligo–Miocene times. Tectonophysics 341, 33–47.

Staunig, R., 2011. The Influence of Extensive Slope Tectonics on the Hydrogeological System Roach Spring (Carinthia/Austria). University of Graz.

Steininger, F.F., Rögl, F., Hochuli, P., Müller, C., 1989. Lignite deposition and marine cycles The Austrian Tertiary lignite deposits - A case history. Österr. Akad. Der Wissenschaften, Biol. Wissenschaften u. Erdwissenschaften (Springer Verlag, Wien) 197, 309–322.

Thalheim, F., 2016. Hydraulic Characterisation of a mass movement-influenced aquifer, Turiawald, Sattnitz Mountains, Carinthia. University of Graz.

Thöni, M., 2006. Dating eclogite-facies metamorphism in the Eastern Alps –

approaches, results, interpretations: a review. Mineralogy and Petrology 88, 123–148. https://doi.org/10.1007/s00710-006-0153-5

van Baak, C.G.C., Krijgsman, W., Magyar, I., Sztanó, O., Golovina, L.A., Grothe, A., Hoyle, T.M., Mandic, O., Patina, I.S., Popov, S. V., Radionova, E.P., Stoica, M., Vasiliev, I., 2017. Paratethys response to the Messinian salinity crisis. Earth-Science Reviews 172, 193–223. https://doi.org/10.1016/j.earscirev.2017.07.015

van Husen, D., 2004. Quaternary glaciations in Austria. Quaternary Glaciations - Extent and Chronology: Part I: Europe. 1–13. https://doi.org/10.1016/S1571-0866(04)80051-4

van Husen, D., 1987. Die Ostalpen und ihr Vorland in der letzten Eiszeit (Würm).

van Husen, D., 1985. Ein prae-würmglazialer Bergsturz vom Spitzegel (Hermagor, Kärnten). Carinthia II 175./95. J, 165–171.

van Husen, D., 1984. Synsedimentäre Gleitschollen großen Ausmaßes im terrestrischen Jungtertiär der Karawanken. Geologische Rundschau, Stuttgart 71, 433–445.

Vasiliev, I., Mezger, E.M., Lugli, S., Reichart, G.-J., Manzi, V., Roveri, M., 2017. How dry was the Mediterranean during the Messinian salinity crisis? Palaeogeography, Palaeoclimatology, Palaeoecology 471, 120–133. https://doi.org/10.1016/j.palaeo.2017.01.032

von Blanckenburg, F., 2005. The control mechanisms of erosion and weathering at basin scale from cosmogenic nuclides in river sediment. Earth and Planetary Science Letters 237, 462–479. https://doi.org/10.1016/j.epsl.2005.06.030

Weber, L., Weiss, A., 1983. Bergbaugeschichte und Geologie der österreichischen Braunkohlenvorkommen, Archiv für Lagerstättenforschung der Geologischen Bundesanstalt.

Wells, S.G., Dohrenwend, J.C., 1985. Relict sheetflood bed forms on late Quaternary alluvial-fan surfaces in the southwestern United States. Geology 13, 512–516.

Willett, S.D., Schlunegger, F., Picotti, V., 2006. Messinian climate change and erosional destruction of the central European Alps. Geology 34, 613–616. https://doi.org/10.1130/G22280.1

Winkler-Hermaden, A., 1957. Geologisches Kräftespiel und Landformung, grundsätzliche Erkenntnisse zur Frage junger Gebirgsbildung und Landformung. Springer, Wien.

Winkler-Hermaden, A., 1914. Über jungtertiäre Sedimentation und Tektonik am Ostrande der Zentralalpen. Mitteilungen Der Österreichischen Geologischen Gesellschaft 7, 256–312.

Winkler, D., 1997. Das Sattnitzkonglomerat / die Genese der “Hohlen Gerölle” und

fazielle Untersuchungen (Neogen, Südkärnten). University of Graz.

Worsch, E., 1937. Geologische Kartierung östlich des Faaker Sees. Carinthia II 127_47, 41–57.